University of Alberta

Motor unit recruitment by intraspinal microstimulation and long-term neuromuscular adaptations

by

Jeremy Andrew Bamford

A thesis submitted to the Faculty of Graduate Studies and Research
in partial fulfillment of the requirements for the degree of

Doctor of Philosophy

Centre for Neuroscience

Fall, 2009
Edmonton, Alberta

Examining Committee

Dr. Vivian Mushahwar, Centre for Neuroscience, University of Alberta
Supervisor

Dr. Charles T. Putman, Centre for Neuroscience, University of Alberta
Co-supervisor

Dr. Tessa Gordon, Centre for Neuroscience, University of Alberta
Committee member

Dr. Kathryn Todd, Centre for Neuroscience, University of Alberta
Committee Chair

Dr. Reggie Edgerton, Department of Physiological Sciences, University of California at Los Angeles
External committee member

Abstract

Spinal cord injury is a devastating neurological disorder partially characterized by a loss of motor function below the lesion. The dramatic loss of activity results in muscle atrophy and slow-to-fast transformation of contractile elements, producing smaller, weaker and more fatiguable muscles. Functional electrical stimulation (FES), has been proposed in order to induce muscular activity and reverse these changes. FES has primarily been applied in the periphery, either at the surface or implanted in or around a nerve or muscle. Although this can excite nervous tissue and produce muscular contractions, these systems often produce reversed recruitment of motor units leading to inappropriate force generation and increased fatigue.

We applied intraspinal microstimulation (ISMS) through fine microwires implanted into the spinal cord of rats. Electrical stimulation through these microwires caused contractions of the quadriceps muscles in both acute and chronically spinalized animals. We showed that muscle recruitment is significantly more gradual with ISMS in intact rats compared to that produced by a standard nerve cuff. Our results further showed that this was due to preferential activation of fatigue resistant muscle fibers.

Given this more orderly recruitment of motor units by ISMS, we tested the muscle phenotypes produced by ISMS or nerve cuffs after

chronic stimulation. Surprisingly, over a 30 day stimulation period the quadriceps muscles chronically activated by either daily ISMS or nerve cuff stimulation underwent similar fast-to-slow transformations in fiber type and functional properties. This indicates that the recruitment order of motor units does not play the only role in determining the muscle phenotype. Other factors such as the total daily time of activity may be critically important to the phenotypic outcome of skeletal muscle.

Finally, we demonstrated that quadriceps force recruitment by ISMS was unchanged following the 30 day stimulation period. In addition, 30 days of chronic ISMS did not cause observable damage in the spinal cord beyond that incurred by the implantation of sham microwires. These studies advance our understanding of the force recruitment properties, neuromuscular plasticity and damage incurred by ISMS and move us closer to developing a clinically viable ISMS procedure.

List of Tables

List of Figures

List of abbreviations

1/2FT - one-half fall time
1/2RT - one-half rise time
ANOVA - analysis of variance
ANCOVA - analysis of covariance
ATP - adenosine tri-phosphate
CNS - central nervous system
CPG - central pattern generator
CSA - cross-sectional area
DBS - deep brain stimulation
EPSP - excitatory post-synaptic potential
FES - functional electrical stimulation
FF - fast, fatiguable motor unit
FR (FFR) - fast, fatigue-resistant motor unit
FNS - functional neuromuscular stimulation
GFAP - glial fibrillary acidic protein
H-reflex - Hoffmann reflex
HDL - high-density lipoprotein
ISMS - intraspinal microstimulation
ISC - intraspinal microwire control
LDL - low-density lipoprotein
Map-2 - microtubule-associated protein 2
MHC - myosin heavy chain
NCC - nerve cuff control
NCS - nerve cuff stimulation
NeuN - neuronal nuclei
PAS - periodic acid Schiff's stain
PBS - phosphate-buffered saline
PNS - peripheral nervous system
pO_2 - partial pressure of oxygen
pps - pulses per second
S - slow motor unit
sc - subcutaneous

SCI - spinal cord injury
SD - standard deviation
SEM - standard error of the mean
SERCA - sarco(endo)plasmic reticulum Ca^{2+}-ATPase
ST - spinal cord transection
TLT - treadmill locomotor training
TNF-α - tumor necrosis factor-alpha
TTP - time-to-peak tension
TWFn - normalized twitch force
VO_2 - volume of oxygen

Chapter 1

Introduction

1.1 Pathophysiology of SCI

Spinal cord injury (SCI) is a devastating neurological impairment with life-threatening implications. A recent survey in the United States indicated that approximately 6 million people live with some form of paralysis and 1.3 million people have undergone SCI (Andresen et al.,2006). In addition to the apparent physical trauma, patients undergo severe psychosocial and socioeconomic disruptions that affect quality of life. Approximately half of all injuries occur as a result of motor vehicle accidents but other significant accident categories include falls, sports injuries and violence. Given these categories it is not surprising that men are 4 times more likely to undergo a spinal cord trauma than women and that the average age of patients when they undergo SCI is 26.4 years (Nobunaga et al., 1999). Persons with SCI must confront a host of neurological sequelae including paralysis, sexual dysfunction, sensory loss and loss of bladder and bowel function. Since the introduction of a rationalized study of SCI in the 1940's the life expectancy of persons with SCI has increased steadily, however, the final neurological outcome is still predicted by the severity of the injury (Ragnarsson, 2008). Currently there is no viable treatment to repair the neurological damage in the spinal cord. In the absence of such a treatment, rehabilitative techniques have focused on lessening the impact of the injury and facilitating accommodation to a new lifestyle.

Current research is focusing on improving existing treatments and offering a better understanding of the basic science of the spinal cord and its response to damage. A large section of the work is focused on restoring the control of movement following SCI (Thuret et al., 2006). This dissertation focuses on the evaluation of a novel, intraspinal method of stimulation designed to reanimate paralyzed or paretic skeletal muscle and restore motor function to the lower limbs. The introductory chapter will: 1) review the pathology of spinal cord injury; 2) discuss the functional consequences of spinal cord injury with respect to the loss of motor function; 3) briefly review the current treatment and rehabilitative options for restoring limb control and motor function; 4) discuss the use of electrical stimulation to restore motor function; 5) introduce an alternative method of electrical stimulation delivered through the spinal cord. Key questions will be addressed regarding the recruitment properties and chronic outcomes of intraspinal stimulation.

1.1.1 Primary Spinal Cord Injury

The primary SCI occurs from blunt traumas that include flexion, extension, axial compression, rotation and distraction of the spinal cord. The most common etiology is that of impact and persistent compression such as in burst fractures, dislocations and disc ruptures (Dumont et al., 2001). Of these, dislocation injuries are the most commonly observed. Further injury can occur due to vertebral segments or fragments of fractured bone that are driven into the spinal cord causing laceration injuries.

According to Bunge et. al. (Bunge et al., 1993) SCIs produce stereotyped gross morphologies of the spinal cord that can be classified into four categories. In a sample database of 180 human patients, most with cervical SCIs due to motor vehicle accidents, 49% presented with contusion/cavity injuries, 21% had laceration injuries, 20% had massive compression injuries and 10% had solid cord injuries which present as grossly normal but display damage when examined histologically (Norenberg et al., 2004). A proper understanding of the primary injury is critical as the patient's neurological grade when reaching the hospital is the most important prognosticator of final outcomes. This may be due to the fact that the primary injury tends to be most damaging to grey matter while relatively sparing white matter (Dumont et al., 2001). In addition there is evidence that certain injury types induce damage in specified regions (Choo et al., 2007). Proper knowledge of these factors may assist in the advancement and specification of future clinical treatments.

1.1.2 Secondary Spinal Cord Injury

The physical trauma that is primary SCI is the causal agent for further damaging events including disruption of axons, hemorrhage, ischemia-reperfusion and neural shock. This period, referred to as secondary injury, features these and other pathophysiological events and is characterized by a worsening of the injury. The original site of injury expands during this period first vertically and then horizontally through the grey matter extending paralysis to higher levels (Schwab et al., 2006).

Damaged axons retract to form stumps while the distal ends undergo Wallerian degeneration. A fluid filled cavity forms surrounded by a scar composed of astrocytes, microglia, fibroblasts and connective tissue. An understanding of this period is critical as much of the final outcome for each patient is determined by the degree to which the original damage is worsened during the secondary phase. Accordingly, this is the first point at which therapeutic interventions can be made to limit damage and improve the final outcome.

1.1.2.1 Ischemia and reperfusion

Ischemia following SCI is primarily associated with disruption of microvasculature and subsequent progression of ischemia rostrally and caudally (for reviews see Tator and Fehlings, 1991; Tator, 1992; Tator, 1995). This expansion of the ischemic area may be attributed to thrombosis and vasospasm as part of the ongoing secondary injury and may provide an early treatment opportunity. Interestingly, many researchers have found that larger blood vessels remain intact following spinal cord trauma. Using a clip-induced SCI model Koyanagi et. al. found that crush damage to the spinal cord of rats was most disruptive to microvasculature networks in the grey matter and posterior columns while larger vessels and white matter were relatively spared (Koyanagi et al., 1993). Using the same model, Wallace et. al. showed a lack of filling of arterioles, capillaries and venules with major arteries still intact (Wallace et al., 1986). Despite the sparing of larger vessels numerous investigators have found a major re-

duction of blood flow in the spinal cord following SCI (Tator and Fehlings, 1991).

The ischemic insult is further compounded by the onset of neurogenic shock and the associated loss of autoregulation which is the ability to maintain constant blood flow in varying pressure conditions (Tator and Fehlings, 1991). Following SCI in animal models many authors have described a period of neurogenic shock characterized by hypotension and reduced cardiac output due to decreased peripheral resistance and bradycardia (Tator and Fehlings, 1991). This is thought to be due to depressed sympathetic drive which decreases heart rate and affects vasomotor systems altering the balance between vasodilation and vasoconstriction (Guha and Tator, 1988). The result of this is both systemic as demonstrated by a drop in blood pressure and decreased cardiac output, and local due to the effects on arterioles and venules within the spinal cord. Specifically, systemic lowering of blood pressure produces further ischemia while localized increases in blood pressure result in hyperemia in areas adjacent to the injury (Guha et al., 1989). The sum effect of all these processes is the production of an ischemic environment that can be particularly damaging to grey matter due to its high metabolic demands (Senter and Venes, 1979).

Following an ischemic period there is often a reperfusion event with concomitant production of free-radical species that further secondary in-

jury (for review see Dumont et al., 2001). This hyperemic event is thought to be due to perivascular decreases in pH due to lactate production (along with the associated hydrogen ion) during ischemia. The onset of hyperemia brings with it the rapidly increased production of reactive oxygen species such as superoxides, nitric oxide and hydroxyl radicals. The rise in reactive oxygen species cannot be buffered by antioxidant molecules and thus the oxidation of key proteins, lipids and nucleic acids ensues. Specifically, reactive oxygen species cause the inactivation of key metabolic enzymes such as glyceraldehyde-3-phosphate dehydrogenase and certain respiratory chain enzymes as well as membrane channels such as the Na^+/K^+ ATPase (Lewen et al., 2000). In addition, the initiation of lipid peroxidation during oxidative stress can lead to the breakdown of membranes and the onset of excitotoxicity. Unfortunately the process of lipid peroxidation includes the production of further reactive oxygen species and the continuance of the cycle.

1.1.2.2 Excitotoxicity

Disruption of cell membranes due to physical trauma or biochemical processes allows the release of glutamate, the primary excitatory neurotransmitter of the CNS. Even before disruption the membrane potential is lost resulting in the activation of presynaptic voltage-gated Ca^{2+} channels triggering a release of excitatory amino acids (Schwab et al., 2006). Once released glutamate accumulates in the extracellular space where it binds to receptors causing the influx of Na^+ and Ca^{2+} into nearby cells

where they initiate a host of processes which contribute to the pathogenesis of secondary injury. The term “excitotoxicity” has been used to describe the process whereby the release of glutamate can mediate the death of CNS neurons (Choi, 1992).

In excitotoxic conditions intracellular Na^+ concentrations rise rapidly in response to the activation of ionotropic glutamate receptors due to the large inward gradient of Na^+ across the cell membrane (Kwon et al., 2004). This inward current of Na^+ ions may also lead to the activation of voltage gated Na^+ channels. Further influx of Na^+ may come from the activation of the Na^+/Ca^{2+} exchanger which imports Na^+ in exchange for the antiport of Ca^{2+}. Normally the influx of Na^+ into the cell during the propagation of an action potential is countered by Na^+/K^+-ATPase which reestablishes the appropriate gradient for both of these ions. However, oxidative and metabolic stress following SCI can lead to a lack of ATP supplying these pumps. In addition, the pumps themselves can be disrupted by reactive oxygen species leading to the accumulation of Na^+ and cytotoxic edema due to osmotically increased H_2O content inside the cell. In addition, the increased Na+ concentration activates Na^+/H^+ exchangers which produce acidosis and the associated deleterious effects (Dumont et al., 2001). The damage caused by increased intracellular Na^+ can be illustrated by the results of experiments blocking Na^+ channels. Injections of tetrodotoxin have been shown to protect against axonal damage and to enhance the recovery of locomotion in animal models if they are administered

shortly after SCI (Teng and Wrathall, 1997; Rosenberg and Wrathall, 2001).

As with Na^+ influx, Ca^{2+} can enter the cell when glutamate binds to ionotropic receptors (Kwon et al., 2004). In addition, damage to cell membranes can cause intracellular concentrations to rise as Ca^{2+} flows in from extracellular sources or from intracellular compartments that sequester Ca^{2+}. Ca^{2+} is a powerful second messenger that can activate a host of proteases and lipases which may damage the cell structure further and encourage lipid peroxidation. In addition, Ca^{2+} interferes with mitochondrial function and cellular respiration. The destructive influence of unregulated intracellular Ca^{2+} content has prompted one author to describe Ca^{2+} as the final common pathway of cell death (Schanne et al., 1979).

1.1.2.3 Necrosis and apoptosis

After SCI the combination of varied traumas such as physical damage, ischemia-reperfusion, oxidative stress and excitotoxicity lead to two paradigms of cellular death (Emery et al., 1998). Necrosis is the process whereby cellular homeostatic mechanisms are overwhelmed and the cell succumbs to its injuries. As such, necrosis is often thought of as a passive mechanism where the cell is "murdered" by extrinsic factors. On the other hand, apoptosis involves the active participation of the cell in its own death including the production of ATP and the alteration of gene expression to bring about programmed cell death or "suicide". Active participation of the cell in its own death can be demonstrated by the fact that the

protein synthesis inhibitor cycloheximide can spare cells and improve recovery after SCI (Liu et al., 1997). At the sites of greatest trauma necrosis is common and obvious while apoptotic cells tend to form around the periphery of the necrotic cell mass. This suggests that as damage increases, the likelihood of necrosis increases (Kwon et al., 2004). Since necrosis involves an overwhelming injury, the death of the cell is relatively quick and interventions to rescue the cell from this fate are less apt to succeed. On the other hand apoptosis involves a lesser trauma and apoptotic cells can be detected for weeks following SCI and at great distances from the original injury site suggesting an opportunity for therapeutic intervention (Crowe et al., 1997; Liu et al., 1997; Emery et al., 1998).

1.1.2.4 Immune response

Following SCI the inflammatory response undergoes distinct stages marked by the activation or recruitment of differing immune cells. In the first day there is an invasion of neutrophils into the lesion site which peaks on the second day and is gone by the third (Norenberg et al., 2004). The main function of neutrophils is to release lytic enzymes which have the effect of furthering damage. As a result, current neuroprotective strategies often involve the suppression of the neutrophil response in order to spare undamaged tissues. As early as the first day resident microglia are activated while blood-borne macrophages are recruited to the site of injury. The primary role of both microglia and macrophages is to phagocytose damaged tissue. This role aids in the removal of lipids and other debris

which may cause the production of free radicals due to lipid peroxidation. In the following days astrocytes are activated and undergo hypertrophy, a process which peaks two to three weeks following injury. They also send out cytoplasmic extensions which form a web of interwoven processes attached via tight junctions and infiltrated with extracellular matrix. This so-called “astroglial scar” functions to isolate the lesion from viable tissue and can be readily visualized by its expression of glial fibrillary acidic protein (GFAP).

The role of inflammatory cells is controversial with ongoing arguments regarding the neurotoxic versus neuroprotective effects of their actions (Lazarov-Spiegler et al., 1998; Bethea, 2000). Most of the immune cells which are present following SCI can be shown to play both damaging and protective roles at varying time points leading to a controversy as to which factors of the immune response should be inhibited and which might be profitably enhanced. For instance macrophages and microglia produce cytokines such as tumor necrosis factor-alpha (TNF-α) which, like many other immune products, has both neurotoxic and neuroprotective effects. The deciding factor may be when TNF-α is released. One view is that TNF-α has neurotoxic effects during the early stages of inflammation and neuroprotective effects at later time points (Kwon et al., 2004). Similarly, the astroglial scar may be the source of molecules such as chondroitin sulfate proteoglycans which retard regeneration, but it is also the source of molecules which promote the growth of neurites. The ablation of

astrocytes in mice following spinal cord damage lead to further invasion of neutrophils and monocytes, neuronal degeneration and decreased function (Bush et al., 1999). The view that the inflammatory response following SCI is only a damaging process is clearly simplistic and further research is required to inform clinical procedures designed to limit damage following SCI.

As healthy tissues are destroyed and phagocytosed they are eventually replaced with dense bundles of connective tissue and cysts. The former are referred to as mesenchymal scars and are distinct from the astroglial scars which form to isolate damaged areas and cysts. Both mesenchymal scars and fluid-filled cysts form impediments to regrowth of axons as they fill large voids in the spinal cord and provide no substrate for axons to grow along. Indeed these are areas where growth inhibiting substances are found in abundance which cause the retraction and collapse of axon growth cones.

1.2 Compromised motor function

Spinal cord injury results in a loss of volitional control of the limbs and the associated loss of freedom and general independence. Furthermore, the decrease in activity represented by this condition has secondary effects over time. It is readily apparent that SCI creates challenges to regular physical activity and may contribute to a sedentary lifestyle. The daily

activities of most individuals with SCI are considered inadequate to maintain fitness and retain bone and muscle mass (Devillard et al., 2007). Cardiorespiratory, musculoskeletal and metabolic health are all detrimentally affected by the dramatic decrease in routine activity and gravitational loading. Although very serious social, emotional and economic consequences are also imposed upon those with spinal cord injuries, the purpose of this section is to examine the physiological consequences of the chronic loss of motor function.

1.2.1 Wasting of bone and muscle

Following SCI there is a dramatic but asynchronous wasting of muscle and bone tissue below the lesion which affects health and quality of life. Muscle mass is significantly reduced in the weeks following SCI in a variety of muscles while bone loss proceeds more slowly, reaching a lowered steady state 1-3 years following injury (Giangregorio and McCartney, 2006). Both muscle and bone loss are site specific with the greatest losses in the lower limbs and little to no loss in the upper extremities except in the case of tetraplegia (Demirel et al., 1998; Spungen et al., 2000).

Not surprisingly, a decrease in muscular activity and weight bearing play a role in the extent of muscle and bone loss. Following SCI, sedentary individuals had higher absolute and relative levels of fat mass than those with greater daily activity levels indicating a shift in body composition and a decrease in fat free mass (Olle et al., 1993). In addition, the loss of muscle and bone mass are correlated with one another suggesting that active

muscle may prevent the loss of bone mass (Modlesky et al., 2005). Spasticity, though often deleterious, does represent an increase in muscle activity which has been associated with increased muscle mass (Wilmet et al., 1995) and in some cases with increased bone mass (Jiang et al., 2006). Other factors that may play a role in bone and muscle mass include hormonal deficiencies and abnormalities in blood circulation (Maimoun et al., 2006).

Complications due to muscle and bone loss include the increased likelihood of fracture, especially low energy fractures which occur during everyday activities such as transferring from a wheelchair or being turned in bed. Common fractures occur at the knee, distal femur or proximal tibia and their prevalence increases with time from 1% in the first 12 months after injury to 4.6% after 20 years or more (Maimoun et al., 2006). Secondary complications include misaligned or delayed healing, pressure sores, infection or osteomyelitis. There have also been case reports of delays in seeking treatment from 1 day to 4 weeks due to loss of pain sensation (Giangregorio and McCartney, 2006). Fractures often require further hospitalization and immobilization reducing quality of life for the individual and leading to greater atrophy and tissue loss.

Chronic spinal cord injury causes not only muscle atrophy but also slow-to-fast transformation of the muscles innervated by nerves originating below the lesion (Burnham et al., 1997; Gerrits et al., 1999; Talmadge

et al., 2002). The observed transformation occurs via the reduced expression of slower isoforms of contractile proteins such as the myosin heavy chains (MHC) (Talmadge, 2000). Slow isoforms of proteins responsible for the handling of Ca^{2+} are also reduced as well as key enzymes of oxidative metabolic pathways. This transformation is complemented by the increased expression of faster contractile isoforms, faster Ca^{2+}-handling proteins and an increase in key enzymes of glycolysis (Shields, 2002). The functional nature of the muscle also changes during fast-to-slow transformation as the expression of key contractile proteins has been tied to the functional capacity of the muscle (Gallo et al., 2004). In most cases, slow-to-fast transformation yields a muscle that is weaker, faster and more fatiguable as demonstrated by lower evoked forces, a shortening of isometric twitch characteristics and increased fatigue during repeated contractions, respectively (Talmadge et al., 2002). This may be explained by the fact that the transformation appears to be coordinated so that a matching of the various contractile and metabolic elements occurs as the muscle becomes faster. There are exceptions to this coordinate relationship which may explain cases where force-, speed- or fatigue-related properties are not altered as would be expected (Bamford et al., 2003); however, the coordinated nature of transformation in muscle has been demonstrated often enough that some have been led to conclude that the expression of these elements are under common control (Hamalainen and Pette, 1997). Although there is evidence for the coordinated control of contractile and

metabolic elements during transformation the transient expression of multiple MHC isoforms in the same muscle fiber is common. Moreover, some reports indicate that the number of these hybrid fibers may remain chronically elevated indicating a breakdown in the control of contractile protein expression (Talmadge et al., 1999). Presumably, the functional properties of these fibers would be a blend of the properties of unadulterated fibers expressing only one MHC isoform. Operatively, this may indicate a decreased range of functional properties and a convergence towards the blended mean.

1.2.2 Decreased activity and the metabolic syndrome

The dramatically reduced activity level following SCI has metabolic consequences in addition to those affecting musculoskeletal health. In recent years the term metabolic syndrome has been used to connote a progressive series of disorders relating to metabolism, adiposity and cardiac function. This syndrome is commonly identified as including the progression of insulin resistance, increased serum triglycerides, hyperinsulinemia, diabetes and cardiac disease. Epidemiological and biochemical links between these conditions have been established in part due to the common and ordered progression from one condition to the next.

The first phase in the metabolic syndrome involves disordered carbohydrate metabolism. In all populations the inability to dispose of glucose leads to elevated blood glucose levels (hyperglycemia), a prolonged increase of circulating insulin (hyperinsulinemia) and finally full-blown

diabetes. However, altered carbohydrate metabolism is more prevalent and more severe in those with SCI than in the general population. This is most likely related to the degree of sedentary immobilization and the associated decrease of fat free tissue following SCI (Bauman et al., 1999). As the proportion of fat free mass including muscle mass diminishes, the ability to dispose of glucose is likewise reduced. Additionally, the modifications of skeletal muscle following SCI contribute to the problem by conversion to fast-twitch muscle fibers which have been found to be less sensitive to insulin than other fiber types (Lillioja et al., 1987). Thus, the foundations of insulin resistance in those with SCI are similar to those for the general population in that inactivity, adiposity and muscular factors are all involved. However, the degree of inactivity caused by immobilization due to SCI is much more severe than found in the typical sedentary population. This is illustrated by the results of standardized tests which show a progressive impairment of glucose tolerance as the severity of spinal cord injury increases. Subjects with tetraplegia had the least effective response to oral glucose followed by those with paraplegia and finally by age-matched controls (Bauman and Spungen, 1994). In the same work these authors found that insulin sensitivity was correlated with increased lean body mass and inversely correlated with fat mass. Moreover, the highest correlation was with measures of cardiopulmonary fitness. The deficits in carbohydrate metabolism in those with SCI are likely due to peripheral insulin re-

sistance rather than altered hepatic glucose release since glucose output in a fasted state is normal in those with SCI (Bauman et al., 1999).

The next phase of the metabolic syndrome is dyslipidemia, a condition secondary to hyperinsulinemia and coexistent with diabetes which involves the increased circulation of harmful lipids and cholesterols associated with cardiovascular disease. In those with SCI a lowering of high-density-lipoprotein cholesterol (HDL) and no change in low-density-lipoprotein cholesterol (LDL) leads to an increase in the LDL/HDL ratio, a key risk factor for cardiovascular disease (Bauman et al., 1999). As with carbohydrate metabolism the deterioration of the LDL/HDL ratio is likely correlated to activity levels as those with tetraplegia and motor complete injuries show the greatest decreases in HDL cholesterol (Bauman et al., 1998). Fortunately, the same work showed that intervention with exercise can increase HDL cholesterol in those with SCI. Indeed, even slight increases in activity can positively affect HDL levels. In addition to the activity related factors high calorie or high fat intake, excessive alcohol consumption and smoking can negatively affect HDL and serum triglyceride levels in those with SCI (Bauman et al., 1999).

Individuals with SCI have a high rate of premature coronary heart disease. Coronary heart disease is the greatest cause of death in those with SCI over 60 years of age or over 30 years after their injury (Whiteneck et al., 1992). The accelerated atherosclerosis in those with SCI is likely the

result of increased insulin resistance, diabetes, and dyslipidemia. These diseases have been well researched in the able-bodied population and have been characterized as the metabolic syndrome. It is noteworthy that this syndrome occurs with greater prevalence in those with SCI and that the severity and prevalence of these disorders are inversely related to the level of injury and thus the level of mobility (Bauman et al., 1999).

1.3 Treatments to restore motor function

Clinical treatment of motor deficits after SCI primarily involves compensation for decreased function and the attempt to achieve the greatest day-to-day improvements in quality of life. Physical therapy practices are generally geared at accommodation of the individual and the environment to the new injury. Accommodation of the individual might include fitting with braces or training on the use of a wheelchair while accommodation of the environment might involve installing ramps and handrails to aid in mobility and transfers. Although these treatments can improve quality of life they are unable to repair the damage incurred during the primary and secondary injuries. The best predictor of the functional outcome remains the severity of damage to the spinal cord after the injury (Ragnarsson, 2008).

1.3.1 Neuroprotection

The first hours following SCI are the first opportunity to intervene to protect the spinal cord and prevent the cascade of damaging processes that will determine the amount of spared tissue. As such, there is a large

body of work examining treatments to protect the spinal cord and perhaps even predispose injured neurons to regeneration. Many injuries that result in the complete disruption of motor and sensory function are not the result of a complete transection. A common gross pathology is characterized by a fluid-filled cyst bordered by intact tracts of tissue that extend below the injury site. This result suggests that early treatments which could attenuate the secondary spinal cord damage might result in improved function. Indeed, there are reports of extant function in individuals with as little as 10% sparing of spinal cord tissue (Kwon et al., 2005).

Neuroprotective therapies following SCI typically involve surgical decompression and the administration of anti-inflammatory drugs. Although commonly performed, surgical decompression of the spinal cord has remained controversial for many years due to conflicting evidence from research trials (Kwon et al., 2005). However, recent evidence from a large, multi-centre trial has shown that 24% of those receiving early decompression had an improvement on the American Spinal Injury Association scale of 2 grades or more (Fehlings and Arvin, 2009). Likewise, the application of anti-inflammatory agents such as methylprednisolone and minocycline remains controversial due to promising results in animal models but conflicting reports of clinical efficacy in humans (Ramer et al., 2005). The equivocal results of clinical trials with these substances, in combination with the potential for serious side-effects have prompted some surgical centers to cease routine usage. For example, the side-effects

of methylprednisolone include an increased risk of infection, bleeding and pancreatitis (Schwab et al., 2006).

1.3.2 Regeneration

While functional regeneration bridging the injury site does not occur spontaneously after SCI it has been shown that treatments can be implemented to encourage axonal growth in the CNS, a region which is naturally hostile to regeneration, even after complete SCI in rats (David and Aguayo, 1981; Cheng et al., 1996; Ramer et al., 2005). These discoveries have led to the development of a field of research investigating the possibility of regenerating neural tissue after traumatic damage such as a spinal cord lesion (for reviews see David and Lacroix, 2003; Schwab et al., 2006). A number of impediments to regrowth in the spinal cord have been identified including physical barriers, the presence of growth-inhibiting molecules and the lack of neurotrophic support for growing axons (Fouad and Pearson, 2004). To counter these challenges a variety of treatments have been attempted. The dissolution of the scar with chondroitinase has produced promising results including the restoration of some forepaw function in rats (Bradbury et al., 2002). Researchers have also implanted a variety of cell types in an attempt to improve upon the original results of Aguayo and colleagues in providing an environment in which axon regeneration might occur. For instance, Schwann cells and olfactory ensheathing glia have been implanted in rats, sometimes in combination, to encourage regrowth (Fouad et al., 2005)(Lu et al., 2002). The application of

antibodies or other substances to inhibit signaling of the Nogo and myelin-associated glycoprotein pathways has proven to promote regeneration (Hasegawa et al., 2004) (GrandPre et al., 2002). In addition, the administration of neurotrophic factors has been used to encourage regrowth and to guide axons to bridge the gap and create beneficial connections below the lesion (Ramer et al., 2000)(Grill et al., 1997). Although these treatments, and others, have proven encouraging the amount of regeneration with each treatment is relatively small, displaying only a few regenerating axons accompanying modest improvements in function. This has engendered combinatorial approaches in recent years which have attempted to gain an additive effect by applying multiple treatments (Fouad et al., 2005). Although this remains an important avenue of research no significant breakthrough has been made to date.

One of the reasons for the interest into neuroprotective and regenerative therapies is the fact that the spinal circuitry below a lesion is largely intact following SCI. The neural networks in the lumbar enlargement are understood to be responsible for generating the walking gait in animals and the same likely holds true for humans (Duysens and Van de Crommert, 1998; Dietz, 2003; Fouad and Pearson, 2004). These networks, commonly referred to as central pattern generators (CPG), generate rhythmic motor patterns in flexors and extensors. Half-center and unit burst generator models of the CPG have been proposed and are useful in predicting and investigating some aspects of locomotion, however, they do

not entirely represent the more complicated networks found in mammalian quadrupeds and bipeds (Grillner, 2003). There is some controversy as to whether humans make use of CPGs or whether the generation of locomotion relies heavily upon descending control. The fact that rhythmic stepping can be generated in humans using electrical stimulation of the spinal cord surface suggests that CPGs do exist and that they can be activated following SCI (Dimitrijevic et al., 1998). It is also possible that stimulation at the surface of the spinal cord may activate afferent pathways which have been proposed to play a large role in the generation of rhythmic locomotion (Edgerton et al., 2006). Although the relative contributions of afferent inputs or putative CPG networks are currently unknown, the protection or regeneration of descending inputs to the lumbar enlargement may restore a significant degree of motor function following SCI.

1.3.3 Locomotor training

Although regenerative therapies hold promise in restoring connection to the lumbar enlargement, other techniques have focused upon activating this circuitry using bodyweight supported treadmill locomotor training (TLT). This technique is originally based on the observations of cats trained to step after spinal cord transection (Lovely et al., 1986; Barbeau and Rossignol, 1987). TLT consists of partially supporting the subject above a treadmill with manual assistance from therapists who move the legs through a walking stride. Over time the amount of support from a

harness is reduced and the subject is able to support more of their own weight (Harkema, 2001). Data from animal work have suggested that a decrease in the inhibition of spinal networks might be responsible for the activity-dependent plasticity observed in this training paradigm (de Leon et al., 1999; Tillakaratne et al., 2002). This evidence supports the view that a CPG can be activated following SCI and that the neural networks that make up this CPG are susceptible to activity-induced plasticity (Edgerton et al., 2004). Many researchers are now attempting to combine TLT with other therapies such as electrical stimulation with the hope of maximizing neurological recovery and function (Barbeau et al., 2002).

1.4 Functional electrical stimulation

Functional electrical stimulation can be defined as the use of electrical current pulses to activate neural tissue in order to restore a functional ability. This can refer to the restoration of either sensory or motor function. Electrical stimulation takes advantage of the irritability of neural tissue by reactivating the flow of neural excitation found in intact neural systems. Classically this has meant the activation of lower motoneurons in order to reanimate paralyzed or paretic muscle in a precise sequence and magnitude. More recently the excitation of central nervous tissue has been proposed to restore auditory and even visual sensation (McCreery, 2008; Normann et al., 2009). Although skeletal muscle tissue is also electrically irritable, the current required is dramatically higher than that required to activate neural tissue, leading most researchers and clinicians to target

neural tissue for excitation. A number of recent reviews have summarized the technologies available in this emerging field (Peckham and Knutson, 2005; Mushahwar et al., 2007; Sheffler and Chae, 2007; Hamid and Hayek, 2008; Ragnarsson, 2008). The current discussion is focused on reviewing the use of FES for the restoration of motor function after a neural lesion or disease such as spinal cord injury.

1.4.1 Activity benefits of FES

There are a number of FES-type systems in various stages of development with the ultimate goal of reanimating paralyzed skeletal muscles. Although these systems address the problem of paralysis in differing ways there are some generalized physiological benefits of FES devices that accrue from the reactivation of immobilized muscle. In general these benefits are similar to those seen in intact but sedentary populations when an increase in exercise and general activity is undertaken. FES exercise has been shown to increase peak oxygen consumption, a key indicator of cardiorespiratory fitness, following rowing, cycling and cycling/arm-crank exercise (reviewed in Hettinga and Andrews, 2008). In addition to targeted exercise programs, the regular use of an FES device to assist walking improves cardiovascular fitness and muscle bulk (Jacobs et al., 1997; Nash et al., 1997). Further work has demonstrated improvements in work capacity, lipid profile and insulin sensitivity following high-intensity voluntary exercise in people with SCI (de Groot et al., 2003). It appears that the physiological capacity to adapt to increased activity in those with SCI ap-

pears to be qualitatively similar to those seen in intact sedentary populations. In fact, the improvements in tetraplegic patients with the greatest degree of paralysis have been extremely encouraging, most likely because these individuals enter any exercise program with extremely low levels of metabolic, muscle and cardiorespiratory fitness and can, therefore, expect the greatest improvements (Haisma et al., 2006; Hettinga and Andrews, 2008).

1.4.2 Fundamentals of electrical excitation of tissue

In order to excite a nerve fiber the applied electrical current must be sufficient in amplitude and duration to produce a depolarization in voltage across the cell membrane. This depolarization must be sufficient to bring the cell to threshold for excitation and produces a self-propagating action potential. Given an infinite pulse duration (practically speaking anything longer than 10 ms) the minimum electrical current that will produce an action potential is termed the rheobase current (Millar and Barnett, 1997). At a current level twice the rheobase, the pulse duration required to excite neural tissue is termed the chronaxie. These two factors, rheobase and chronaxie, are used to characterize the extent of a tissue's irritability. For instance, the rheobase and chronaxie of neural tissues are considerably less than those of muscle tissue. As already mentioned, this makes the muscle an impractical place to apply FES.

Current pulses are delivered in mono or biphasic configurations. Although monophasic waveforms can be used to excite tissue they are apt

to involve the electrolysis of elements in the tissues surrounding the anode and cathode. This leads to the production of free oxygen radicals and acid at the anode and the reduction of oxygen and alkali at the cathode. This is especially true if large amplitudes or repetitive trains of stimuli are delivered. These reactions also erode the electrode surface and further perturb pO_2 and pH near the electrode causing tissue damage (Mortimer, 1981). In order to avoid electrolytic reactions biphasic waveforms can be used. These are usually balanced in terms of the total charge delivered during each phase (charge balanced) thus depositing no net current and lessening the possibility of damaging reaction products. If stimulus amplitude is high enough it remains possible to produce irreversible electrolytic reactions with biphasic stimulation but the chance of this is greatly reduced over monophasic waveforms (Mortimer, 1981).

The excitation threshold for a nerve axon is a function of pulse amplitude, pulse duration, distance to the electrode and diameter of the axon. If pulse amplitude, duration and distance are held constant, axons of the greatest diameter will reach threshold first. Essentially, given a uniform electrical field, the largest diameter axons in a nerve bundle have the lowest input resistance and will, therefore, receive the greatest current flow across the cell membrane. As a result, the greatest drop in voltage across the cell membrane will occur in axons of the largest diameter. These axons will reach threshold first and recruit the motor units which they innervate. This is termed “reversed recruitment order” as it is the reverse of the

physiologically normal condition where the smallest motoneurons are activated first due to the generation of larger excitatory post-synaptic potentials in small cells with higher input resistance (Kernell, 1966). Physiologically ordered recruitment according to size is also known as Henneman's size principle which states that motor units will be recruited in order from smallest to largest (Henneman, 1957; Henneman et al., 1965).

Reversed recruitment order is a challenge for most FES systems as they all involve the flow of current across the membranes of axons of varying diameter (Popovic, 2004). At the muscle, the reversed recruitment order results in the preferential recruitment of the largest motor units which are innervated by the most-easily recruited, large diameter axons (Totosy de Zepetnek et al., 1992). These motor units are exclusively made up of fast-twitch, fatiguable muscle fibers. Thus any muscle action comprising larger motor units will be extremely powerful and suffer from a rapid decline in sustained force. This is unsuitable for movements requiring grace or fine motor control, or those which need to be maintained for long periods such as standing or walking.

1.4.3 Transcutaneous stimulation

Perhaps the most common clinical application of FES has been at the skin via the application of large, flexible electrodes adhered to the surface. These electrodes are positioned over the motor point and can excite motoneurons transcutaneously. The clinical requirements for surface electrodes are summarized by Popovic as: low impedance, flexibility to main-

tain skin contact, easy donning and doffing and producing little skin irritation in order to be worn chronically (Popovic, 2004). Surface stimulation has the advantage of being applied easily and non-invasively. Electrodes are inexpensive, relatively simple and may be donned/doffed and adjusted by the user. However, muscle selectivity suffers as it is difficult to recruit smaller muscles and deeper muscles without first activating superficial muscles (Peckham and Knutson, 2005). Compounding the muscle selectivity problem is the fact that surface electrodes can shift during contractions with respect to the motor point. This may result in variable responses in muscle selection and force. Furthermore, the preferential activation of large diameter nerve fibers produces a very sharp force recruitment profile. This is the classic reversed recruitment order mentioned above which limits the ability to select stable submaximal forces and produces a variable and highly fatiguable muscle response.

1.4.4 Implanted devices

In an attempt to overcome some of the limitations of surface stimulation researchers have proposed the use of implanted FES devices. Although implantation is a necessarily invasive procedure, implanted devices generally offer better selectivity, lower current requirements and more stable responses. The electrodes of devices implanted into the peripheral nervous system fall into two general categories: those secured to the muscle, targeting the motor point; and those secured to the nerve targeting motoneurons in the nerve bundle. Although these devices are implanted in

different areas, both types excite the motoneuron axons somewhere between their exit from the spinal column at the ventral roots and their termination at the muscle motor point.

Electrodes secured at the motor point are termed intramuscular or epimysial electrodes. Intramuscular or epimysial electrodes produce a high degree of selectivity by placing the electrode in or close to the muscle, below the level of motor nerve arborization (Mortimer, 1981). Thus the motoneurons excited by stimulation are bound to be a selective population that innervate only one muscle or one portion of a muscle. This selectivity also allows intramuscular electrodes to produce a mixed recruitment order (Singh et al., 2000) if they are located near a motor point innervated with a high proportion of small diameter axons. However, these stimulation paradigms require multiple implants in order to recruit large portions of the muscle or multiple muscles. In addition, they are placed in highly mobile muscle tissues leading to increased lead breakage and an increased possibility for the electrode to shift position or even be forced to the surface. In one report, intramuscular electrodes suffered a 20% failure rate after one year with one third of these failures due to structural failure such as lead breakage while the remaining two thirds were due to physiological responses such as excess encapsulation and/or physical displacement (Popovic, 2004).

Nerve cuff electrodes wrap around the nerve and can be implanted in relatively immobile areas. These, and other electrodes target the peripheral nerve have the capability to recruit large amounts of muscle and produce high force. However, they sometimes lack the ability to selectively recruit individual muscles or motor units if they are implanted on large nerve trunks such as the sciatic nerve. Muscle selectivity with nerve cuff FES can be improved with multiple implants on smaller branches of the main nerve trunks, however, this requires greater surgical intervention and a more sophisticated control system.

Although the recruitment properties of peripherally implanted neural electrodes appear somewhat disappointing at first, recent improvements in electrode design have, to some degree, ameliorated these disadvantages. Peripheral neural implants that lie in (intraneural), on (epineural) or around (perineural) the nerve can benefit from designs which employ multiple electrode contact points to improve the selectivity of nerve fibers. For instance, Yoshida and Horch have employed intrafascicular electrodes sown into the nerve in pairs to individually activate nerve fascicles (Yoshida and Horch, 1993a). Normann and colleagues have published recent reports highlighting the effectiveness of a penetrating intrafascicular electrode array in producing multijoint movements such as standing after spinal cord injury (Normann, 2007). They have employed multielectrode arrays implanted into peripheral nerves able to penetrate individual fascicles. The lengths of electrode shafts vary from 1.5 mm to 0.5 mm so

that the electrode tips are at varying depths, targeting individual axons or small groups of axons with each electrode tip. Using this system they have reported the ability to activate individual muscles or agonist muscle groups selectively and the ability to recruit force more gradually than with conventional nerve cuffs (Branner et al., 2001).

A conceptually similar strategy has been employed by other groups using perineural implants. Increasing the number of electrode contact points can improve the selectivity and force recruitment properties of nerve cuff electrodes (Veraart et al., 1993; Grill and Mortimer, 1996). Others have employed nerve cuffs with multiple electrode contacts after reshaping the geometry of peripheral nerves in order to expose a greater number of axons (Tyler and Durand, 2002). The reshaped geometry forces axons buried within the centre of the nerve bundle to the surface, and improves muscle selectivity while maintaining the ability to recruit large amounts of muscle.

Any FES system with the ability to select independent populations of motor units innervating the target muscle can deploy interleaved stimulation strategies which produce smooth, fatigue-resistant force (Yoshida and Horch, 1993b; McDonnall et al., 2004a; McDonnall et al., 2004b). Interleaving involves the presentation of stimulus pulses from multiple electrodes at evenly spaced intervals. For example, if two electrodes were used the pulses from the second electrode would be introduced midway be-

tween pulses from the first electrode. As a result, two electrodes stimulating at 20 pulses per second (pps) would produce an aggregate 40 twitches of the muscle per second. In many muscles this would summate to produce a fused tetanus even though the pulse rate from a single electrode would not. Implantation into multiple sites on the sciatic and femoral nerves has allowed sufficient control of the hip, knee and ankle to produce a standing synergy (Mushahwar et al., 2007). The success of this system lies in its ability to expose motor axons to numerous electrode sites and thus improve the selectivity of neural excitation.

1.5 Intraspinal microstimulation

Although the implantation of electrodes into the peripheral nervous system has received more attention, it has been known for many years that central nervous tissue can be excited in a similar manner (Penfield and Rasmussen, 1950). Stimulation in the CNS is fundamentally similar to that in the PNS. The flow of electrical current can depolarize membranes and establish self-propagating action potentials. However, the CNS contains a more complicated arrangement of projections and cell bodies from different neurons lying in close proximity to one another. It is understood that the excitability of large, myelinated axons is greater than that of cell bodies (Ranck, 1975; Tehovnik, 1996; Nowak and Bullier, 1998), however, given the decay of the stimulus pulse the selection of neurites or cell bodies will be determined by the interaction between their latent excitability and their distance to the current source. As a result, there exists both the possibility

of direct excitation of cell bodies if the current source is close and transsynaptic excitation if the source is farther away (Gustafsson and Jankowska, 1976). The latter phenomenon illustrates how a larger network of neurons can be activated in the CNS.

Stimulation of the spinal cord surface has been applied for the treatment of intractable pain (Shealy et al., 1970) and spasticity (Dimitrijevic, 1998). The application of epidural stimulation at the lumbar enlargement has also produced rhythmic stepping movements in humans with complete SCI (Dimitrijevic et al., 1998) and in spinalized animals (Iwahara et al., 1992; Gerasimenko et al., 2003). In combination with TLT, epidural stimulation generated an immediate improvement in walking gait and an increase in speed (Herman et al., 2002). The ability of epidural stimulation to produce complex movements such as stepping has been attributed to the activation of a larger network of neurons, although the exact mechanism remains uncertain (Edgerton et al., 2006). A proposed explanation is that the activation of afferent projections in a tonic manner can organize motoneuron pools and may be interpreted as a descending command to initiate the movement program (Minassian et al., 2004). However this result is achieved, it is an example of how stimulation in a discrete area of the CNS can spread due to the activation of a larger network.

Perhaps the most common clinical application of central nervous system stimulation has been the implantation of electrodes targeting the subthalamic nucleus in order to reduce tremor, dyskinesia, akinesia and rigidity in those with Parkinson's disease (Benabid et al., 2009). Deep brain stimulation (DBS) procedures have been performed in tens of thousands of patients worldwide despite both the invasive nature of the procedure and an incomplete understanding of the treatment's mechanism of action (Birdno and Grill, 2008). Unfortunately, despite the promising results of DBS a number of physical and cognitive side-effects occur commonly as a result of stimulation (Benabid et al., 2009). These complications can occur even when electrodes are placed accurately and at voltage levels required to achieve the positive benefits of treatment. This is likely due to the fact that DBS stimulation is known to activate a larger network of fibers in passage (Dostrovsky and Lozano, 2002). The activation of a larger network of fibers creates uncertainty as to what downstream elements are being excited. This illustrates the opportunity and the challenge of CNS stimulation. The ability to tap into the extant network of circuitry below a transmission blockage such as a lesion to the auditory nerve, optic nerve or corticospinal tract also comes with the possibility of activating undesired elements that could produce deleterious side-effects.

1.5.1 Intraspinal microstimulation

In a manner conceptually similar to DBS, a number of research groups have attempted to stimulate neurons in the spinal cord. Termed

intraspinal microstimulation (ISMS), this novel FES method uses penetrating microelectrodes with exposed tips inserted into the spinal cord to reactivate networks below a spinal cord lesion. Attempts have been made to reestablish functional voiding of the bladder (Grill et al., 1999; McCreery et al., 2004), penile erection (Tai et al., 1998) and reanimation of paralyzed muscle (Tai et al., 1999). As with other forms of central stimulation both axons and cell bodies can be excited depending upon the latent excitability of the tissue and the proximity to the microwire tip. To produce movement of the lower limbs, implants can be targeted at the lumbar enlargement which is ideally suited for implantation as it contains all of the motoneurons that innervate the lower limbs as well as the networks responsible for generating locomotion (Jankowska, 1992; Dietz, 2003). Other advantages include the fact that spinal cord tissue is relatively immobile and the vertebral column provides a degree of protection for the implant. As with DBS, the procedure is necessarily invasive yet with the appropriate caution ISMS implants have proven to be mechanically stable, to cause only limited damage and to produce consistent responses over periods of up to 6 months in cats (Prochazka et al., 2001).

1.5.2 Recruitment properties

The thresholds for activation of muscle (motor threshold) with ISMS are considerably lower than those for other methods of electrical stimulation (Mushahwar et al., 2000). This corresponds to previous work showing that spinal cord tissue can be excited at stimulus amplitudes be-

low 5 μA (Jankowska and Roberts, 1972). Average threshold amplitudes for ISMS in an acute implant have been reported at 32 ± 2.4 μA (Guevremont et al., 2006), at a pulse duration of 200 μs. ISMS motor thresholds from chronically implanted microwires ranged from 15 - 30 μA at first but subsequently rose to near double those levels over the first month following implantation, remaining stable thereafter (Mushahwar et al., 2000). Presumably this doubling in motor threshold is related to the aforementioned encapsulation of implanted FES electrodes. The low levels of current needed to excite CNS tissue and to reach motor threshold have implications for the development of implantable neuroprosthetic devices with respect to battery life and size (Ragnarsson, 2008). In addition, stimulation at lower amplitudes maintains a buffer between the charge needed to excite neuronal networks and the level of charge where unsafe, irreversible reactions may occur (Mortimer, 1981).

Previous work with ISMS has demonstrated that increases in stimulus strength result in gradual increases in force. Force recruitment curves generated from cat quadriceps, tibialis anterior and triceps surae/plantaris demonstrated a graded force response to increasing stimulus amplitude (Mushahwar and Horch, 2000a). This result is in contrast to the typically rapid recruitment of force by conventional peripheral nerve stimulation whereby maximal force is recruited with small increases in stimulus amplitude, indicating reversed recruitment order (Singh et al., 2000). In a direct comparison of force recruitment, the average slope of the force re-

cruitment curves from cat quadriceps muscle was found to be 2.9 times shallower with ISMS than with a bipolar nerve cuff (Snow et al., 2006). In addition to producing graded force, simple tonic ISMS can maintain an evoked motor task for extended periods with relatively little decay of force (Tai et al., 1999). This property can be greatly enhanced by implanting multiple microwires and employing interleaved stimulation (Mushahwar and Horch, 1997). Using interleaved ISMS in combination with a close-loop control system has produced prolonged, weight-bearing standing in cats lasting up to 32 minutes (Lau et al., 2007). The use of interleaved stimulation improves fatigue resistance by exciting individual motoneurons at frequencies closer to their natural firing rate, while still producing a fused tetanic contraction at the muscle (Mushahwar et al., 2007). In contrast, motor unit fatigue can be encouraged by driving the excitation of motor units with synchronous, tonic stimulation (Prochazka, 1993). Although ISMS recruits graded, fatigue-resistant force, most reports also indicate that ISMS through a single microwire is unable to produce the maximal force that can be achieved with peripheral nerve stimulation. This suggests that not all motor units can be recruited by single ISMS microwires within the limits of safe stimulation (Mushahwar and Horch, 1998).

These two properties of ISMS, gradual force recruitment and fatigue resistance suggest that motor units are being recruited in a manner resembling the physiologically normal recruitment of motor units by size

(i.e. mixed or near-normal recruitment). This is supported by the fact that the duration of muscle twitches was found to decrease with increasing stimulus strength, indicating the recruitment of slow and then fast-twitch motor units as stimulus strength increased (Mushahwar and Horch, 2000a). This points to the transsynaptic, indirect activation of motoneurons through the excitation of fibers in passage, a phenomenon that has been demonstrated during stimulation of the spinal cord (Jankowska and Roberts, 1972; Gustafsson and Jankowska, 1976; Gaunt et al., 2006). Although the ventral grey matter contains the motoneuron pools it also contains a rich network of axonal processes from a variety of interneurons, propriospinal neurons and afferent projections. As an example, the connectivity of Ia afferents can be considered. Each Ia afferent branches to synapse with every motoneuron in the homonymous motoneuron pool and a large proportion of motoneurons in heteronymous pools that innervate synergistic muscles (Mendell and Henneman, 1971). This creates a dense web of Ia axons in the ventral horn which can be excited by external stimulation. The excitation of afferents or the activation of a reflex arc has been shown to recruit motoneurons in order from smallest to largest (Henneman and Mendell, 1981). In combination with some direct activation of motoneurons, especially at higher intensities of stimulus, this would explain why ISMS might produce a mixed or near-normal recruitment order and recruit graded, fatigue-resistant force.

The activation of a broader network of afferent projections, interneurons and propriospinal neurons with a microwire point-source of current has greater implications for motor control. ISMS has already demonstrated a high degree of muscle selectivity (Mushahwar and Horch, 2000b), but also the ability to recruit muscle synergies and even produce locomotion. ISMS produces whole limb synergies and fatigue-resistant standing and stepping in intact and spinalized cats (Mushahwar et al., 2000; Mushahwar et al., 2002; Saigal et al., 2004; Lau et al., 2007). The discrete nature of motoneuron pools and the distance between those which govern complex movements such as walking strongly suggest that the activation of synergies by stimulating through a few microwires is the result of exciting a network of neurons that connect motoneuron pools into functional groups. These networks are known to exist in the ventral horn, to establish connections between synergistic motoneuron pools and to process the reciprocal activation of agonist and antagonist muscles (Jankowska, 1992).

1.6 Dissertation summary and overview

Currently, ISMS is a promising experimental technique that bears further investigation. In order to move towards the clinical application of this technique a number of questions must be asked and modifications made based upon the answers. This dissertation addresses some of these remaining questions and attempts to shed light on the basic mechanisms

of the neuromuscular system that produce the responses observed during ISMS.

Although ISMS can produce gradual recruitment of force, a detailed understanding of this phenomenon has not been gained. A study was conducted (chapter 2) to observe directly the muscle fibers activated during acute ISMS as compared to those activated with a nerve cuff. I compared the force recruitment properties of these two stimulation paradigms and determined directly which muscle fibers were activated by each stimulation protocol. For each stimulation protocol I considered whether the activated muscle fibers were drawn proportionally from within the whole population or whether each protocol was selectively activating slow or fast muscle fibers, respectively.

Given these acute results I hypothesized that the chronic application of ISMS or nerve cuff stimulation would produce disparate muscular plasticity following spinal transection. I conducted a study (chapter 3) to examine the muscle transformations that would occur following spinal transection and subsequent daily stimulation for 30 days with either ISMS or the nerve cuff. I considered MHC-based fiber type as well as functional measurements of twitch-characteristics and fatigue resistance.

In addition to examining muscular plasticity following chronic ISMS, I conducted a final study (chapter 4) to examine the plastic adaptations and damage that might occur with microwire implantation and

chronic ISMS. I examined immunohistochemical markers of damage, inflammation and neuronal content in the spinal cord and compared these around stimulated and sham unstimulated microwires implanted in the spinal cord. I also considered whether neural plasticity following transection and chronic ISMS might have altered the force recruitment properties of ISMS.

A general discussion of these studies is provided in chapter 5 along with some recommendations for future work. An evaluation of the efficacy of ISMS with regards to recruiting stable, fatigue-resistant force is given and the safety of ISMS implantation is discussed. The goal of this dissertation is not just to provide practical understanding of the properties of ISMS but also to shed light on the basic neural structures which ISMS utilizes to produce muscle recruitment.

The work described in this dissertation is the culmination of years of effort using a challenging animal model. The first study brings novel data about muscle recruitment using peripheral and central means of electrical stimulation. In concert with other works into the nature of neuronal network activation by ISMS (Gaunt et al., 2006; Mushahwar et al., 2007) this provides us with a mechanistic picture of how peripheral and central means of stimulation produce force, and why ISMS so readily produces gradual, fatigue-resistant force. In addition, these results have been extended chronically in order to provide a significant contribution to our un-

derstanding of the phenotypic transformations of skeletal muscle in response to chronic electrical stimulation. Finally, our results provide critical indications that the spinal cord tolerates chronic ISMS well, even in the current example of extreme mismatch between the stiffness of the microwires and the size of the spinal cord. This work provides important encouragement to continue the investigation of ISMS and the advancement towards a clinically implantable device for the reanimation of skeletal muscle after spinal cord injury.

1.7 Bibliography

Andresen E, Barrington W, Cahill A, et al. (2006) One degree of separation: Paralysis and spinal cord injury in the United States. Paralysis consensus conference 1-28.

Bamford JA, Lopaschuk GD, MacLean IM, Reinhart ML, Dixon WT & Putman CT (2003). Effects of chronic AICAR administration on the metabolic and contractile phenotypes of rat slow- and fast-twitch skeletal muscles. *Can J Physiol Pharmacol* 81, 1072-1082.

Barbeau, H, Ladouceur, M, Mirbagheri, MM, Kearney, RE (2002) The effect of locomotor training combined with functional electrical stimulation in chronic spinal cord injured subjects: walking and reflex studies. Brain Res Brain Res Rev, 40:274–291.

Barbeau, H, Rossignol, S (1987) Recovery of locomotion after chronic spinalization in the adult cat. Brain Res, 412:84–95.

Bauman, WA, Adkins, RH, Spungen, AM, Kemp, BJ, Waters, RL (1998) The effect of residual neurological deficit on serum lipoproteins in individuals with chronic spinal cord injury. Spinal Cord, 36:13–17.

Bauman, WA, Kahn, NN, Grimm, DR, Spungen, AM (1999) Risk factors for atherogenesis and cardiovascular autonomic function in persons with spinal cord injury. Spinal Cord, 37:601–616.

Bauman, WA, Spungen, AM (1994) Disorders of carbohydrate and lipid metabolism in veterans with paraplegia or quadriplegia: a model of premature aging. Metabolism, 43:749–756.

Benabid, AL, Chabardes, S, Mitrofanis, J, Pollak, P (2009) Deep brain stimulation of the subthalamic nucleus for the treatment of Parkinson's disease. Lancet Neurol, 8:67–81.

Bethea, JR (2000) Spinal cord injury-induced inflammation: a dual-edged sword. Prog Brain Res, 128:33–42.

Birdno, MJ, Grill, WM (2008) Mechanisms of deep brain stimulation in movement disorders as revealed by changes in stimulus frequency. Neurotherapeutics, 5:14–25.

Bradbury, EJ, Moon, LD, Popat, RJ, King, VR, Bennett, GS, Patel, PN, Fawcett, JW, McMahon, SB (2002) Chondroitinase ABC promotes functional recovery after spinal cord injury. Nature, 416:636–640.

Branner, A, Stein, RB, Normann, RA (2001) Selective stimulation of cat sciatic nerve using an array of varying-length microelectrodes. 85:1585–1594.

Bunge, RP, Puckett, WR, Becerra, JL, Marcillo, A, Quencer, RM (1993) Observations on the pathology of human spinal cord injury. A review and classification of 22 new cases with details from a case of chronic cord compression with extensive focal demyelination. Adv Neurol, 59:75–89.

Burnham, R, Martin, T, Stein, R, Bell, G, MacLean, I, Steadward, R (1997) Skeletal muscle fibre type transformation following spinal cord injury. Spinal Cord, 35:86–91.

Bush, TG, Puvanachandra, N, Horner, CH, Polito, A, Ostenfeld, T, Svendsen, CN, Mucke, L, Johnson, MH, Sofroniew, MV (1999) Leukocyte infiltration, neuronal degeneration, and neurite outgrowth after ablation of scar-forming, reactive astrocytes in adult transgenic mice. Neuron, 23:297–308.

Cheng, H, Cao, Y, Olson, L (1996) Spinal cord repair in adult paraplegic rats: partial restoration of hind limb function. Science, 273:510–513.

Choi, DW (1992) Excitotoxic cell death. J Neurobiol, 23:1261–1276.

Choo, AM, Liu, J, Lam, CK, Dvorak, M, Tetzlaff, W, Oxland, TR (2007) Contusion, dislocation, and distraction: primary hemorrhage and membrane permeability in distinct mechanisms of spinal cord injury. J Neurosurg Spine, 6:255–266.

Crowe, MJ, Bresnahan, JC, Shuman, SL, Masters, JN, Beattie, MS (1997) Apoptosis and delayed degeneration after spinal cord injury in rats and monkeys. Nat Med, 3:73–76.

David, S, Aguayo, AJ (1981) Axonal elongation into peripheral nervous system "bridges" after central nervous system injury in adult rats. Science, 214:931–933.

David, S, Lacroix, S (2003) Molecular approaches to spinal cord repair. Annu Rev Neurosci, 26:411–440.

de Groot, PC, Hjeltnes, N, Heijboer, AC, Stal, W, Birkeland, K (2003) Effect of training intensity on physical capacity, lipid profile and insulin sensitivity in early rehabilitation of spinal cord injured individuals. Spinal Cord, 41:673–679.

de Leon, RD, Tamaki, H, Hodgson, JA, Roy, RR, Edgerton, VR (1999) Hindlimb locomotor and postural training modulates glycinergic inhibition in the spinal cord of the adult spinal cat. J Neurophysiol, 82:359–369.

Demirel, G, Yilmaz, H, Paker, N, Onel, S (1998) Osteoporosis after spinal cord injury. Spinal Cord, 36:822–825.

Devillard, X, Rimaud, D, Roche, F, Calmels, P (2007) Effects of training programs for spinal cord injury. Ann Readapt Med Phys, 50:490–8, 480-9.

Dietz, V (2003) Spinal cord pattern generators for locomotion. Clin Neurophysiol, 114:1379–1389.

Dimitrijevic, MR (1998) Chronic spinal cord stimulation for spasticity. In: Textbook for stereotactic and functional surgery (Gildelber, PM, Tasker, RRM, eds), pp 1267–1274. New York: McGraw-Hill.

Dimitrijevic, MR, Gerasimenko, Y, Pinter, MM (1998) Evidence for a spinal central pattern generator in humans. Ann N Y Acad Sci, 860:360–376.

Dostrovsky, JO, Lozano, AM (2002) Mechanisms of deep brain stimulation. Mov Disord, 17 Suppl 3:S63–8.

Dumont, RJ, Okonkwo, DO, Verma, S, Hurlbert, RJ, Boulos, PT, Ellegala, DB, Dumont, AS (2001) Acute spinal cord injury, part I: pathophysiologic mechanisms. Clin Neuropharmacol, 24:254–264.

Duysens, J, Van de Crommert, HW (1998) Neural control of locomotion; The central pattern generator from cats to humans. Gait Posture, 7:131–141.

Edgerton, VR, Tillakaratne, NJ, Bigbee, AJ, De Leon, RD, Roy, RR (2004) Plasticity of the spinal neural circuitry after injury. 27:145–167.

Edgerton, VR, Kim, SJ, Ichiyama, RM, Gerasimenko, YP, Roy, RR (2006) Rehabilitative therapies after spinal cord injury. J Neurotrauma, 23:560–570.

Emery, E, Aldana, P, Bunge, MB, Puckett, W, Srinivasan, A, Keane, RW, Bethea, J, Levi, AD (1998) Apoptosis after traumatic human spinal cord injury. J Neurosurg, 89:911–920.

Fehlings, MG, Arvin, B (2009) The timing of surgery in patients with central spinal cord injury. J Neurosurg Spine, 10:1–2.

Fouad, K, Pearson, K (2004) Restoring walking after spinal cord injury. Prog Neurobiol, 73:107–126.

Fouad, K, Schnell, L, Bunge, MB, Schwab, ME, Liebscher, T, Pearse, DD (2005) Combining Schwann cell bridges and olfactory-ensheathing glia grafts with chondroitinase promotes locomotor recovery after complete transection of the spinal cord. J Neurosci, 25:1169–1178.

Gallo, M, Gordon, T, Tyreman, N, Shu, Y, Putman, CT (2004) Reliability of isolated isometric function measures in rat muscles composed of different fibre types. Exp Physiol, 89:583–592.

Gaunt, RA, Prochazka, A, Mushahwar, VK, Guevremont, L, Ellaway, PH (2006) Intraspinal Microstimulation Excites Multisegmental Sensory Afferents at Lower Stimulus Levels Than Local {alpha}-Motoneuron Responses. J Neurophysiol, 96:2995–3005.

Gerasimenko, YP, Avelev, VD, Nikitin, OA, Lavrov, IA (2003) Initiation of locomotor activity in spinal cats by epidural stimulation of the spinal cord. Neurosci Behav Physiol, 33:247–254.

Gerrits, HL, De Haan, A, Hopman, MT, Der Woude, LH, Jones, DA, Sargeant, AJ (1999) Contractile properties of the quadriceps muscle in individuals with spinal cord injury. Muscle Nerve, 22:1249–1256.

Giangregorio, L, McCartney, N (2006) Bone loss and muscle atrophy in spinal cord injury: epidemiology, fracture prediction, and rehabilitation strategies. J Spinal Cord Med, 29:489–500.

Grandpre T Li S & Strittmatter S (2002) Nogo-66 receptor antagonist peptide promotes axonal regeneration. Nature, 417:547-551.

Grill R Murai K Blesch A Gage F & Tuszynski M (1997) Cellular delivery of neurotrophin-3 promotes corticospinal axonal growth and partial functional recovery after spinal cord injury. J Neurosci, 17:5560-5572.

Grill, WM, Bhadra, N, Wang, B (1999) Bladder and urethral pressures evoked by microstimulation of the sacral spinal cord in cats. Brain Res, 836:19–30.

Grill, WMJ, Mortimer, JT (1996) Quantification of recruitment properties of multiple contact cuff electrodes. IEEE Trans Rehabil Eng, 4:49–62.

Grillner, S (2003) The motor infrastructure: from ion channels to neuronal networks. Nat Rev Neurosci, 4:573–586.

Guevremont, L, Renzi, CG, Norton, JA, Kowalczewski, J, Saigal, R, Mushahwar, VK (2006) Locomotor-related networks in the lumbosacral enlargement of the adult spinal cat: activation through intraspinal microstimulation. IEEE Trans Neural Syst Rehabil Eng, 14:266–272.

Guha, A, Tator, CH (1988) Acute cardiovascular effects of experimental spinal cord injury. J Trauma, 28:481–490.

Guha, A, Tator, CH, Rochon, J (1989) Spinal cord blood flow and systemic blood pressure after experimental spinal cord injury in rats. Stroke, 20:372–377.

Gustafsson, B, Jankowska, E (1976) Direct and indirect activation of nerve cells by electrical pulses applied extracellularly. J Physiol, 258:33–61.

Haisma, JA, van der Woude, LH, Stam, HJ, Bergen, MP, Sluis, TA, Bussmann, JB (2006) Physical capacity in wheelchair-dependent persons with a spinal cord injury: a critical review of the literature. Spinal Cord, 44:642–652.

Hamalainen, N, Pette, D (1997) Coordinated fast-to-slow transitions of myosin and SERCA isoforms in chronically stimulated muscles of euthyroid and hyperthyroid rabbits. J Muscle Res Cell Motil, 18:545–554.

Hamid, S, Hayek, R (2008) Role of electrical stimulation for rehabilitation and regeneration after spinal cord injury: an overview. Eur Spine J, 17:1256–1269.

Harkema, SJ (2001) Neural plasticity after human spinal cord injury: application of locomotor training to the rehabilitation of walking. Neuroscientist, 7:455–468.

Hasegawa, Y, Fujitani, M, Hata, K, Tohyama, M, Yamagishi, S, Yamashita, T (2004) Promotion of axon regeneration by myelin-associated glycoprotein and Nogo through divergent signals downstream of Gi/G. J Neurosci, 24:6826–6832.

Henneman, E (1957) Relation between size of neurons and their susceptibility to discharge. Science, 126:1345–1347.

Henneman, E, Mendell, LM (1981) Functional organization of motoneuron pool and its inputs. In: Vol II, Motor Control (Brooks, VD, ed), pp 423–507. Bethesda: American Physiological Society.

Henneman, E, Somjen, G, Carpenter, DO (1965) Excitability and inhibitability of motoneurons of different sizes. Journal of Neurophysiology, 28:599–620.

Herman, R, He, J, D'Luzansky, S, Willis, W, Dilli, S (2002) Spinal cord stimulation facilitates functional walking in a chronic, incomplete spinal cord injured. Spinal Cord, 40:65–68.

Hettinga, DM, Andrews, BJ (2008) Oxygen consumption during functional electrical stimulation-assisted exercise in persons with spinal cord injury: implications for fitness and health. Sports Med, 38:825–838.

Iwahara, T, Atsuta, Y, Garcia-Rill, E, Skinner, RD (1992) Spinal cord stimulation-induced locomotion in the adult cat. Brain Res Bull, 28:99–105.

Jacobs, PL, Nash, MS, Klose, KJ, Guest, RS, Needham-Shropshire, BM, Green, BA (1997) Evaluation of a training program for persons with SCI paraplegia using the Parastep 1 ambulation system: part 2. Effects on physiological responses to peak arm ergometry. Arch Phys Med Rehabil, 78:794–798.

Jankowska, E, Roberts, WJ (1972) An electrophysiological demonstration of the axonal projections of single spinal interneurones in the cat. J Physiol, 222:597–622.

Jankowska, E (1992) Interneuronal relay in spinal pathways from proprioceptors. Prog Neurobiol, 38:335–378.

Jiang, SD, Dai, LY, Jiang, LS (2006) Osteoporosis after spinal cord injury. Osteoporos Int, 17:180–192.

Kernell, D (1966) Input resistance, electrical excitability, and size of ventral horn cells in cat spinal cord. Science, 152:1637–1640.

Koyanagi, I, Tator, CH, Theriault, E (1993) Silicone rubber microangiography of acute spinal cord injury in the rat. Neurosurgery, 32:260–8; discussion 268.

Kwon, BK, Fisher, CG, Dvorak, MF, Tetzlaff, W (2005) Strategies to promote neural repair and regeneration after spinal cord injury. Spine, 30:S3–13.

Kwon, BK, Tetzlaff, W, Grauer, JN, Beiner, J, Vaccaro, AR (2004) Pathophysiology and pharmacologic treatment of acute spinal cord injury. Spine J, 4:451–464.

Lau, B, Guevremont, L, Mushahwar, VK (2007) Strategies for generating prolonged functional standing using intramuscular stimulation or intraspinal microstimulation. IEEE Trans Neural Syst Rehabil Eng, 15:273–285.

Lazarov-Spiegler, O, Rapalino, O, Agranov, G, Schwartz, M (1998) Restricted inflammatory reaction in the CNS: a key impediment to axonal regeneration? Mol Med Today, 4:337–342.

Lewen, A, Matz, P, Chan, PH (2000) Free radical pathways in CNS injury. J Neurotrauma, 17:871–890.

Lillioja, S, Young, AA, Culter, CL, Ivy, JL, Abbott, WG, Zawadzki, JK, Yki-Jarvinen, H, Christin, L, Secomb, TW, Bogardus, C (1987) Skeletal muscle capillary density and fiber type are possible determinants of in vivo insulin resistance in man. J Clin Invest, 80:415–424.

Liu, XZ, Xu, XM, Hu, R, Du, C, Zhang, SX, McDonald, JW, Dong, HX, Wu, YJ, Fan, GS, Jacquin, MF, Hsu, CY, Choi, DW (1997) Neuronal and glial apoptosis after traumatic spinal cord injury. J Neurosci, 17:5395–5406.

Lovely, RG, Gregor, RJ, Roy, RR, Edgerton, VR (1986) Effects of training on the recovery of full-weight-bearing stepping in the adult spinal cat. Exp Neurol, 92:421–435.

Lu J Feron F Mackay-Sim A & Waite P (2002) Olfactory ensheathing cells promote locomotor recovery after delayed transplantation into transected spinal cord. Brain, 125:14-21.

Maimoun, L, Fattal, C, Micallef, JP, Peruchon, E, Rabischong, P (2006) Bone loss in spinal cord-injured patients: from physiopathology to therapy. Spinal Cord, 44:203–210.

McCreery, D, Pikov, V, Lossinsky, A, Bullara, L, Agnew, W (2004) Arrays for chronic functional microstimulation of the lumbosacral spinal cord. IEEE Trans.Neural Syst.Rehabil.Eng, 12:195–207.

McCreery, DB (2008) Cochlear nucleus auditory prostheses. Hear Res, 242:64–73.

McDonnall, D, Clark, GA, Normann, RA (2004a) Interleaved, multisite electrical stimulation of cat sciatic nerve produces fatigue-resistant, ripple-free motor responses. IEEE Trans.Neural Syst.Rehabil.Eng, 12:208–215.

McDonnall, D, Clark, GA, Normann, RA (2004b) Selective motor unit recruitment via intrafascicular multielectrode stimulation. 82:599–609.

Mendell, LM, Henneman, E (1971) Terminals of single Ia fibers: location, density, and distribution within a pool of 300 homonymous motoneurons. J Neurophysiol, 34:171–187.

Millar, J, Barnett, TG (1997) The zeta pulse: a new stimulus waveform for use in electrical stimulation of the nervous system. J Neurosci Methods, 77:1–8.

Minassian, K, Jilge, B, Rattay, F, Pinter, MM, Binder, H, Gerstenbrand, F, Dimitrijevic, MR (2004) Stepping-like movements in humans with complete spinal cord injury induced by epidural stimulation of the lumbar cord: electromyographic study of compound muscle action potentials. 42:401–416.

Modlesky, CM, Slade, JM, Bickel, CS, Meyer, RA, Dudley, GA (2005) Deteriorated geometric structure and strength of the midfemur in men with complete spinal cord injury. Bone, 36:331–339.

Mortimer, JP (1981) Motor Prostheses. In: Vol II, Motor Control (Brooks, VD, ed), pp 155–187. Bethesda: American Physiological Society.

Mushahwar, VK, Collins, DF, Prochazka, A (2000) Spinal cord microstimulation generates functional limb movements in chronically implanted cats. Exp.Neurol, 163:422–429.

Mushahwar, VK, Gillard, DM, Gauthier, MJ, Prochazka, A (2002) Intraspinal micro stimulation generates locomotor-like and feedback-controlled movements. IEEE Trans.Neural Syst.Rehabil.Eng, 10:68–81.

Mushahwar, VK, Horch, KW (1997) Proposed specifications for a lumbar spinal cord electrode array for control of lower extremities in paraplegia. IEEE Trans.Rehabil.Eng, 5:237–243.

Mushahwar, VK, Horch, KW (1998) Selective activation and graded recruitment of functional muscle groups through spinal cord stimulation. 860:531–535.

Mushahwar, VK, Horch, KW (2000a) Muscle recruitment through electrical stimulation of the lumbo-sacral spinal cord. IEEE Trans.Rehabil.Eng, 8:22–29.

Mushahwar, VK, Horch, KW (2000b) Selective activation of muscle groups in the feline hindlimb through electrical microstimulation of the ventral lumbosacral spinal cord. IEEE Trans.Rehabil.Eng, 8:11–21.

Mushahwar, VK, Jacobs, PL, Normann, RA, Triolo, RJ, Kleitman, N (2007) New functional electrical stimulation approaches to standing and walking. J Neural Eng, 4:S181–97.

Nash, MS, Jacobs, PL, Montalvo, BM, Klose, KJ, Guest, RS, Needham-Shropshire, BM (1997) Evaluation of a training program for persons with SCI paraplegia using the Parastep 1 ambulation system: part 5. Lower extremity blood flow and hyperemic responses to occlusion are augmented by ambulation training. Arch Phys Med Rehabil, 78:808–814.

Nobunaga, AI, Go, BK, Karunas, RB (1999) Recent demographic and injury trends in people served by the Model Spinal Cord Injury Care Systems. Arch Phys Med Rehabil, 80:1372–1382.

Norenberg, MD, Smith, J, Marcillo, A (2004) The pathology of human spinal cord injury: defining the problems. J Neurotrauma, 21:429–440.

Normann, RA (2007) Technology insight: future neuroprosthetic therapies for disorders of the nervous system. Nat Clin Pract Neurol, 3:444–452.

Normann, RA, Greger, BA, House, P, Romero, SF, Pelayo, F, Fernandez, E (2009) Toward the development of a cortically based visual neuroprosthesis. J Neural Eng, 6:035001.

Nowak, LG, Bullier, J (1998) Axons, but not cell bodies, are activated by electrical stimulation in cortical gray matter. I. Evidence from chronaxie measurements. Exp Brain Res, 118:477–488.

Olle, MM, Pivarnik, JM, Klish, WJ, Morrow, JRJ (1993) Body composition of sedentary and physically active spinal cord injured individuals estimated from total body electrical conductivity. Arch Phys Med Rehabil, 74:706–710.

Peckham, PH, Knutson, JS (2005) Functional electrical stimulation for neuromuscular applications. Annu Rev Biomed Eng, 7:327–360.

Penfield, W, Rasmussen, T (1950) The cerebral cortex of man; a clinical study of localization of function. Macmillan: New York.

Popovic, DB (2004) Neural Prostheses for Movement Restoration. In: Biomedical Technology and Devices Handbook (Moore, J, Zouridakis, G, eds), pp 28–21. CRC Press LLC.

Prochazka, A (1993) Comparison of natural and artificial control of movement. Rehabilitation Engineering, IEEE Transactions on Rehabilitation Engineering, IEEE Transactions on, Rehabilitation Engineering, IEEE Transactions on:7–17.

Prochazka, A, Mushahwar, VK, McCreery, DB (2001) Neural prostheses. J.Physiol, 533:99–109.

Ragnarsson, KT (2008) Functional electrical stimulation after spinal cord injury: current use, therapeutic effects and future directions. Spinal Cord, 46:255–274.

Ramer, LM, Ramer, MS, Steeves, JD (2005) Setting the stage for functional repair of spinal cord injuries: a cast of thousands. Spinal Cord, 43:134–161.

Ramer, MS, Priestley, JV, McMahon, SB (2000) Functional regeneration of sensory axons into the adult spinal cord. Nature, 403:312–316.

Ranck, JBJ (1975) Which elements are excited in electrical stimulation of mammalian central nervous system: a review. Brain Res, 98:417–440.

Rosenberg, LJ, Wrathall, JR (2001) Time course studies on the effectiveness of tetrodotoxin in reducing consequences of spinal cord contusion. J Neurosci Res, 66:191–202.

Saigal, R, Renzi, C, Mushahwar, VK (2004) Intraspinal microstimulation generates functional movements after spinal-cord injury. IEEE Trans.Neural Syst.Rehabil.Eng, 12:430–440.

Schanne, FA, Kane, AB, Young, EE, Farber, JL (1979) Calcium dependence of toxic cell death: a final common pathway. Science, 206:700–702.

Schwab, JM, Brechtel, K, Mueller, C-A, Failli, V, Kaps, H-P, Tuli, SK, Schluesener, HJ (2006) Experimental strategies to promote spinal cord regeneration--an integrative perspective. Prog Neurobiol, 78:91–116.

Senter, HJ, Venes, JL (1979) Loss of autoregulation and posttraumatic ischemia following experimental spinal cord trauma. J Neurosurg, 50:198–206.

Shealy, CN, Mortimer, JT, Hagfors, NR (1970) Dorsal column electroanalgesia. J Neurosurg, 32:560–564.

Sheffler, LR, Chae, J (2007) Neuromuscular electrical stimulation in neurorehabilitation. Muscle Nerve, 35:562–590.

Shields, RK (2002) Muscular, skeletal, and neural adaptations following spinal cord injury. J Orthop Sports Phys Ther, 32:65–74.

Singh, K, Richmond, FJ, Loeb, GE (2000) Recruitment properties of intramuscular and nerve-trunk stimulating electrodes. IEEE Trans.Rehabil.Eng, 8:276–285.

Snow, S, Horch, KW, Mushahwar, VK (2006) Intraspinal microstimulation using cylindrical multielectrodes. IEEE Trans Biomed Eng, 53:311–319.

Spungen, AM, Wang, J, Pierson, RNJ, Bauman, WA (2000) Soft tissue body composition differences in monozygotic twins discordant for spinal cord injury. J Appl Physiol, 88:1310–1315.

Tai, C, Booth, AM, de Groat, WC, Roppolo, JR (1998) Penile erection produced by microstimulation of the sacral spinal cord of the cat. IEEE Trans Rehabil Eng, 6:374–381.

Tai, C, Booth, AM, Robinson, CJ, de Groat, WC, Roppolo, JR (1999) Isometric torque about the knee joint generated by microstimulation of the cat L6 spinal cord. IEEE Trans Rehabil Eng, 7:46–55.

Talmadge, RJ (2000) Myosin heavy chain isoform expression following reduced neuromuscular activity: potential regulatory mechanisms. Muscle Nerve, 23:661–679.

Talmadge, RJ, Roy, RR, Caiozzo, VJ, Edgerton, VR (2002) Mechanical properties of rat soleus after long-term spinal cord transection. J.Appl.Physiol, 93:1487–1497.

Talmadge, RJ, Roy, RR, Edgerton, VR (1999) Persistence of hybrid fibers in rat soleus after spinal cord transection. Anat Rec, 255:188–201.

Tator, CH (1992) Hemodynamic issues and vascular factors in acute experimental spinal cord injury. J Neurotrauma, 9:139–40; discussion 141.

Tator, CH (1995) Update on the pathophysiology and pathology of acute spinal cord injury. Brain Pathol, 5:407–413.

Tator, CH, Fehlings, MG (1991) Review of the secondary injury theory of acute spinal cord trauma with emphasis on vascular mechanisms. J Neurosurg, 75:15–26.

Tehovnik, EJ (1996) Electrical stimulation of neural tissue to evoke behavioral responses. J Neurosci Methods, 65:1–17.

Teng, YD, Wrathall, JR (1997) Local blockade of sodium channels by tetrodotoxin ameliorates tissue loss and long-term functional deficits resulting from experimental spinal cord injury. J Neurosci, 17:4359–4366.

Thuret, S, Moon, LDF, Gage, FH (2006) Therapeutic interventions after spinal cord injury. Nat Rev Neurosci, 7:628–643.

Tillakaratne, NJ, De Leon, RD, Hoang, TX, Roy, RR, Edgerton, VR, Tobin, AJ (2002) Use-dependent modulation of inhibitory capacity in the feline lumbar spinal cord. J Neurosci, 22:3130–3143.

Totosy de Zepetnek, JE, Zung, HV, Erdebil, S, Gordon, T (1992) Innervation ratio is an important determinant of force in normal and reinnervated rat tibialis anterior muscles. Journal of Neurophysiology, 67:1385–1403.

Tyler, DJ, Durand, DM (2002) Functionally selective peripheral nerve stimulation with a flat interface nerve electrode. IEEE Trans Neural Syst Rehabil Eng, 10:294–303.

Veraart, C, Grill, WM, Mortimer, JT (1993) Selective control of muscle activation with a multipolar nerve cuff electrode. IEEE Trans Biomed Eng, 40:640–653.

Wallace, MC, Tator, CH, Frazee, P (1986) Relationship between posttraumatic ischemia and hemorrhage in the injured rat spinal cord as shown by colloidal carbon angiography. Neurosurgery, 18:433–439.

Whiteneck, GG, Charlifue, SW, Frankel, HL, Fraser, MH, Gardner, BP, Gerhart, KA, Krishnan, KR, Menter, RR, Nuseibeh, I, Short, DJ, et, a (1992) Mortality, morbidity, and psychosocial outcomes of persons spinal cord injured more than 20 years ago. Paraplegia, 30:617–630.

Wilmet, E, Ismail, AA, Heilporn, A, Welraeds, D, Bergmann, P (1995) Longitudinal study of the bone mineral content and of soft tissue composition after spinal cord section. Paraplegia, 33:674–677.

Yoshida, K, Horch, K (1993a) Selective stimulation of peripheral nerve fibers using dual intrafascicular electrodes. IEEE Trans Biomed Eng, 40:492–494.

Yoshida, K, Horch, K (1993b) Reduced fatigue in electrically stimulated muscle using dual channel intrafascicular electrodes with interleaved stimulation. Ann Biomed Eng, 21:709–714.

Chapter 2

Intraspinal microstimulation preferentially recruits fatigue-resistant muscle fibres and generates gradual force in rat*

2.1 Introduction

Spinal cord injury (SCI) represents a devastating neurological impairment with potentially life-threatening implications. The quality of life for a person with SCI often centers on the challenges to bladder and bowel function, respiration, skin and muscle health, freedom of movement, and general independence. One of the associated difficulties following SCI is the dramatic muscle atrophy and slow-to-fast transformation of skeletal muscle downstream of the lesion (Burnham *et al.*, 1997;Castro *et al.*, 1999). These result in a muscle that is highly fatiguable and incapable of performing at workloads required for standing or stepping. Previous rehabilitative interventions for restoring stepping which have utilized functional neuromuscular stimulation (FNS) have been employed with some success (Stein *et al.*, 2002;Prochazka & Mushahwar, 2001). Unfortunately, these systems have inherent disadvantages. Because they employ peripheral electrodes tunneled subcutaneously for long distances, such as with epimysial and intramuscular forms of stimulation, they suffer from problems associated with electrode lead breakage (Popovic, 1992). In addition,

* A version of this chapter has been published. Bamford JA Putman CT & Mushahwar VK (2005) Intraspinal microstimulation preferentially recruits fatigue-resistant muscle fibres and generates gradual force in rat. *J Physiol***569**, 873-884.

the normal order of motor-unit recruitment is reversed so that the lowest currents recruit the fastest, most fatiguable units, which leads to inappropriate, excessive force recruitment and high fatiguability (Prochazka, 1993).

Recently, intraspinal microstimulation (ISMS) has been suggested for therapeutic restoration of stable stepping. This technique involves implanting microwires into the ventral horns of the lumbosacral spinal cord. Stimulation through implanted microwires has previously been effective in establishing coordinated single, and multi-joint movements in both intact (Mushahwar *et al.*, 2002) and spinalized (Saigal *et al.*, 2004) cats including consistent bilateral stepping. Furthermore, previous reports showed that ISMS produces graded force recruitment and activates muscles selectively (Mushahwar & Horch, 1998;Mushahwar & Horch, 2000b). Therefore, ISMS may avoid some of the difficulties associated with peripheral forms of FNS, including improper motor-unit recruitment pattern and electrode lead-breakage because the stimulus is applied through existing central nervous system structures and the electrodes are placed in comparatively non-mobile tissue.

The purpose of this study was to compare the muscle recruitment properties of peripheral FNS in the form of a nerve cuff electrode over the femoral nerve with ISMS through electrodes targeting the quadriceps motoneuron pool. Two sets of experiments were performed to study the prop-

erties of these stimulation paradigms. In the first experimental series, pulse frequency and amplitude were varied and a glycogen depletion method was used to determine which muscle fibres were activated by ISMS or by nerve cuff stimulation (NCS) protocols. In a second series of experiments, force recruitment data from quadriceps muscles were collected to analyze the functional properties of muscle under the direction of each stimulation protocol. Previous studies suggested that ISMS recruits motor units in a mixed order (Mushahwar & Horch, 2000a), however, this is the first study to compare directly the recruitment properties of ISMS and NCS at the muscle level.

The results of this study show that ISMS preferentially recruited fatigue-resistant (FR) fibres out of proportion to their corresponding myosin heavy chain (MHC) content in quadriceps muscles. Contrarily, NCS chiefly recruited fast-twitch fatigable fibres. The difference between the proportion of FR fibres activated by ISMS and NCS was significantly different at the stimulation condition most likely to be used in a clinical setting. Furthermore, the rate of force recruitment with ISMS was significantly more gradual than that with NCS. The results of this investigation further our understanding of muscle recruitment by ISMS and provide support for the efficacy of ISMS as a novel rehabilitative therapy.

2.2 Methods

2.2.1 Animal Treatment and Care

All animal procedures were carried out under the guidelines of the Canadian Council for Animal Care and approved by the University of Alberta Animal Welfare Committee. Female Sprague–Dawley rats were housed in pairs in a controlled environment with 50–55% humidity, at 20 °C, with alternating 12 h light: 12 h dark cycles and received food and water ad libitum. Animals were randomly assigned to experimental groups for either glycogen depletion or force recruitment experiments. For all surgical experiments animals were anaesthetised using 2.5% isofluorane delivered in gaseous form. Upon completion of the experiments all animals were immediately euthanised by cardiac excision whilst under anaesthesia. Fifty-four animals were used for this study with a mean mass of 349.6 ± 8.7 g (mean ± SEM).

2.2.2 Glycogen Depletion Experiments

Glycogen depletion was accomplished by stimulating one hindlimb while the contralateral hindlimb served as a sham control. For NCS experiments a bipolar nerve cuff with 1-2 mm inter-electrode separation was placed around the femoral nerve, further insulated from surrounding muscles with mineral oil and sutured securely closed. For ISMS experiments a laminectomy was performed at T12-T13 to expose spinal cord segments L3-L4. Following this, 30 μm diameter, Teflon-insulated microwires (stainless steel 304, California Fine Wire Company, Grover Beach, CA) were inserted 2-3 mm past the dura mater of the spinal cord.

Specifically, microwire tips exposed for 30-60 μm were inserted into the quadriceps motoneuron pool in the ventral grey matter. Mono-polar stimulation with the return electrode placed in the back musculature was used for all ISMS experiments. The ISMS target area has been mapped by Mushahwar *et al.* (Mushahwar & Horch, 1998;Mushahwar & Horch, 2000b) in cats and is thought to be maintained in other species such as rabbit and humans (Sharrard, 1955;Portal *et al.*, 1991;Romanes, 1964). Placement of microwires in the quadriceps motoneuron pool was confirmed with practice twitches and ultimately by the glycogen-depleted fibres themselves. A stimulator (STG1008, Multi-channel Systems Inc, Reutlingen, Germany) was used to deliver 400 μs, biphasic, cathodic-first, charge-balanced pulses through the electrodes at each frequency and amplitude. For both NCS and ISMS, stimulation consisted of five bouts of five-minute stimulation periods (1 s on, 1 s off) interspersed with two-minute rest periods between each bout. Since the duty cycle was 50%, total stimulation time was twelve and one half minutes. Stimulation procedures were designed to produce depletion of glycogen in the activated quadriceps muscle fibres. Our own preliminary experiments showed that glycogen depletion of slow-twitch fibres was undetectable for up to 1 hour of stimulation. Presumably, this is due to the increased propensity of slow-twitch fibers to rely upon oxidative metabolism, thereby sparing muscle glycogen stores. Similarly, Rafuse and Gordon found that slow-twitch motor units required as long as 3 hours of stimulation to produce fatigue and

glycogen depletion (Rafuse & Gordon, 1996). Previous reports demonstrated that glycogen depletion can be accelerated and enhanced with ischemia of the selected muscles (Hudlicka *et al.*, 1994;Totosy de Zepetnek *et al.*, 1992). Therefore, in the present experiments, ischemia was produced by placing sutures around the femoral artery of both stimulated and contralateral sham control hindlimbs. Muscles were made ischemic at the beginning of the stimulation period by tightening the sutures around the femoral arteries. Sham hindlimbs were made ischemic for the same duration. This procedure did not disrupt blood flow to the femoral nerve, which is supplied by the internal iliac artery.

Previous reports conducted ISMS at a range of amplitudes, including near-threshold levels (Saigal *et al.*, 2004;Mushahwar *et al.*, 2003). For near-threshold stimulation both NCS and ISMS protocols were carried out with the amplitude held at 1.2X threshold. Threshold was defined as the lowest stimulation amplitude that produced a visible twitch. In light of the possibility that interneuronal pathways are differentially activated according to stimulus frequency (Minassian et al., 2004;Jilge et al., 2004) we performed stimulation at 1, 20 or 50 s-1 to determine the effect of frequency on muscle fibre type recruitment by ISMS. NCS experiments were carried out with matching frequencies as a control. Each NCS and ISMS group at the 1.2X threshold condition contained 6 animals for a total of 36. High-amplitude stimulation was also performed at 3.0X threshold to determine the recruitment properties of ISMS and NCS at stimulation ampli-

tudes more likely to be used in clinical FNS applications. The stimulation frequency of 20 s^{-1} was chosen for these experiments because it represents a frequency that is similar to the maximum natural rate of motor unit firing in humans (Fuglevand & Johns, 2004;Taylor & Enoka, 2004). This stimulation rate has also been successfully used in the past for ISMS experiments from our group (Saigal *et al.*, 2004) and is likely to be the most clinically relevant frequency for ISMS therapy. Six animals were included in each of the 3.0X threshold groups (ISMS and NCS) for a total of 12.

Following stimulation, the *vastus lateralis* and *rectus femoris* muscles were quickly excised as a group from experimental and control legs and placed into ice-cold saline for 30 s with gentle stirring. *Rectus femoris* and *vastus lateralis* muscles were chosen because they represent a large portion of the quadriceps muscle mass and they contain mixed MHC isoform based fibre types which allowed for identification of the full spectrum of fibre types. Handling and separation of these muscles was performed on a metal platform embedded in ice. Once separated, muscles were placed in a slightly stretched position on aluminum foil and frozen in melting isopentane (-156 °C) cooled in liquid nitrogen. Muscles were stored at -80 °C until sectioned to a thickness of 10 μm.

To determine which fibres were activated by stimulation, frozen muscle cross-sections of the *rectus femoris* and *vastus lateralis* were stained for glycogen using the periodic acid-Schiff (PAS) reaction. Acti-

vated fibres were identified as those lacking glycogen, a technique commonly known as the glycogen depletion method (Kim *et al.*, 1995;Kugelberg & Edstrom, 1968). The absence of glycogen depletion in any of the contralateral sham control muscles confirmed that neither ischemia due to occlusion of the femoral artery nor the muscle collection procedure induced glycogen degradation.

2.2.3 Muscle Fibre type Analysis

Immunohistochemical detection of MHC isoforms was completed on frozen muscle sections according to Putman *et al.* (Putman *et al.*, 2001;Putman *et al.*, 2003). Monoclonal antibodies directed against adult MHC isoforms were harvested from hybridoma cell lines obtained from the American Type Culture Collection (Manassa, VA) (Schiaffino *et al.*, 1989) and applied at the following dilutions: anti-MHCI clone BA-D5 (MHCI, 1:400, culture supernatant); anti-MHCIIa clone SC-71 (MHCIIa, 1:100, culture supernatant); anti-MHCIIb clone BF-F3 (MHCIIb, 1:400, culture supernatant). Negative controls were run in parallel by substituting a non-specific IgG (mouse IgG, 1:2000, Santa Cruz Biotechnology, Inc., Santa Cruz, CA) or by omitting the primary antibody. Each MHC stain also served as a positive control for the others. This panel of monoclonal antibodies allowed direct identification of pure type-I, -IIA, and -IIB fibres, as well as associated hybrid fibre combinations. Pure type-IID/X fibres were identified as those fibres that remained unstained by this panel of antibodies.

Stained serial sections were digitally imaged at 40X magnification (Olympus IX70, Olympus Microscopes, Melville, NY) with an attached camera (Spot RT, Diagnostic Instruments, Sterling Heights, MI) and analyzed using the Image Pro Plus software suite (ver 4.5.0.27, Media Cybernetics, Silver Spring, MD). Fibres activated by stimulation were identified by the absence of glycogen staining (Kim *et al.*, 1995;Kugelberg & Edstrom, 1968). Image Pro Plus software was used to ensure that the identification procedure was carried out consistently. Briefly, an observer set the staining intensity threshold by which the software package identified depleted fibres. The computer then applied this threshold throughout the image, ensuring uniformity. This manner of identifying fibres cannot altogether remove subjectivity, however, it can ensure that the threshold set by the observer is always applied by the computer in an unbiased manner. Serial sections stained for the various adult MHC isoforms were used to classify stimulated fibres. Glycogen depletion results for *rectus femoris* and *vastus lateralis* muscles were combined and further grouped according to the fatigue-resistance of the fibre types. Type-I, -I/IIA and -IIA fibres were grouped into the fatigue-resistant category (FR) while type-IID/X and -IIB fibres were grouped into the fast fatiguable category (FF) (Pette & Vrbova, 1992;Pette & Staron, 1997).

2.2.4 Myosin Heavy Chain Electrophoresis

To determine whether glycogen depletion of each fibre type was proportional to its whole muscle content, MHCI, MHCIIa, MHCIId/x, and

MHCIIb isoform contents were quantified by SDS-PAGE in 8 *rectus femoris* and 8 *vastus lateralis* muscles (Bamford *et al.*, 2003). Previous reports have shown that electrophoretic quantification of MHC isoform content provides an accurate estimation of MHC isoform based fibre type content (Putman *et al.*, 2003;Hamalainen & Pette, 1996;Putman *et al.*, 2004). Briefly, muscles were homogenized in ice-cold buffer containing 100 mM $Na_4P_2O_7$ (pH 8.5), 5 mM EGTA, 5 mM $MgCl_2$, 0.3 M KCl, 10 mM DTT and 5 mg/ml of a protease inhibitor cocktail (Complete™, Roche Diagnostics Corporation, Indianapolis, IN). Samples were centrifuged at 4 °C, diluted 1:1 with glycerol and stored at –20 °C until analyzed. Total protein content of the extracts was analyzed using the Bio-Rad Protein Assay (Bio-Rad Laboratories, Hercules, CA) (Bowers-Komro *et al.*, 1989), diluted to 0.2 μg/μl in Laemmli-lysis buffer (Laemmli, 1970) and boiled for 10 minutes. Five μl of each extract were electrophoresed for 24 hours and 275 V at 12 °C on 7% polyacrylamide gels containing glycerol, under denaturing conditions. MHC isoforms were detected by silver staining (Oakley *et al.*, 1980) and evaluated with integrated densitometry using the Syngene GeneSnap and GeneTools software package (Chemigenius Gel Documentation System, Syngene, U.K.).

2.2.5 Force Recruitment Experiments

Isometric twitch force was measured during application of NCS or ISMS to generate recruitment curves for these two stimulation paradigms. Nerve cuffs were placed around the femoral nerve and a laminectomy was

performed to expose spinal cord segments L3-L4. The animal was fixed at the iliac crest and at the epicondyles of the femur with a stereotaxic array to prevent movement. The patellar tendon was dissected from its point of insertion and attached to a force transducer (Interface MB-5, Interface Inc, Scottsdale, AZ). Stimulation (single, 400 μs, biphasic, cathodic-first, charge-balanced pulses) proceeded with the nerve cuff over the femoral nerve or with intraspinal microwires inserted within the quadriceps motoneuron pool in the ventral spinal cord (Mushahwar & Horch, 2000a). Data were amplified 100-fold and captured at a sampling rate of 1000 s^{-1} using a data acquisition interface (Power 1401, Cambridge Electronic Design, Cambridge, England) with associated software (Signal ver 2.13, Cambridge Electronic Design). Stimulation amplitude was varied upwards from subthreshold levels in quasi-random order and the force of the evoked twitch was measured with rest periods of approximately 30 s between pulses to avoid potentiation between twitches. Isometric force was recorded from the same hindlimb using both NCS and ISMS methods to allow paired comparisons. In some cases multiple ISMS curves obtained by stimulating different locations in the same pool were gathered on the same hindlimb to compare against a single NCS curve. Recruitment curves were gathered from 6 animals providing 6 NCS and 7 ISMS curves.

To compare twitch forces evoked by NCS and ISMS, forces were normalized to the maximum twitch force obtained by the nerve cuff for each hindlimb and plotted against pulse amplitude (μA). Linear regression

was used to calculate slopes for the recruitment curves between threshold and 250 μA or between threshold and the onset of force plateau if this occurred before 250 μA.

2.2.6 Confirmation of Microwire Placement in ISMS Trials

Spinal cords from ISMS glycogen depletion and force recruitment experiments were excised following stimulation, placed in a slightly stretched position on aluminum foil and frozen in melting isopentane (-156 °C) cooled in liquid nitrogen. Cords were later sectioned to verify ISMS microwire placement. Typically, an electrolytic lesion is produced at the end of the experiment to aid in confirming the microwire location (Mushahwar & Horch, 1998). However, this procedure was not possible in this experiment because of the need to control muscle activation and fibre depletion in each condition. This made locating microwire tips more difficult. Thus, only 17 of 33 microwires were retrieved and their locations positively confirmed. The other 16 microwire locations were not confirmable, either because of inadvertent dislodging of the microwire during extraction and sectioning, or because of an inability to find the exact tip location without the presence of an electrolytic lesion. Nevertheless, stimulation through each of these microwires did produce gradual force recruitment following insertion. In our experience, this is a clear indication that the tips of these microwires were located correctly within the ventral grey matter (Saigal et al., 2004).

2.2.7 Statistical Analysis

The same statistical analysis was used for both glycogen depletion and force recruitment experiments. All analyses were performed with a computerized software statistics package (SPSS 11.0, SPSS Inc, Chicago, IL). Differences between group means were determined via independent samples *t*- test or one-way ANOVA with a Scheffe *post-hoc* test. All planned comparisons were undertaken with one-tailed analysis, whereas unplanned comparisons were analyzed using a two-tailed test. Differences were considered significant at $p < 0.05$. All results are presented as means ± SEM.

2.3 Results

2.3.1 Threshold Levels for ISMS were Significantly Lower than those for NCS

Following either the glycogen depletion or force recruitment experiments, spinal cords were extracted, frozen, and sectioned on a cryostat. The purpose of this procedure was to confirm that ISMS microwires were properly located within the ventral spinal cord. Figure 2-1 summarises, on a single cross-section, the tip locations for 17 of 33 intraspinal microwires used in this investigation. Mean stimulation threshold in the glycogen depletion experiments was 12.1 ± 1.0 μA and 25.0 ± 3.0 μA for ISMS and NCS, respectively, a highly significant difference ($p < 0.0002$). Differences in mean threshold generated during the force recruitment experiments were larger than for the glycogen depletion experiments. Mean

threshold was 7.7 ± 0.1 μA and 39.1 ± 5.7 μA for ISMS and NCS, respectively ($p < 0.0006$).

2.3.2 ISMS Caused Greater Depletion of Fatigue-Resistant Fibres at High Amplitudes of Stimulation

Glycogen depletion experiments were carried out in order to determine which fibres were activated by either NCS or ISMS under different stimulation conditions. Figure 2-2 shows an example of the method used to identify glycogen-depleted fibres in one ISMS animal and one NCS animal, both stimulated at 1 s^{-1} 1.2X threshold. Depleted fibres were identified by the PAS stain (figure 2-2A) and then characterized according to their MHC content in serial sections (type-I, -IIA, -IIB in figures 2-1B,C,D, respectively). In the example shown, ISMS primarily depleted type-I and -IIA fibres while NCS depleted type-IIB and -IID fibres. PAS staining of control muscles demonstrated that neither the ischemia, nor the extraction procedure produced detectable glycogen depletion (figure 2-2E). In the 1.2X threshold condition, the mean number of depleted fibres per animal was 176.6 ± 27.5 and 181.2 ± 44.6 for ISMS and NCS, respectively. In the 3.0X threshold condition, the mean number of fibres depleted per animal was 150.5 ± 49.5 and 1,215.7 ± 363.6 for ISMS and NCS, respectively. The sum of all fibres depleted and analyzed in this study was 14,637.

Figure 2-3 shows the cumulative proportion of each fibre type depleted in each stimulation condition from all animals. The total number of fibres depleted in the 1 s^{-1} 1.2X threshold, 20 s^{-1} 1.2X threshold, 50 s^{-1} 1.2X

threshold and 20 s^{-1} 3.0X threshold were 726, 1,481, 1,055 and 7,294, respectively, for NCS, and 1,249, 1,178, 751 and 1,188, respectively, for ISMS. NCS stimulation at 3.0X threshold depleted significantly more fibres than any other condition ($p < 0.004$). All other conditions were not significantly different in terms of total fibres depleted. The only condition that resulted in greater depletion of type I, I/IIA and IIA fibres by ISMS was 20 s^{-1} 3.0X threshold. Figure 2-4 shows the proportion of glycogen-depleted fibres that were FR type (type I + type I/IIA + type IIA) in each experimental group (n=6 animals per group). At 1.2X threshold, the proportion of FR fibres recruited by ISMS was 1.7- ($p < 0.23$), 2.8- ($p < 0.059$) and 0.67-fold ($p < 0.24$) that of NCS at 1, 20 and 50 s^{-1} frequencies, respectively. Although both 1 and 20 s^{-1} ISMS recruited proportionally more FR fibres than NCS, this trend did not reach statistical significance in either case. Specifically, in the 1.2X threshold conditions, some ISMS samples did not display depleted FR fibres, producing large variances in the data. (e.g. min 0.0% – max 97.8% in the 1 s^{-1} condition). In contrast, the 3.0X threshold condition produced consistent and highly significant increases ($p < 0.0001$) in the proportion of FR fibres recruited by ISMS over NCS. Only 0.4% of fibres recruited by 20 s^{-1} 3.0X threshold NCS were FR fibres, whereas 44.4% of the total fibres depleted by ISMS at 20 s^{-1} 3.0X threshold were FR.

2.3.4 Fibre Type Recruitment by ISMS and NCS in Mixed Fast-Twitch Muscle

Electrophoresis was performed to measure the MHC-isoform contents of activated muscles. This allowed us to determine whether the number of FR fibres activated by ISMS or NCS was proportional to their distribution within the *vastus lateralis* and *rectus femoris*, or if these fibres were selectively recruited. The MHC-isoform contents of the *vastus lateralis* and *rectus femoris* are shown in figure 2-5. There was no difference in MHCI content between *rectus femoris* and *vastus lateralis* ($p = 0.99$), however, the *rectus femoris* displayed significantly more MHCIIa ($p < 0.001$), MHCIId/x ($p < 0.003$), and less MHCIIb ($p < 0.003$). For the purposes of this study the MHC-isoform contents of the *rectus femoris* and *vastus lateralis* were grouped into FR and FF categories. FR MHC content was 22.8 ± 2.0% and 16.0 ± 1.4% in the *rectus femoris* and *vastus lateralis*, respectively ($p < 0.02$). These data were further summarized to compare with the grouped *rectus femoris* and *vastus lateralis* glycogen depletion results. Using these broad classifications, the proportion of FR and FF fibres were 19.4 ± 1.5% and 80.6 ± 1.5%, respectively. Comparison of the cumulative proportion of FR fibres depleted in each stimulation condition revealed that ISMS recruited FR fibres at 2.9-, 1.9-, 1.7- and 2.5-fold the FR MHC content at 1, 20 and 50 s^{-1} 1.2X threshold and 20 s^{-1} 3.0X threshold, respectively. In contrast, NCS recruited FR fibres at 1.2-, 1.0-, 2.1- and 0.0-times the FR MHC content at 1, 20 and 50 s^{-1} 1.2X threshold and 20 s^{-1} 3.0X threshold, respectively (figure 2-5C).

2.3.5 ISMS Recruited Force More Gradually than NCS

Force recruitment experiments were performed to compare the functional characteristics of ISMS and NCS with the results from the glycogen depletion experiments. Twitch recruitment curves obtained via intraspinal and nerve cuff stimulation from 0 to 250 μA are shown in figure 2-6. The mean slope of the recruitment curves for NCS was 0.020 ± 0.006 and was thus 4.9-fold steeper ($P < 0.02$) than the mean slope of recruitment curves for ISMS (0.0041 ± 0.0008).

A charge level of 90 nC has previously been identified as the maximum level for safe charge injection in central nervous system tissue (Agnew & McCreery, 1990). Since the pulse width for all stimulation experiments was 400 μs, the maximum safe charge of 90 nC corresponds to 225 μA. Mean peak twitch force at 225 μA was 1.56 ± 0.49 N and 0.34 ± 0.06 N for NCS and ISMS, respectively ($p < 0.03$). At 225 μA, ISMS through a single microwire recruited a mean of 36.8 ± 11.1% of twitch force recruited by NCS at the same charge level.

2.4 Discussion

2.4.1 Overview

The purpose of this study was to compare the muscle recruitment characteristics of NCS, a peripheral method of stimulation, with the novel rehabilitative therapy, ISMS. In the first set of experiments muscle fibres activated at three different frequencies and two different amplitudes by each stimulation paradigm were identified by the glycogen depletion

method and classified according to their corresponding MHC-based fibre types. In the second set of experiments, data were gathered from ISMS and NCS twitch force recruitment curves to assess force recruitment characteristics. During high-amplitude stimulation ISMS activated a significantly larger proportion of fatigue-resistant fibres than NCS. In accordance with this result we found that NCS twitch force recruitment was steeper than ISMS. ISMS through a single electrode produced a considerable amount of force with more gradual recruitment. Whole nerve stimulation through the nerve cuff required significantly more charge at threshold but produced higher forces at the same charge level. Other work from our laboratory has shown that ISMS likely recruits motoneurons through interneurons or afferent pathways (Mushahwar *et al.*, 2003). This would explain the more gradual recruitment of force and increased activation of fatigue-resistant muscle fibres by ISMS compared with NCS. This study corroborates and enhances previous evidence for the efficacy of ISMS and is the first work to compare directly the muscle recruitment properties of ISMS and NCS.

2.4.2 ISMS Causes Greater Depletion of Fatigue-Resistant Fibres at High Amplitudes of Stimulation

In this study, glycogen depletion was enhanced using ischemia. Our preliminary experiments, as well as the work of others (Rafuse & Gordon, 1996), showed that stimulation alone required up to 3 hours to produce detectable glycogen depletion in slow-twitch muscle fibres. Therefore,

ischemia was induced in the quadriceps muscles, but not in the femoral nerve, by occlusion of arterial flow through the femoral artery. PAS staining in control muscles showed that ischemia alone did not induce detectable glycogen depletion, thus proving the validity of this technique. Glycogen depletion via ISMS or NCS resulted in differences in the proportions of FR fibres depleted. In the 1.2X threshold condition these differences approached significance at 20 s^{-1} ($p < 0.059$) but not in the 1 or 50 s^{-1} conditions.

In all of the 1.2X threshold conditions, there were at least a few ISMS samples that did not deplete FR fibres. Although fibre recruitment resulting from low-amplitude stimulation may be especially sensitive to electrode placement, at 3.0X threshold, small differences in electrode placement are less likely to affect the outcome due to increased current spread. Indeed, the differences between ISMS and NCS at 3.0X threshold were particularly consistent, where the former recruited a significantly higher proportion of FR fibres (figure 2-3). It is interesting that the 3.0X threshold ISMS condition did not deplete a significantly larger number of fibres than other ISMS conditions. This suggests a limited spread of current as has been shown in the past (Mushahwar & Horch, 1997;Pikov & McCreery, 2004;Lemay & Grill, 2004;Snow *et al.*, 2005).

When comparing the proportion of FR fibres depleted by each condition it is illuminating to consider the contents of MHC-isoforms in *rec-*

tus femoris and *vastus lateralis* muscles. Electrophoretic analyses revealed that 19.4% of the total MHC content can be placed in the FR category. Thus, the cumulative proportion of FR fibres recruited by ISMS represents a 2.9-, 1.9-, 1.7- and 2.5-fold increase over the FR MHC content at 1, 20, and 50 s^{-1} 1.2X threshold and at 20 s^{-1} 3.0X threshold, respectively (figure 2-4). In contrast, NCS recruited FR fibres at 1.2-, 1.0-, 2.1- and 0.0-fold the FR MHC content at 1, 20 and 50 s^{-1} 1.2X threshold and at 20 s^{-1} 3.0X threshold, respectively. Although ISMS preferentially recruited FR fibres in the *rectus femoris* and *vastus lateralis*, only the 50 s^{-1} NCS 1.2X threshold condition did the same.

Surprisingly, the 50 s^{-1} condition not only recruited FR fibres out of proportion to their MHC isoform content, but 50 s^{-1} NCS depleted a larger proportion of FR fibres than the 50 s^{-1} ISMS condition (figures 2-3 and 2-4). The proportion of FR fibres depleted by ISMS did not decrease significantly compared with other frequencies. Instead, there was an increase in the number of FR fibres depleted by NCS at 50 s^{-1}. Other authors have used peripheral, low amplitude stimulation at 100 s^{-1} to produce contractions which may contain both peripheral and central components (Collins *et al.*, 2001;Collins *et al.*, 2002). These authors suggested that their results were due to motoneuron activation through Ia afferents and the generation of plateau potentials. Although the frequencies used in this study were not as high as the 100 s^{-1} used by Collins *et al.* (2001; 2002), it is possible that the higher proportion of FR fibres at the 50 s^{-1} 1.2X threshold NCS

condition is due to activation of Ia afferents. These afferents make physiologically normal connections to motoneurons and could recruit fibres in a near-normal order. Although our data suggest that it is possible for NCS-type systems at 50 s^{-1} to recruit FR fibres, they would likely still suffer from problems encountered by peripheral stimulation methods (Popovic, 1992). Furthermore, this result would only be present at lower stimulation amplitudes where low levels of force are produced. Indeed, our results suggest that at 3.0X threshold stimulation this effect is abolished due to the overriding influence of whole nerve stimulation through motor axons at higher amplitudes.

There is one report of surface stimulation recruiting fibres in a mixed manner (Thomas *et al.*, 2002), however, the results of this experiment are difficult to interpret (Enoka, 2002). It is likely that the authors showed neither normal recruitment nor truly random recruitment. Rather, it is more likely that the authors showed pseudorandom recruitment order due to the spread of current from the point-source surface electrode used in these experiments. Although the largest axons are characterized by their low recruitment thresholds (Henneman *et al.*, 1965), the spatial orientation of axons in the nerve trunk could result in a situation where the smallest axons receive current above threshold level while larger axons, located further away do not. This “depth effect” phenomenon could also explain the pseudorandom recruitment order reported by Singh et al. when using intramuscular BION™ electrodes (Singh *et al.*, 2000).

2.4.3 ISMS Recruits Force More Gradually than NCS

Similar to other work in our lab (Snow *et al.*, 2005) we found that the mean slope for ISMS force recruitment curves was 4.9-fold lower than for NCS. A range of force recruitment curves generated by ISMS has previously been reported for electrodes targeting feline quadriceps motoneuron pools (Mushahwar & Horch, 2000a) and intermediate grey matter (Aoyagi *et al.*, 2004). It has been proposed that differences in electrode placement within a motoneuron pool may activate different subsets of motoneurons targeting different compartments in skeletal muscle (English *et al.*, 1993;Lieber & Friden, 2000). The fibre type distribution of these compartments may vary, thus the force recruitment characteristics can change depending on microwire placement. This may point to another advantage of activating motoneurons in the ventral horn. Not only is it possible to activate muscles selectively with ISMS (Mushahwar & Horch, 2000b;Mushahwar & Horch, 1998;Mushahwar & Horch, 2000a), this selectivity may also extend to subsets of motoneuron pools comprised of different types of motor units. Thus, ISMS seems capable of activating the muscles in a more gradual manner, as required for postural support for extended periods, and in a steep manner as needed for standing from a chair. A multi-electrode array has been proposed for ISMS (Mushahwar & Horch, 1997;Snow *et al.*, 2005) and our results suggest that such a system could be used not just to activate individual muscles selectively but popu-

lations of fibre types within the muscle. This would represent a significant improvement over current forms of peripheral nerve stimulation.

Although NCS recruited higher forces, ISMS through a single microwire recruited mean force approaching 37% of that normalized to the nerve cuff at 225 μA. This result is surprising given that it was produced with only one electrode and a single pulse. Other authors have compared single pulses with 50 s^{-1} stimulation trains and concluded that tetanic force levels produced by single ISMS microwires can match those of whole nerve stimulation through peripheral nerve cuffs (Snow *et al.*, 2005). The use of higher frequencies, multiple electrodes and/or interleaved stimulation paradigms might allow ISMS to activate the muscle fully without producing damaging effects. This approach has already proven successful in creating consistent, fatigue-resistant weight-bearing stepping in spinalized animals (Saigal *et al.*, 2004).

2.4.4 Potential Mechanisms for ISMS Stimulation Results

At the 1.2X threshold condition the differences between NCS and ISMS did not reach significance. In fact the NCS and ISMS results from near-threshold stimulation were so similar that it is tempting to speculate that both stimulation procedures might have been acting through similar mechanisms. It has already been shown that ISMS activates afferent fibres before motoneurons (Mushahwar *et al.*, 2003) and may also activate interneurons contained within the ventral spinal cord. In the NCS condition,

Ia afferents were likely responsible for the twitch response at near-threshold conditions, otherwise known as the Hoffmann (H) reflex (Zehr, 2002). Ia afferents directly synapse on motoneurons, thus the resulting synaptic activation of motoneurons produces a normal or near-normal physiological recruitment order. Reversed recruitment order is commonly seen at higher amplitudes with peripheral methods such as NCS or surface stimulation (Levy *et al.*, 1990). As charge levels increase, ISMS is expected to activate more interneurons and afferents thereby recruiting force more gradually than NCS. In contrast, direct stimulation of motoneuron axons during NCS leads to rapid recruitment of fast-twitch motor units and abolition of the slow-twitch response at higher amplitudes. Neurophysiologically, this is confirmed by the increasing dominance of the muscle-wave response and disappearance of the H-reflex as stimulus amplitude increases beyond the maximal H-reflex response (Zehr, 2002). If stimulus amplitude is increased further, F-waves will be produced by NCS because of antidromic activation of motor axons in possible combination with the Ia afferent reflex arc (Mesrati & Vecchierini, 2004). In the present study, as stimulation amplitude increased, NCS reached peak twitch force quickly due to the preferential activation of FF fibres. In contrast, ISMS twitch force continued to rise gradually due to the delayed recruitment of large, fast-twitch fatiguable motor units. Our results with 3.0X threshold stimulation demonstrated that ISMS preferentially recruited FR fibres in *rectus femoris* and *vastus lateralis* muscle while NCS almost exclusively re-

cruited FF fibres (figure 2-3). Ultimately, the pattern of ISMS activation is similar to the physiologically normal activation of motor units in which the smallest, most fatigue-resistant motor units are activated first, holding the larger units in reserve for activities requiring large force or power (Henneman, 1957;Henneman *et al.*, 1965).

Previous work has provided insight into how muscle fibre type is specified over the long-term. Periods of tonic motoneuron activity promote a slow-fibre program while periods of inactivity interspersed with bursts of high frequency activity promote the fast-fibre program (Pette & Vrbova, 1992). Evidence for this position has been enhanced by the discovery of the calcineurin signaling pathway, which transduces this activity pattern signal into the nucleus and alters gene expression (Schiaffino & Serrano, 2002). In accordance with this theory there is a dramatic slow-to-fast transformation of muscle fibre type following SCI (Burnham *et al.*, 1997;Castro *et al.*, 1999). Due to the plastic nature of skeletal muscle (Pette & Staron, 1997), previous authors have performed chronic low-frequency stimulation through a peripheral FNS system to rehabilitate skeletal muscle following SCI. The ultimate goal of these interventions is the upregulation of FR fibre types and restoration of fatigue-resistance (Martin *et al.*, 1992;Andersen *et al.*, 1996).

Although fatigue-resistant movements are an important goal for FNS it is also important to ensure that the potential for high force produc-

tion in stimulated muscle is preserved over the long-term. The mixed fibre type content of intact quadriceps muscle (figure 2-5) represents the capacity of this muscle to undertake both fatigue-resistant and high-force movements. Thus, maintaining mixed muscle fibre types should remain the goal for FNS therapies following SCI. Unfortunately, long-term stimulation with peripheral forms of FNS entails the possibility of complete transformation of the muscle such that no fast fibres remain to produce high-force movements. Andersen *et al.* performed 30 minutes of stimulation through surface electrodes 3 times a week at 60 s^{-1} and approximately 3.25-7.25X threshold for up to 12 months in 5 male spinal cord injured subjects (Andersen *et al.*, 1996). Following stimulation, fibres expressing pure IID/X MHC (the fastest isoform expressed in humans) dropped from 37.2 ± 15.5% to 2.3 ± 1.4% of the total fibre content with concomitant increases in pure IIA fibre content from 21.2 ± 13.9% to 91.2 ± 2.8% (Andersen *et al.*, 1996). This dramatic transformation is to be expected from peripheral forms of stimulation, which entail a reversed recruitment order of motor unit firing. The fastest fibres, which undergo a phasic duty cycle in intact muscle, are also the first activated by peripheral systems, thus being highly susceptible to transformation. In contrast, ISMS through a single electrode allowed for fibre type selectivity and recruited a mixed fibre type at both 1.2X and 3.0X threshold conditions. The capacity of ISMS to recruit slow fibres while leaving fast fibres in reserve should aid in maintaining a mixed fibre type and should prove helpful in rescuing the normal

mixed-muscle phenotype in chronic SCI cases. Further studies with ISMS should be designed to address the capacity of this novel rehabilitative therapy to rescue the normal mixed-muscle phenotype in a chronic SCI model.

2.5 Figures

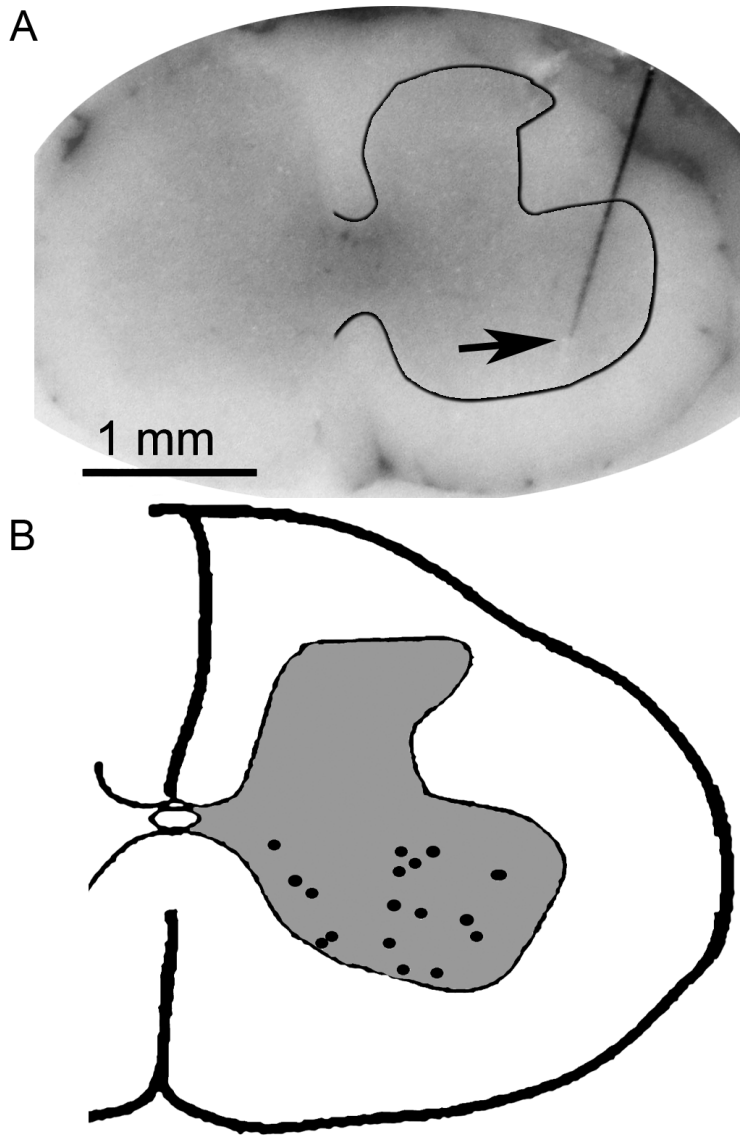

Figure 2-1: ISMS electrode locations.

Frozen spinal cords were sectioned on a cryostat and representative photomicrographs (A) were taken in order to verify electrode placement within the ventral grey matter. A composite schematic for electrode tip locations (B) was generated by plotting 17 ISMS electrodes used in this study.

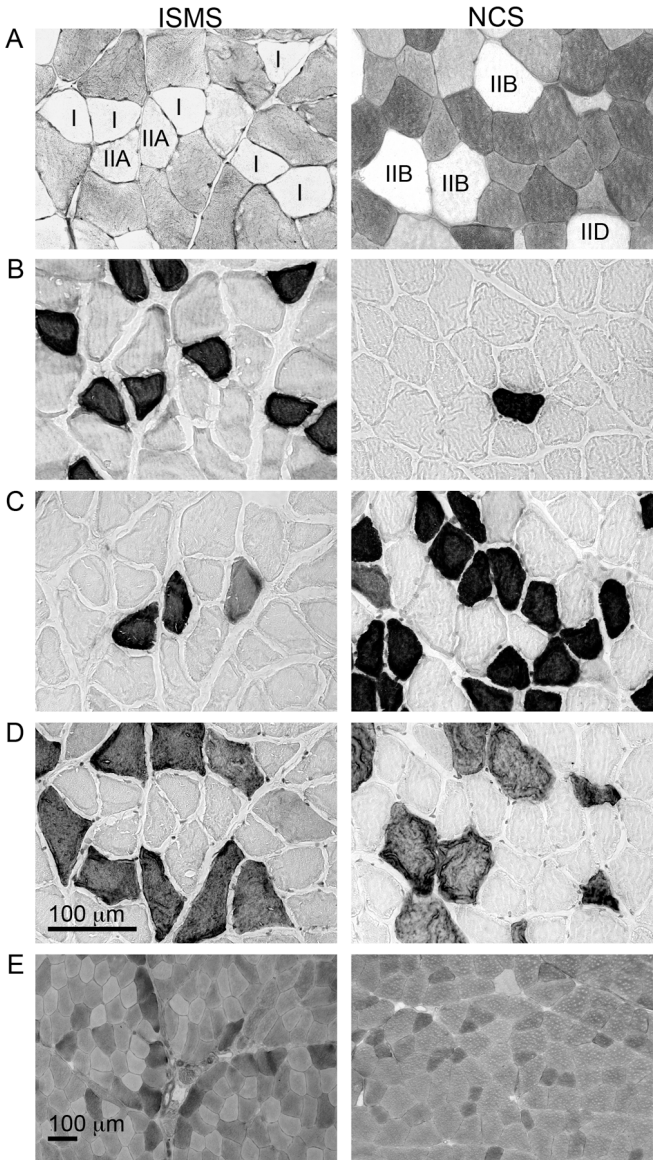

Figure 2-2: Glycogen depletion protocol.

Representative photomicrographs of histological and immunohistochemical stains, pictured here at 300 X, were used to identify (A) glycogen content (periodic acid Schiff's), (B) type-I (anti-MHCI), (C) type-IIA (anti-MHCIIa), (D) type-IIB (anti-MHCIIb). Control stains for glycogen (E), pictured here at 100 X were performed on sham control hindlimb muscle in order to verify that neither the ischemia nor the extraction procedure produced glycogen depletion. Fibres were identified by their reaction with the corresponding MHC antibody, while type-IID/X fibres were identified by the absence of immunohistochemical staining. Although the IIA fibre marked with * in (C) appears depleted to the naked eye, it fell just below the threshold for detection according to computer analysis.

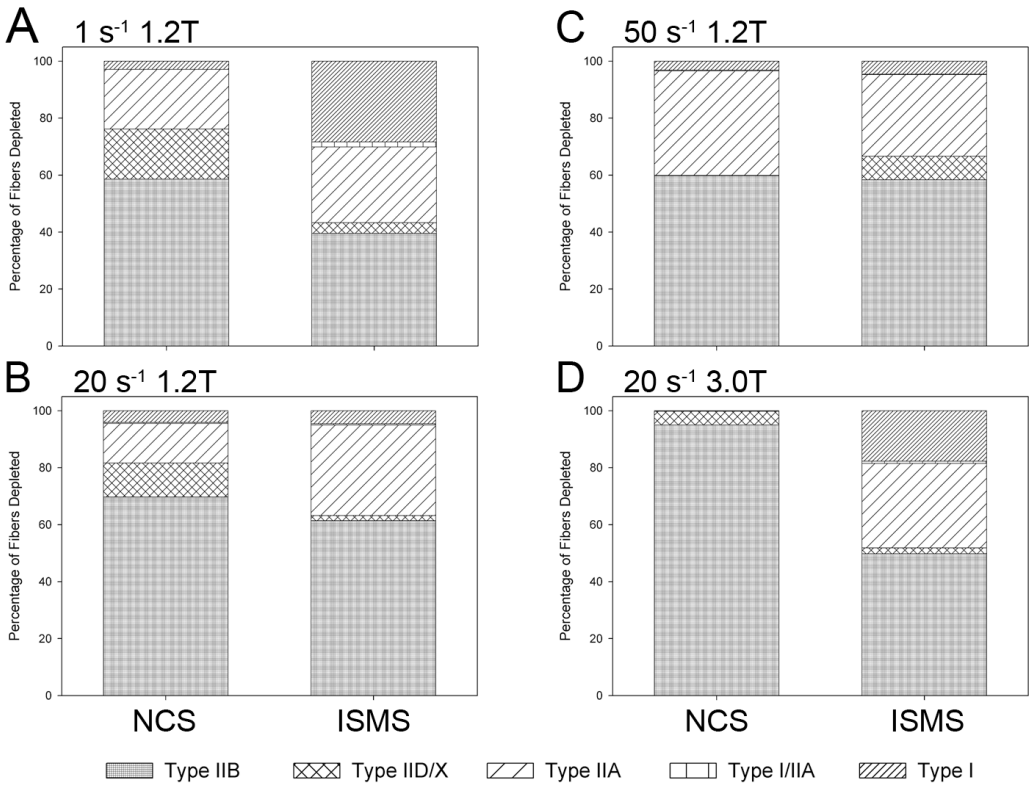

Figure 2-3: Glycogen depletion results.

Graphs show MHC type-I, -I/IIA, -IIA, -IID/X and -IIB fibres depleted by either NCS or ISMS as a proportion of the total fibres depleted in (A) 1 s^{-1} 1.2X threshold (B) 20 s^{-1} 1.2X threshold (C) 50 s^{-1} 1.2X threshold and (D) 20 s^{-1} 3.0X threshold conditions. Six animals were used for each stimulation condition.

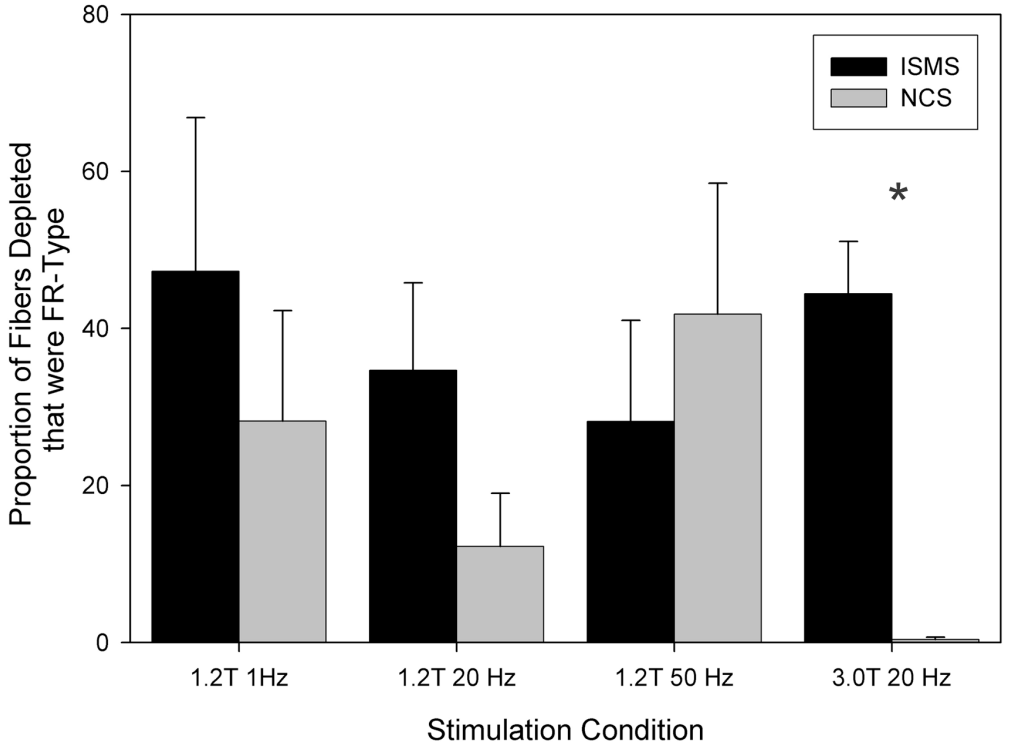

Figure 2-4: Fatigue-resistant fibres depleted in each condition.

Proportion of glycogen-depleted fibres that were FR type (MHC type-I, -I/IIA and –IIA) in each experimental group (n=6) by either NCS or ISMS. The nerve cuff caused the depletion of 726, 1,481, 1,055 and 7,294 fibers in the 1 Hz 1.2X threshold, 20 Hz 1.2X threshold, 50 Hz 1.2X threshold and 20 Hz 3.0X threshold groups, respectively. ISMS caused depletion of 1,249, 1,178, 751 and 1,188 muscle fibers in the 1 Hz 1.2X threshold, 20 Hz 1.2X threshold, 50 Hz 1.2X threshold and 20 Hz 3.0X threshold groups, respectively. Results are shown as means ± SEM for both 1.2X and 3.0X threshold. Statistical significance was set at $p < 0.05$.

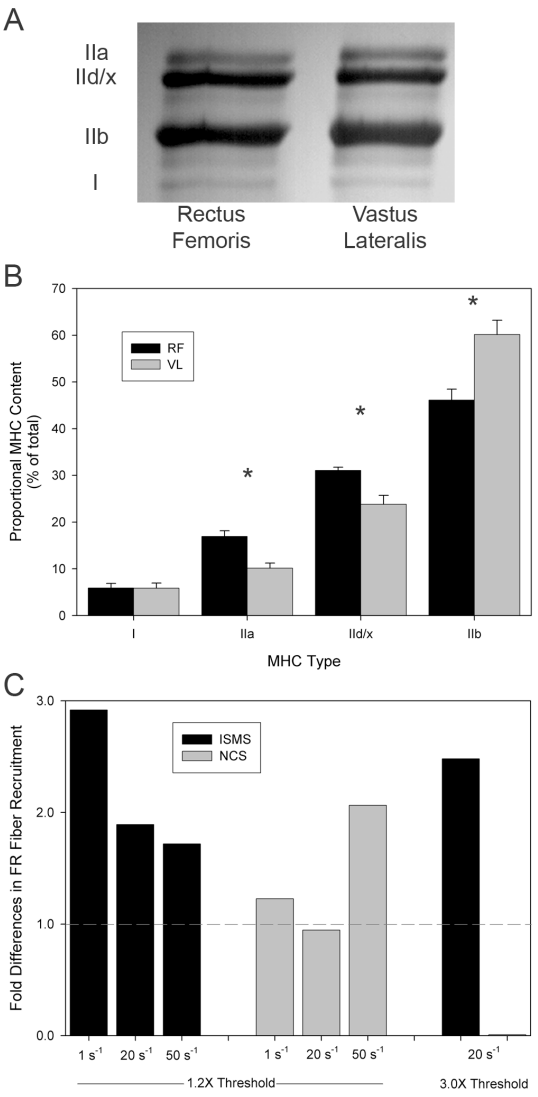

Figure 2-5: Depletion of fatigue-resistant fibres as a function of myosin heavy chain content.

Relative MHC isoform content in 8 *rectus femoris* and 8 *vastus lateralis* muscles from 8 different animals as determined by one-dimensional electrophoresis. (A) Representative gel blot of *rectus femoris* and *vastus lateralis* muscles with type-IIa, -IId/x, -IIb and -I MHC bands delineated. (B) Bar-plot showing results of SDS-PAGE for MHC isoform content in *rectus femoris* (RF) and *vastus lateralis (VL)* muscles. (C) After grouping MHC isoform content results into FR and FF categories the total number of FR fibres depleted by each condition was divided by the FR MHC content yielding fold differences in the recruitment of FR fibre types. Note that statistical significance in (B) was set at $p < 0.05$.

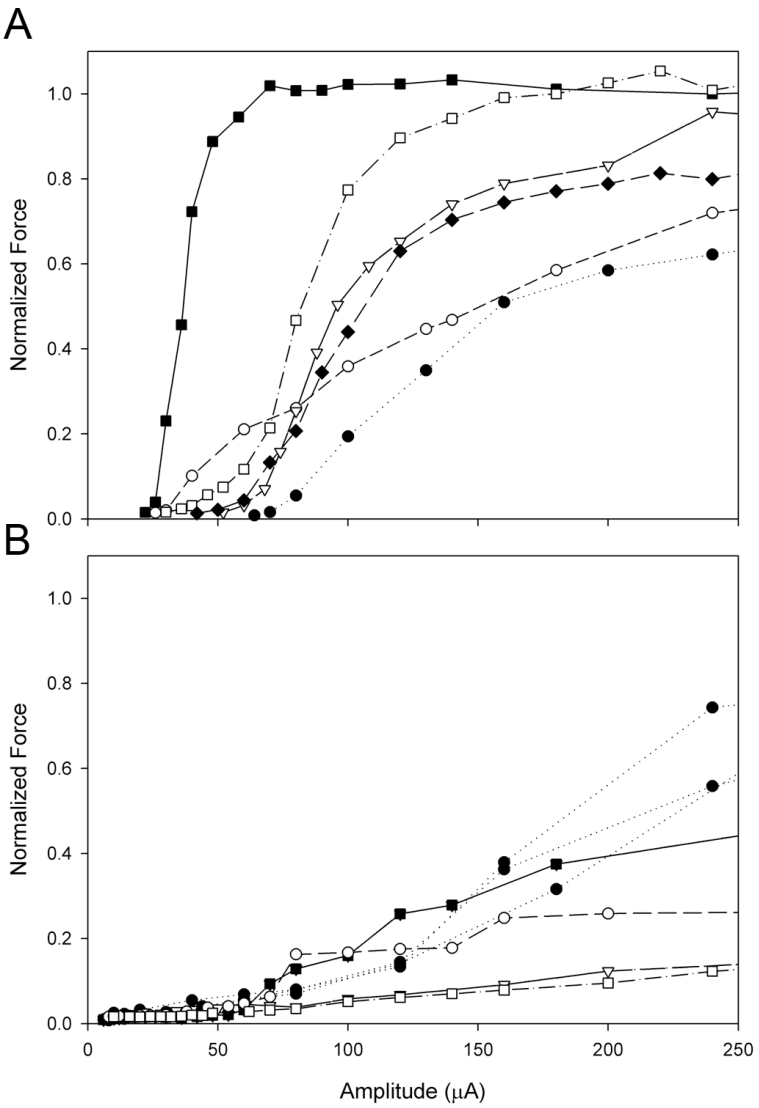

Figure 2-6: Peak twitch force results.

Force recruitment curves produced by either (A) NCS of the femoral nerve or (B) ISMS in the quadriceps motoneuron pool in the ventral grey matter. Force is normalized to the peak twitch force produced by the nerve cuff in each hindlimb and is expressed as a function of pulse amplitude in μA. The same symbols in (A) and (B) indicate that the NCS and ISMS curves were obtained from the same animals.

2.6 Bibliography

Agnew WF & McCreery DB (1990). *Neural Prostheses: Fundamental Studies*. Prentice-Hall, Englewood Cliffs, NJ.

Andersen JL, Mohr T, Biering-Sorensen F, Galbo H & Kjaer M (1996). Myosin heavy chain isoform transformation in single fibres from m. vastus lateralis in spinal cord injured individuals: effects of long-term functional electrical stimulation (FES). *Pflugers Arch* 431, 513-518.

Aoyagi Y, Mushahwar VK, Stein RB & Prochazka A (2004). Movements elicited by electrical stimulation of muscles, nerves, intermediate spinal cord, and spinal roots in anesthetized and decerebrate cats. *IEEE Trans Neural Syst Rehabil Eng* 12, 1-11.

Bamford JA, Lopaschuk GD, MacLean IM, Reinhart ML, Dixon WT & Putman CT (2003). Effects of chronic AICAR administration on the metabolic and contractile phenotypes of rat slow- and fast-twitch skeletal muscles. *Can J Physiol Pharmacol* 81, 1072-1082.

Bowers-Komro DM, Yamada Y & McCormick DB (1989). Substrate specificity and variables affecting efficiency of mammalian flavin adenine dinucleotide synthetase. *Biochemistry* 28, 8439-8446.

Burnham R, Martin T, Stein R, Bell G, MacLean I & Steadward R (1997). Skeletal muscle fibre type transformation following spinal cord injury. *Spinal Cord* 35, 86-91.

Castro MJ, Apple DF, Jr., Staron RS, Campos GE & Dudley GA (1999). Influence of complete spinal cord injury on skeletal muscle within 6 mo of injury. *J Appl Physiol* 86, 350-358.

Collins DF, Burke D & Gandevia SC (2001). Large involuntary forces consistent with plateau-like behavior of human motoneurons. *J Neurosci* 21, 4059-4065.

Collins DF, Burke D & Gandevia SC (2002). Sustained contractions produced by plateau-like behaviour in human motoneurones. *J Physiol* 538, 289-301.

English AW, Wolf SL & Segal RL (1993). Compartmentalization of muscles and their motor nuclei: the partitioning hypothesis. *Phys Ther* 73, 857-867.

Enoka RM (2002). Activation order of motor axons in electrically evoked contractions. *Muscle Nerve* 25, 763-764.

Fuglevand A & Johns RK (2004). Saturation of Motor Unit Firing Rate. *Active Dendrites in Motor Neurons: Conference Proceedings*.

Hamalainen N & Pette D (1996). Slow-to-fast transitions in myosin expression of rat soleus muscle by phasic high-frequency stimulation. *FEBS Lett* 399, 220-222.

Henneman E (1957). Relation between size of neurons and their susceptibility to discharge. *Science* 126, 1345-1347.

Henneman E, Somjen G & Carpenter DO (1965). Excitability and inhibitability of motoneurons of different sizes. *J Neurophysiol* 28, 599-620.

Hudlicka O, Brown MD, Egginton S & Dawson JM (1994). Effect of long-term electrical stimulation on vascular supply and fatigue in chronically ischemic muscles. *J Appl Physiol* 77, 1317-1324.

Jilge B, Minassian K, Rattay F & Dimitrijevic MR (2004). Frequency-dependent selection of alternative spinal pathways with common periodic sensory input. *Biol Cybern* 91, 359-376.

Kim CK, Bangsbo J, Strange S, Karpakka J & Saltin B (1995). Metabolic response and muscle glycogen depletion pattern during prolonged electrically induced dynamic exercise in man. *Scand J Rehabil Med* 27, 51-58.

Kugelberg E & Edstrom L (1968). Differential histochemical effects of muscle contractions on phosphorylase and glycogen in various types of fibres: relation to fatigue. *J Neurol Neurosurg Psychiatry* 31, 415-423.

Laemmli UK (1970). Cleavage of structural proteins during the assembly of the head of bacteriophage T4. *Nature* 227, 680-685.

Lemay MA & Grill WM (2004). Modularity of motor output evoked by intraspinal microstimulation in cats. *J Neurophysiol* 91, 502-514.

Levy M, Mizrahi J & Susak Z (1990). Recruitment, force and fatigue characteristics of quadriceps muscles of paraplegics isometrically activated by surface functional electrical stimulation. *J Biomed Eng* 12, 150-156.

Lieber RL & Friden J (2000). Functional and clinical significance of skeletal muscle architecture. *Muscle Nerve* 23, 1647-1666.

Martin TP, Stein RB, Hoeppner PH & Reid DC (1992). Influence of electrical stimulation on the morphological and metabolic properties of paralyzed muscle. *J Appl Physiol* 72, 1401-1406.

Mesrati F & Vecchierini MF (2004). F-waves: neurophysiology and clinical value. *Neurophysiol Clin* 34, 217-243.

Minassian K, Jilge B, Rattay F, Pinter MM, Binder H, Gerstenbrand F & Dimitrijevic MR (2004). Stepping-like movements in humans with complete spinal cord injury induced by epidural stimulation of the lumbar cord: electromyographic study of compound muscle action potentials. *Spinal Cord* 42, 401-416.

Mushahwar VK, Gillard DM, Gauthier MJ & Prochazka A (2002). Intraspinal micro stimulation generates locomotor-like and feedback-controlled movements. *IEEE Trans Neural Syst Rehabil Eng* 10, 68-81.

Mushahwar VK & Horch KW (1997). Proposed specifications for a lumbar spinal cord electrode array for control of lower extremities in paraplegia. *IEEE Trans Rehabil Eng* 5, 237-243.

Mushahwar VK & Horch KW (1998). Selective activation and graded recruitment of functional muscle groups through spinal cord stimulation. *Ann N Y Acad Sci* 860, 531-535.

Mushahwar VK & Horch KW (2000a). Muscle recruitment through electrical stimulation of the lumbo-sacral spinal cord. *IEEE Trans Rehabil Eng* 8, 22-29.

Mushahwar VK & Horch KW (2000b). Selective activation of muscle groups in the feline hindlimb through electrical microstimulation of the ventral lumbo-sacral spinal cord. *IEEE Trans Rehabil Eng* 8, 11-21.

Mushahwar VK, Prochazka A, Ellaway PH, Guevremont LG & Gaunt RA (2003). Microstimulation in CNS Excites Axons Before Neuronal Cell Bodies. *Society for Neuroscience 33rd Annual Meeting: Conference Proceedings*.

Oakley BR, Kirsch DR & Morris NR (1980). A simplified ultrasensitive silver stain for detecting proteins in polyacrylamide gels. *Anal Biochem* 105, 361-363.

Pette D & Staron RS (1997). Mammalian skeletal muscle fiber type transitions. *Int Rev Cytol* 170, 143-223.

Pette D & Vrbova G (1992). Adaptation of mammalian skeletal muscle fibers to chronic electrical stimulation. *Rev Physiol Biochem Pharmacol* 120, 115-202.

Pikov V & McCreery DB (2004). Mapping of spinal cord circuits controlling the bladder and external urethral sphincter functions in the rabbit. *Neurourol Urodyn* 23, 172-179.

Popovic DB (1992). Functional Electrical Stimulation for Lower Extremities. In *Neural Prostheses: Replacing Motor Function After Disease or Disuse*, ed. Stein RB, Peckham PH & Popovic DB, pp. 233-251. Oxford University Press, New York.

Portal JJ, Corio M & Viala D (1991). Localization of the lumbar pools of motoneurones which provide hindlimb muscles in the rabbit. *Neurosci Lett* 124, 105-107.

Prochazka A (1993). Comparison of natural and artificial control of movement. *IEEE Trans Rehabil Eng,* 1, 7-17.

Prochazka A & Mushahwar VK (2001). Spinal cord function and rehabilitation - an overview. *J Physiol* 533, 3-4.

Putman CT, Dixon WT, Pearcey JA, MacLean IM, Jendral MJ, Kiricsi M, Murdoch GK & Pette D (2004). Chronic low-frequency stimulation upregulates uncoupling protein-3 in transforming rat fast-twitch skeletal muscle. *Am J Physiol Regul Integr Comp Physiol* 287, R1419-R1426.

Putman CT, Kiricsi M, Pearcey J, MacLean IM, Bamford JA, Murdoch GK, Dixon WT & Pette D (2003). AMPK activation increases uncoupling protein-3 expression and mitochondrial enzyme activities in rat muscle without fibre type transitions. *J Physiol* 551, 169-178.

Putman CT, Sultan KR, Wassmer T, Bamford JA, Skorjanc D & Pette D (2001). Fiber-type transitions and satellite cell activation in low-frequency-stimulated muscles of young and aging rats. *J Gerontol A Biol Sci Med Sci* 56, B510-B519.

Rafuse VF & Gordon T (1996). Self-reinnervated cat medial gastrocnemius muscles. I. comparisons of the capacity for regenerating nerves to form enlarged motor units after extensive peripheral nerve injuries. *J Neurophysiol* 75, 268-281.

Romanes GJ (1964). The Motor Pools of the Spinal Cord. *Prog Brain Res* 11, 93-119.

Saigal R, Renzi C & Mushahwar VK (2004). Intraspinal microstimulation generates functional movements after spinal-cord injury. *IEEE Trans Neural Syst Rehabil Eng* 12, 430-440.

Schiaffino S, Gorza L, Sartore S, Saggin L, Ausoni S, Vianello M, Gundersen K & Lomo T (1989). Three myosin heavy chain isoforms in type 2 skeletal muscle fibres. *J Muscle Res Cell Motil* 10, 197-205.

Schiaffino S & Serrano A (2002). Calcineurin signaling and neural control of skeletal muscle fiber type and size. *Trends Pharmacol Sci* 23, 569-575.

Sharrard WJ (1955). The distribution of the permanent paralysis in the lower limb in poliomyelitis; a clinical and pathological study. *J Bone Joint Surg Br* 37-B, 540-558.

Singh K, Richmond FJ & Loeb GE (2000). Recruitment properties of intramuscular and nerve-trunk stimulating electrodes. *IEEE Trans Rehabil Eng* 8, 276-285.

Snow S, Horch KW & Mushahwar VK. (2005) Intraspinal Microstimulation using Cylindrical Multielectrodes. *IEEE Trans Biomed Eng,* In Press.

Stein RB, Chong SL, James KB, Kido A, Bell GJ, Tubman LA & Belanger M (2002). Electrical stimulation for therapy and mobility after spinal cord injury. *Prog Brain Res* 137, 27-34.

Taylor AM & Enoka RM (2004). Quantification of the factors that influence discharge correlation in model motor neurons. *J Neurophysiol* 91, 796-814.

Thomas CK, Nelson G, Than L & Zijdewind I (2002). Motor unit activation order during electrically evoked contractions of paralyzed or partially paralyzed muscles. *Muscle Nerve* 25 , 797-804.

Totosy de Zepetnek JE, Zung HV, Erdebil S & Gordon T (1992). Innervation ratio is an important determinant of force in normal and reinnervated rat tibialis anterior muscles. *J Neurophysiol* 67, 1385-1403.

Zehr PE (2002). Considerations for use of the Hoffmann reflex in exercise studies. *Eur J Appl Physiol* 86, 455-468.

Chapter 3

Muscle plasticity in rat following spinal transection and chronic instraspinal microstimulation[†]

3.1 Introduction

Following spinal cord injury a characteristic pattern of muscle wasting and transformation is observed in muscle innervated by nerves originating below the lesion. Skeletal muscle in rat becomes weaker, faster and more fatiguable (Talmadge et al., 2002). These attributes are demonstrated functionally by lower evoked forces, a shortening of isometric twitch characteristics and increased fatigue during repeated contractions. Given that these functional measures are tied to the expression of key contractile proteins it is not surprising that muscles affected by a chronic spinal cord transection (ST) also exhibit characteristic changes in contractile protein expression (Gallo et al., 2004).

Adult rat skeletal muscle expresses four myosin heavy chain (MHC) isoforms, slow type-I and fast types-IIa, -IId/x and -IIb (Pette and Vrbova, 1999). MHC content is a key determinant of contractile properties and can be used to delineate between a number of pure muscle fibre types named type-I, -IIA, IID/X and IIB according to their corresponding MHC content (Pette and Staron, 2001). These fibre types form a continuum from slowest to fastest of increasing ATPase activity, maximum isometric tension and

[†] A version of this chapter has been submitted for publication to the Journal of Physiology.

shortening velocity while the economy of contraction decreases from slowest to fastest (Pette and Staron, 2001). After ST, rat skeletal muscles undergo a slow-to-fast transformation of MHC isoforms that is characteristic of many inactivity paradigms (Talmadge, 2000). The muscles exhibit decreases in slow (MHC type-I) and fast fatigue-resistant (MHC type-IIA) muscle fibres with concomitant increases in fast fatiguable (MHC type-IID/X and type-IIB) fibres (Talmadge et al., 1999). Muscle atrophy is also commonly noted following ST (Talmadge et al., 1999).

Just as skeletal muscle responds to paradigms of inactivity, there is also a characteristic response to increased activity which can be induced even after complete spinal lesion (Harris et al., 2007). In humans with spinal cord injury, electrically evoked muscle training leads to increased fatigue resistance and a lengthening of muscle twitch properties (Gerrits et al., 2000). Contractile proteins such as MHC also undergo dramatic fast-to-slow isoform transformations in subjects following electrically evoked cycle training (Andersen et al., 1996). Similar fast-to-slow transformations in contractile proteins are seen following increased activity in chronically spinalized animals (Roy et al., 1998). Exercise training in subjects with spinal lesions can also ameliorate some of the atrophy associated with muscle disuse; however, this effect seems limited to training paradigms involving contractions against external loads (Dudley-Javoroski and Shields, 2008).

Intraspinal microstimulation (ISMS) is a new model of functional electrical stimulation (FES) that has been investigated for its ability to produce weight-bearing standing (Lau et al., 2007) and stepping (Saigal et al., 2004) in cats. Previous reports showed that, in contrast to many peripheral FES approaches, ISMS produces graded force recruitment, activates muscles selectively and produces coordinated multi-joint synergies (Mushahwar and Horch, 1998; Mushahwar and Horch, 2000; Mushahwar et al., 2000; Saigal et al., 2004; Snow et al., 2006; Lau et al., 2007). We have attributed the gradual force recruitment characteristics of ISMS to its ability to activate motoneurons in a near normal physiological order based upon their size (Bamford et al., 2005). Presumably the ordered recruitment of motoneurons is due to the preferential activation of fibres-in-passage, and the resultant trans-synaptic activation of motoneurons (Gaunt et al., 2006; Mushahwar et al., 2007).

The purpose of this study was to evaluate the muscle transformations that would occur following complete ST and the potential for ISMS to rescue a normal muscle fibre phenotype. In the rectus femoris muscle, this would mean the maintenance of a mixed concentration of MHC type-I and type-IIA fibres in the deepest portion of the muscle and a large concentration of type-IID/X and type-IIB fibres in the intermediate and superficial regions. Accordingly, this mixed muscle would maintain the functional properties of an intact muscle with regards to isometric twitch properties, fatigue resistance and sag profile.

We have shown previously that acute ISMS produces near normal motor unit recruitment and preferential activation of slow, fatigue-resistant muscle fibres while peripheral stimulation through a nerve cuff produces reversed recruitment and activation of fast, fatiguable fibres (Bamford et al., 2005). Given these results we hypothesized that chronic ISMS in spinal cord transected rats would rescue many of the functional properties of an intact muscle and its corresponding contractile proteins. On the other hand we hypothesized that chronic nerve cuff stimulation (NCS) in spinal cord transected rats would cause a dramatic fast-to-slow transformation in MHC-based fibre content and corresponding functional measures. We tested these hypotheses by transecting the spinal cords of rats at the eighth thoracic (T8) level and stimulating one leg of each rat with either ISMS or NCS for thirty days while the contralateral leg served as an unstimulated control. We found that chronic ISMS in rat reverses the slow-to-fast transformation following ST and, surprisingly, that the nature of the transformation was similar to that produced by chronic stimulation through a nerve cuff. This study is the first to evaluate the muscle transformations induced by chronic ISMS, a method of ISMS which produces near-normal recruitment of motoneurons.

3.2 Methods

3.2.1 Animals

Experiments were performed on female Sprague-Dawley rats weighing 225-275 g. All procedures were approved by the University of Al-

berta Animal Welfare Committee and were in keeping with the Canadian Council on Animal Care's guidelines for scientific research in animals.

3.2.2 Transection surgery

Aseptic transection of the spinal cord at T8 was carried out as follows. Animals were deeply anesthetized using 2.0% isofluorane and a laminectomy was performed to expose the spinal cord at the T8 level. A complete transection of the cord was performed followed by close visual inspection of the inner circumference of the spinal column to ensure that no tracts remained intact. A small piece of surgical mesh was inserted to promote vascular coagulation and a layer of thin plastic film was affixed over the laminectomy site with discrete drops of cyanoacrylate to prevent invasion of connective tissue into the transection site. The muscle and skin layers were sutured closed and analgesics (buprenorphine 0.015 mg/kg sc), and antibiotics (enroflaxacin 1.0 mg/kg sc) were administered. Further analgesics were administered as needed while antibiotics were administered daily for one week following surgery. The bladders of the rats were manually expressed three times per day for two weeks until voiding became reflexive. Following this period the bladders were expressed at least once per day to check for bladder infections and to ensure complete voiding. Cages were inspected daily and changed at least two times per week. Two weeks after the transection procedure each animal underwent a second aseptic surgical procedure to implant either a nerve cuff or an ISMS array.

3.2.3 Nerve cuff implant

Bipolar, split ring nerve cuffs were implanted in 6 animals around the femoral nerve of one leg as previously described (Cuoco and Durand, 2000; Bamford et al., 2005). Contralateral control legs received no implant and are hereafter referred to as nerve cuff control (NCC). Lead wires were tunneled subcutaneously to a headpiece connector (MS363, PlasticsOne, Roanoke, VA, USA) affixed with screws and dental acrylic to the skull. Muscle and skin layers were sutured and analgesics were administered (buprenorphine 0.015 mg/kg sc).

3.2.4 Intraspinal microwire implant

In another 6 animals with complete ST a second laminectomy was performed at thoracic level 13 and lumbar 1 (T13 and L1) and ISMS microwires were implanted as described in rats (Bamford et al., 2005; Yakovenko et al., 2007). Chronic microwire arrays for ISMS were manufactured as described previously for cats except that microwire depth was shortened to 1.5 mm to accommodate the smaller spinal cord of the rat (Guevremont et al., 2006). An array of four 30 μm diameter platinum-iridium microwires (California Fine Wire, Grover Beach, CA, USA) was implanted. Two microwires were inserted in each side of the spinal cord with 2 mm inter-wire rostro-caudal spacing and tips targeting the quadriceps motoneuron pool (Nicolopoulos-Stournaras and Iles, 1983). The targeting of the quadriceps pool was confirmed by delivering test trains of stimuli and observing quadriceps activation. Microwires were fixed to the

dura mater using discrete drops of cyanoacrylate at their point of insertion into the cord and run along the surface of the dura mater to the base of the T12 vertebra. Here they were carefully sutured to the dura mater using 8-0 silk before a layer of thin plastic film was affixed with cyanoacrylate to cover the exposed cord and prevent connective tissue from dislodging the microwires. The microwires were routed through a silastic tube which was attached to the T12 spinous process and then to a connector headpiece as described for the nerve cuff implant. Muscle and skin layers were sutured and analgesics were administered (buprenorphine 0.015 mg/kg sc). As with the nerve cuff animals, one leg was used for stimulation while the other leg was used as a contralateral intraspinal microwire control (ISC). All animals were given a one week recovery period prior to initiating nerve cuff or intraspinal stimulation.

3.2.5 Nerve cuff stimulation

Supramaximal stimulation at levels 4.0 ± 0.0 times the activation threshold (the lowest stimulus amplitude that produced a muscle twitch) was delivered through the nerve cuff four hours every day for thirty days while the contralateral NCC leg received no stimulation. Stimulus trains of 50 pulses per second (pps) were maintained for 1 second followed by 1 second of rest. Stimuli were composed of biphasic, cathodic-first, 200 μs, charge balanced pulses. The use of supramaximal stimulation was necessary to produce stable contractions in the quadriceps muscle. In all cases,

NCS produced strong extension of the leg at the knee throughout the thirty day stimulation period.

3.2.6 Intraspinal microwire stimulation

Stimulation for the ISMS animal group proceeded as above with the following differences. Stimulation to the treatment leg was carried out using two ipsilateral microwires while the contralateral control ISC leg received no stimulation. Stimulation trains were delivered through each microwire at 25 pps which, when both microwires were interleaved, produced 50 pps contractions at the muscle. This frequency of stimulation was selected for both ISMS and NCS legs (as noted above) in order to produce fused contractions of the quadriceps muscle, thereby ensuring stable forces during the contraction. Stability of force is a critical component in achieving a functional motor task and, as such, fused contractions would be part of the stimulation strategy for a clinical device.

Stimulation through the ISMS microwires produced a more complex response than stimulation through a nerve cuff. Stimulation at activation threshold caused weak quadriceps contractions. As stimulus amplitude increased, quadriceps activation became more apparent with resultant extension of the leg at the knee. If amplitude was increased even further, coordinated muscle synergies were produced. Out of 12 microwires that were used for stimulation 8 produced extension synergies of the whole leg involving hip and knee extension. The other 4 microwires produced a forward movement involving knee extension and hip flexion. In

order to standardize the muscle recruitment across all nerve cuff and ISMS animals, the experimental legs were stimulated at the maximal amplitude that produced knee extension but not muscle synergies. Activation thresholds were routinely checked and stimulus amplitudes were adjusted to maintain this movement pattern. When expressed as a function of activation threshold these stimulus amplitudes were a mean of 2.55 ± 0.87 times the activation threshold. This level of stimulation produced strong activation of the quadriceps muscle in each animal throughout the thirty day stimulation period.

3.2.7 Terminal surgery

One day following the final stimulation bout, animals were anesthetized and functional muscle data were collected from stimulated NCS and ISMS legs, contralateral NCC and ISC control legs and from intact control animals (IC) according to previously established protocols (Gallo et al., 2004). Under deep anesthesia new nerve cuffs were implanted around the femoral nerve of all legs except for those that had received a chronic nerve cuff implant (the NCS group). The animals were then positioned in a stereotaxic array and each patellar tendon was dissected from its point of insertion and attached to a force transducer (Interface MB-5, Interface Inc., Scottsdale, AZ, USA). The force recordings were amplified 100-fold and captured at a sampling rate of 1000 Hz using a data acquisition interface (Power 1401, Cambridge Electronic Design, Cambridge, UK) with associated software (Signal v. 2.13, Cambridge Electronic Design).

3.2.8 Tests of the functional properties of stimulated muscles

The following tests were performed in all animals by stimulating through a nerve cuff. Tests were carried out to determine: 1) the peak twitch force and twitch velocity; 2) the presence of whole muscle sag; and 3) the fatiguability profile of the muscle.

1) Peak twitch force and twitch velocity: Four individual supra-maximal twitches were evoked and averaged. Peak force was averaged from the same 4 twitches and later divided by the wet weight of the corresponding quadriceps muscle to calculate normalized twitch force (TWFn). Time-to-peak tension (TTP) was determined by averaging the time taken for force to rise from zero to peak force. Half-rise-time (1/2RT) was obtained by averaging the time taken for force to rise from zero to one half of peak force. Half-fall-time (1/2FT) was obtained by averaging the time taken for force to decay from peak to one half of peak force. These twitch characteristics are useful indicators of muscle fibre-type phenotypic conversions because MHC content varies with whole-muscle isometric measures of contractile speed during muscle transformation (Gallo et al., 2004). Measurements of twitch duration are indicators of underlying contractile and metabolic proteins that govern the speed of contraction (1/2RT, TTP) or relaxation (1/2FT) of the muscle fibres. While 1/2RT and TTP are best correlated to contractile proteins, especially the MHC isoforms (Gallo et al., 2004), 1/2FT is more strongly correlated with compo-

nents of muscle relaxation such as fast or slow sarco(endo)plasmic reticulum Ca^{2+}-ATPase (SERCA) (Hämäläinen and Pette, 1997).

2) Detection of whole muscle sag: An 800 ms-train of stimuli with inter-pulse interval of 1.25 x TTP was used to test for the presence of muscle sag. This test provided information regarding the collective motor unit type makeup of the muscle.

3) Fatigue: A Burke fatigue test (Burke et al., 1971) was performed by sending repeated 40 pps stimulus trains for 330 ms of every second for up to 5 minutes and recording the decline in the evoked tetanic force. A fatigue ratio was calculated by dividing the force level at the 2 minute mark by the peak force evoked during the test. Information regarding changes in the overall fatigue resistance of the muscle was obtained using this test.

3.2.9 Tests of recruitment order following chronic spinal cord transection

There is some uncertainty regarding the recruitment order of motor units after spinal transection with one report suggesting temporarily disordered recruitment (Durkovic, 2006). In order to 1) determine the recruitment order of motor units following chronic ST and 2) compare the recruitment order produced by ISMS and NCS, force recruitment curves were constructed and compared to those obtained from intact animals (Bamford et al., 2005). Force recruitment curves were generated using 5 chronically implanted microwires in the ISMS legs and 6 nerve cuffs in the

NCS legs. Stimulation amplitude was varied upwards from sub-threshold levels in random order and the force evoked by 50 pps stimulus trains was recorded. Evoked tetanic forces were normalized to peak force and plotted against stimulation amplitude. Linear regression was used to calculate the slopes from 10% to 90% of peak force for each recruitment curve and group means were calculated.

3.2.10 Confirmation of microwire tip locations

To determine the locations of the ISMS microwire tips animals with ISMS implants were perfused through the heart with saline followed by 4% formaldehyde in saline solution. This was conducted immediately after the muscles were extracted for analysis (see Immunohistochemical Staining below). The spinal cords were removed, cryoprotected in 20% sucrose/ phosphate buffered solution (PBS) and frozen. They were then sectioned in 20 μm cross-sections to locate the microwire tips. Out of 12 microwires used for stimulation 7 were located during sectioning. All located microwire tips were positioned in the ventral horn of the grey matter (figure 1).

3.2.11 Immunohistochemical staining

Following functional data collection quadriceps muscles from both legs were excised, weighed and frozen in melting isopentane cooled in liquid nitrogen before sectioning in 10 μm cross-sections. Immunohistochemical detection of MHC isoforms at pH 7.4 was performed on frozen rectus femoris muscle sections as previously described (Bamford et al.,

2005). Culture supernatant from anti-MHC type-I clone BA-D5, anti-MHC type-IIA clone SC-71 and anti-MHC type-IIB clone BF-F3 had been previously collected from our own tissue culture facilities. Sections were incubated in 3% H_2O_2 in methanol for 15 minutes then washed and incubated for 1 hour at room temperature in blocking solution containing PBS-tween, 1% bovine serum albumin, 10% horse serum and Avidin-D blocking agent (Vector Laboratories, Burlingame, CA, USA). The blocking step for the MHC-IIB clone BF-F3 was identical except for the substitution of goat serum for horse serum. Primary monoclonal antibodies from culture supernatant were applied overnight at 4° C at the following dilutions in blocking solution: anti-MHC type-I clone BA-D5 (1:400); anti-MHC type-IIA clone SC-71 (1:100); anti-MHC type-IIB clone BF-F3 (1:400). The primary antibody solution also included Biotin Blocking Reagent (Vector Laboratories). Sections were washed in PBS-tween and PBS and then incubated for 1 hour at room temperature with biotinylated horse anti-mouse IgG (Vector Laboratories, for BA-D5 and SC-71) diluted 1:400 in blocking solution or with biotinylated goat anti-mouse IgM (Vector Laboratories, for BF-F3) diluted 1:400 in blocking solution. Sections were washed as before and incubated for 1 hour at room temperature with Vectastain ABC Reagent (Vector Laboratories) in PBS and washed again. Immunoreactivity was visualized by applying diaminobenzidine, H_2O_2 and NiCl in 50 mM tris-HCl (Vector Laboratories).

3.2.12 Image analysis

Pictures of stained serial cross-sections were taken through a microscope with a 10X objective (Leica DMLS, Leica Microsystems, Wetzlar, Germany). A digital camera (Spot Insight, Diagnostic Instruments, Sterling Heights, MI, USA) was used to record the images which were stored and analyzed using the ImageJ software package (ImageJ, U. S. National Institutes of Health, Bethesda, Maryland, USA). This software allowed for counting of fibres and determination of cross-sectional area (CSA). The panel of applied monoclonal antibodies allowed direct identification of stained pure type-I, -IIA, -IIB fibres and, in the absence of any staining, -IID/X fibres. Hybrid fibres could also be detected when more than one MHC isoform was detected in a given fibre (i.e. type-I/IIA and type-IIA/IIB).

The slowest area in each muscle was chosen for detailed analysis since it contained a mixture of fibre types, and could be used to detect either fast-to-slow or slow-to-fast transformations (figure 2). Counting was used to show the direction of the transformation occurring in each muscle and to evaluate changes in fibre CSA. This allowed for detailed analysis of the slowest region of each muscle.

Given the size and total number of fibres in rectus femoris muscles counting of immunohistochemically stained fibres was not used as an indicator of total proportional content of each MHC-based fibre type. A broader analysis of the MHC type-IIA content in the whole muscle was

used to compliment the detailed analysis of the slow region of each muscle. Whole muscle images of MHC type-IIA were binarized (figure 3) according to established image analysis procedures (Sedgewick, 2008) and the black pixels which represent stained areas of the tissue were counted and expressed as a proportion of all pixels within the muscle boundary. In this way an area fraction was calculated which represented the area of muscle positively stained for MHC type-IIA as a proportion of the whole muscle area.

3.2.13 Statistical Analysis

All analyses were performed with a computerized software package (SPSS 17.0, SPSS Inc., Chicago, IL, USA). Differences were determined with one-way ANOVA and Tukey HSD post hoc test. Where indicated, paired *t*-tests were run on data from animals with paired control legs. Differences were considered significant at $P < 0.05$. All data are presented as mean (± SD).

3.3 Results

3.3.1 Activation thresholds for ISMS decreased over time

The threshold amplitudes for quadriceps muscle activation were checked on the first day of stimulation and approximately every ten days thereafter (figure 4). Mean threshold for nerve cuff muscle activation was 118.3 μA ± 69.4 μA at the beginning of the thirty day stimulation period and 123.3 μA ± 46.8 μA at the end. Mean threshold for muscle activation with ISMS microwires dropped significantly from 118.2 μA ± 45.1 μA to

67.8 μA ± 25.1 μA by the end of the thirty days of stimulation. At the end of stimulation period the mean activation threshold for ISMS was also significantly lower than that for NCS.

Regression curves were fitted for each plot of threshold changes over time. The mean slope of these curves was significantly lower for ISMS (-1.61 ± 1.67) than for NCS (-0.16 ± 1.20). Out of 12 microwires used for ISMS, 11 lasted throughout the thirty day stimulation period while one failed permanently on the fourteenth day. Of these 11 microwires, 8 showed decreases, 2 showed increases, and 1 showed no overall change in activation threshold.

3.3.2 Muscle mass decreased with ST while normalized force increased with NCS

Mean mass of the quadriceps muscle of the contralateral unstimulated NCC and ISC legs dropped significantly compared to the IC legs (see table 1); however, TWFn was not significantly different from the IC legs. This suggests that decreases in force produced by NCC and ISC control muscles were entirely accounted for by decreases in quadriceps muscle mass.

Mean mass of the quadriceps muscle decreased significantly in NCS and ISMS legs compared to IC legs (see table 1). Furthermore, mean quadriceps mass of NCS legs was significantly less than that of NCC legs (paired *t*-test) but mean mass of the ISMS legs was similar to that of the ISC legs.

In the NCS legs, TWFn increased significantly compared to the NCC and IC legs.

The isometric force profile of sub-tetanic motor unit contraction is commonly used to identify motor unit type based on the presence of either sag or potentiation of force in fast and slow motor units, respectively (Burke et al., 1971). The same approach has been extended to the whole muscle level since the force profile of sub-tetanic whole muscle contraction can be considered to be an aggregate of all the individual motor units (Gallo et al., 2004). Force recordings were visually inspected for the presence of whole muscle sag. The results are displayed in table 1 and representative examples are provided in figure 5. We found that thirty days of stimulation resulted in the absence of sag in all 6 NCS legs and in 5 of 6 ISMS legs, indicating a slowing of the stimulated quadriceps muscle compared to IC, NCC and ISC unstimulated controls (table 1).

Mean force curves showing the decline in force during the fatigue test are shown in figure 6. The mean fatigue resistance index of the IC legs was found to be near 0.5 (table 1), meaning that after 2 minutes of electrically evoked contractions the quadriceps muscle of the IC legs produced ~50% of its peak force. Mean fatigue resistance decreased significantly in the NCC legs as compared to the contralateral NCS legs and the IC legs. There were no significant differences in mean fatigue resistance between the stimulated NCS and ISMS legs and the IC legs.

Interestingly, the fatigue index of the ISC legs was not significantly different from that of the IC legs or the contralateral ISMS legs. This was surprising given the result from the NCC legs and our expectation that unstimulated muscle in chronically transected animals would fatigue more rapidly than muscle from intact controls.

3.3.3 Stimulation caused slowing of the muscle twitch

Thirty days of stimulation through either intraspinal microwires or a nerve cuff caused a significant slowing of twitch lengths in stimulated NCS and ISMS legs (table 1). Normalized mean muscle twitches evoked with a nerve cuff in ISMS and NCS legs, contralateral ISC and NCC legs and IC legs are shown in figure 7. Thirty days of stimulation caused a significant lengthening in TTP, 1/2RT and 1/2FT in NCS and ISMS legs compared to the respective NCC and ISC legs (paired *t*-test, figure 8). Furthermore, the NCS and ISMS legs also exhibited significant lengthening of both TTP and 1/2RT when compared to the IC legs.

Only the ISMS group showed significant lengthening of 1/2FT in comparison to the IC legs. This difference suggests that the intraspinal stimulation paradigm caused a stronger transformation in the components of muscle relaxation; however, the exact nature of these changes is unclear. Contralateral control ISC and NCC legs were not significantly different from the IC legs for any measurements of isometric twitch length.

3.3.4 Stimulation caused a fast-to-slow transformation

A mean of 432.3 ± 96.1 rectus femoris muscle fibres were analyzed in each leg for a total of 12970 analyzed fibres. The slowing of muscle twitch in stimulated legs was matched by a fast-to-slow transformation of MHC content in the stimulated NCS and ISMS legs (see figures 9 and 10). The slowest muscle region in NCS and ISMS stimulated legs showed significant increases in mean type-IIA fibre content and corresponding decreases in mean type-IID/X fibre content compared to the NCC and ISC control legs, and to the IC legs. This finding was verified with whole muscle analysis which showed an increase in the area fraction for MHC IIA fibres in stimulated NCS and ISMS legs compared to the IC control legs (figure 11). Mean type-IIA/IIB hybrid fibre content was significantly increased in the stimulated NCS and ISMS legs compared to the contralateral NCC legs, ISC legs and the IC legs. There was no significant difference in mean type-IIB fibre content between the stimulated legs and the IC legs in the slow region. Mean type-I fibre content in the NCS but not the ISMS legs was significantly decreased compared to the IC legs.

In contrast to the stimulated legs, a mild slow-to-fast transformation was observed in unstimulated NCC and ISC legs compared to the IC legs. The slowest rectus femoris region in NCC and ISC legs showed significant decreases in the mean number of type-IIA fibres and corresponding increases in the mean number of type-IIB fibres compared to the IC legs and to the stimulated NCS and ISMS legs. Mean type-IID/X fibre content was not changed in NCC and ISC unstimulated legs compared to the

IC legs. Mean type-I fibre content was also not changed in NCC and ISC legs compared to their respective contralateral stimulated legs. There was a significant decrease in the mean type-I fibre content in the ISC but not in the NCC legs compared to the IC legs. Despite the increase in fast MHC isoforms in the slow region of unstimulated muscles there were no indications from isometric twitch measures that these legs were functionally faster than the IC legs. This is presumably because the content of slower type-I and -IIA fibres in the rectus femoris muscle of the IC legs is small and the functional measures from the whole quadriceps muscle are dominated by the far greater content of the faster type-IID/X and -IIB fibres. The slow-to-fast transformations in unstimulated NCC and ISC muscles did not play a large role in altering isometric functional measures since they took place in a relatively small population of slower fibres.

Surprisingly, mean fibre-type cross-sectional area was not significantly different between unstimulated NCC and ISC legs and the IC legs (see table 2). The muscles in the NCC and ISC legs did undergo a significant decrease in muscle mass which would presumably be related to a decrease in fibre CSA and to any transformations in fibre type. We have previously shown that rectus femoris muscles display a very fast phenotype in rat as shown by a combined proportional content of IId/x and IIb MHC that is greater than 75% (Bamford et al., 2005). It is possible that a non-significant decrease in type-IID/X or -IIB fibre CSA could result in a sig-

nificant decrease in whole muscle mass given the large proportion of type-IID/X and -IIB fibres in rectus femoris.

Mean cross-sectional areas for both type-IID/X and type-IIB fibres declined significantly in both NCS and ISMS stimulated legs compared to the IC legs. The corresponding decreases in mean muscle mass were greatest in the stimulated NCS and ISMS muscles, perhaps reflecting the decrease in CSA in type-IID/X and -IIB fibres as well as the increased expression of slower fibres with smaller CSA. No other significant differences in mean cross-sectional area were found.

The activity-induced transformations in muscle fibre type in all legs paralleled the observed functional changes except in the case of mean fatigue resistance index in the ISC legs (table 1, figure 6). Although fatigue resistance is correlated to MHC content and muscle twitch characteristics (Talmadge et al., 2002) fatigue is a more complex phenomenon as it is also influenced by factors such as capillary density, myoglobin content and mitochondrial density, and the concomitant expression of key oxidative enzymes such as citrate synthase and succinate dehydrogenase (Allen et al., 2008). Although these factors are expected to be coordinately regulated with MHC content, the relationship between fatigue resistance and MHC expression is not as tightly coupled as that between MHC expression and isometric twitch speed.

3.3.5 Force recruitment through NCS and ISMS is unchanged following chronic spinal cord transection

The mean slope of recruitment curves generated through ISMS microwires in the ISMS legs was 0.0048 ± 0.0027, while that generated through nerve cuffs in NCS legs was significantly sharper at 0.016 ± 0.010. This represents a 3.4 fold sharper recruitment of force through the nerve cuff compared to recruitment through ISMS microwires (see figure 12). While this is less than the 4.9 fold difference previously found for intact animals (Bamford et al., 2005) it represents a significantly more gradual recruitment of force through the ISMS microwires. Furthermore, the mean slope of the recruitment curves generated through ISMS microwires after transection and thirty days of stimulation (0.0048 ± 0.0027) was nearly identical to the previously reported mean slope generated through ISMS microwires in intact animals (0.0041 ± 0.0021) (Bamford et al., 2005). This suggests that the recruitment order of motor units through ISMS and NCS was not altered following spinal cord transection.

3.4 Discussion

3.4.1 Overview

Skeletal muscle is a highly adaptive tissue that responds to imposed demands by altering its functional properties including fatigue resistance, sag profile and the speed of isometric twitches. Tests for these properties can be used to reveal the direction and extent of the muscle transformation. Key contractile proteins such as the MHCs can be used to reveal the

direction of transformation as they are tightly correlated with these functional properties (Pette and Vrbova, 1999).

Motor units recruited during voluntary or reflex actions follow a specified order proceeding from smallest to largest. This is known as the size-principle and is explained by the rheobase current for motoneurons as well as the organization of synaptic input to motoneurons (Cope and Pinter, 1995). The smallest, slowest motor units receive a more tonic activity pattern while the largest and fastest motor units are reserved for a more phasic pattern. Thus, the size-principle engenders muscle fibre phenotype based upon the cumulative daily activity pattern of individual motor units (Kernell et al., 1987).

The overall goal of this study was to assess the long-term effects of ISMS on the functional characteristics and phenotypic make up of muscles that had been paralyzed due to a complete ST. We reasoned that if ISMS could recruit motoneurons in a more normal order, as we have shown previously (Mushahwar and Horch, 2000; Bamford et al., 2005; Snow et al., 2006), this would lead to a maintenance of the mixed phenotype in the rat quadriceps muscle since the activity patterns delivered to small and large motor units would be similar to their normal tonic and phasic activity patterns, respectively. Conversely, we hypothesized that because of the reversed recruitment order of NCS, its chronic application would lead to a

slow-to-fast fibre-type transformation in the quadriceps muscle, leaving it with predominantly slow twitch characteristics.

We found that chronic ST resulted in a mild slow-to-fast transformation in contralateral, unstimulated ISC and NCC legs. The extent of this transformation was limited by the fact that rat quadriceps muscles already demonstrate a fast phenotypic profile which cannot be made substantially faster (Bamford et al., 2005). Both ISMS and NCS legs showed nearly identical slowing of quadriceps function and corresponding fast-to-slow transformations in rectus femoris muscle. This suggests that the nature of the transformations produced by these different stimulation paradigms was similar in many respects, a result we did not anticipate given that findings in acute experiments showed that NCS recruits greater force than ISMS and the recruitment of force is more gradual with ISMS than NCS (Bamford et al., 2005).

Several explanations could account for this unanticipated finding. These include: 1) location of the microwire tips outside the ventral grey matter; 2) loss of recruitment order due to ST or chronic stimulation; 3) damage of fibres-in-passage in the grey matter due to microwire implantation and chronic ISMS; 4) delayed onset of stimulation relative to the time of complete ST; and 5) the stimulation paradigm used.

3.4.2 Location of ISMS microwire tips

One of the main characteristics of ISMS is its recruitment of motor units in a near normal order based on their size, resulting in graded production of force with increments of stimulus amplitude (Mushahwar and Horch, 1998; Mushahwar et al., 2007). This is achieved when the microwire tips are placed within the grey matter of the ventral horn. This characteristic is lost if the microwire tips are advanced ventrally beyond the grey matter and placed in the white matter. More specifically, if the microwire tips are positioned ventrally in the white matter, a steep generation of force is obtained mimicking that seen with NCS. As such, this differentiation between placement in the grey and white matter of the ventral spinal cord can be used to determine the proper positioning of the microwires in each implant. Given the apparent similarity in motor unit recruitment between ISMS and NCS when ISMS is applied in the ventral white matter, the fast-to-slow muscle fibre-type transformation seen after thirty days of ISMS could be explained by inappropriate targeting of microwire tips.

The locations of implanted pulsed and unpulsed intraspinal microwires were verified directly in cross-sectional slices of the spinal cord (figure 1). Of 24 microwires a total of 16 were located on stained tissues. Seven (7) of the identified tips were from pulsed microwires. Some sections containing the unlocated microwire tips were presumably lost during tissue processing. Since the diameter of implanted microwires is only 30 μm it is possible that the loss of a few 20 μm thick tissue sections in cer-

tain areas would make the localization of microwire tips impossible. Without direct localization of the remaining 8 microwire tips (including 5 pulsed) it is impossible to be certain whether or not they were properly implanted in the ventral grey matter. Nonetheless, as shown in figure 1, all of the located microwire tips were in the ventral grey horn. In addition, since all microwires were 1.5 mm in depth, the range of microwire tip locations was limited to an area of the rat spinal cord dominated by the ventral grey horn. Finally, during the microwire implantation procedure, test stimulus trains were used to ensure that the quadriceps muscle was activated selectively and that force was recruited in a gradual manner. These hallmarks of ISMS indicate that microwire tips were indeed located in the ventral grey matter in or near the quadriceps motoneuron pool. Given these factors it seems likely that the unlocated microwire tips were placed in the ventral grey matter as 16 of the 24 microwires were determined to be.

3.4.3 Recruitment order after ST and chronic stimulation

Although the pattern of ordered recruitment of motor units according to size is often treated as immutable, there are studies showing exceptions to the principle of ordered recruitment following denervation and reinnervation of a muscle (Gordon et al., 2004). Similarly, following spinal transection or hemisection in cats ordered recruitment of motor units can be lost and a disordered recruitment profile can be observed transiently (Heckman, 1994; Durkovic, 2006). Although the reasons for disrupted re-

cruitment order are uncertain, it may be explained by an increase in the magnitude of heteronymous EPSPs to extensor motoneuron pools following transection (Frigon and Rossignol, 2006). One report of this phenomenon also suggested that the increase in EPSPs is largest in fast-fatiguable and fast, fatigue-resistance motoneurons shortly after transection (Munson et al., 1986). The size of EPSP magnitude does return to normal after several months, a time course which roughly coincides with the return of an ordered recruitment pattern.

In the current work a reversal or disordering of motor unit recruitment might explain the results in the ISMS animals. Although ISMS activates motoneurons in a near-normal order in intact animals (Bamford et al., 2005), a reversal of recruitment following spinal transection would cause the preferential activation of the largest and fastest motor units as occurs with the nerve cuff. However, the mean slope of recruitment curves generated from quadriceps muscle via the nerve cuff in the ISMS animals was 3.4 fold sharper than those recruited through ISMS microwires in the same muscles (figure 12). In addition, the mean slope of the recruitment curves generated through ISMS microwires after transection and thirty days of stimulation was nearly identical to the previously reported mean slope generated through ISMS microwires in intact animals (Bamford et al., 2005). It remains possible that recruitment order is transiently altered following transection, as other authors have shown (Durkovic, 2006), and that normal recruitment order is reestablished by this time point.

Damage of fibers-in-passage after chronic ST and ISMS

The orderly recruitment of motor units seen with ISMS is due to its preferential activation of fibres-in-passage in the ventral horn which in turn activate the motoneurons trans-synaptically (Gaunt et al., 2006; Mushahwar et al., 2007). These fibres-in-passage include afferent projections into the ventral horn, propriospinal neurons and interneurons. Damage to such fibre-in-passage systems due to chronic ST or chronic stimulation could preclude ISMS from activating motoneurons trans-synaptically, essentially stripping it of its ability to recruit motor units in a normal physiological order. In the absence of fibres-in-passage, ISMS would act in a manner similar to NCS and would impose a reversed recruitment order on the motoneurons, an event that would explain the similarity of functional and phenotypic fast-to-slow transformations seen in the quadriceps muscle using both stimulation methods.

While some damage of fibres-in-passage may have occurred due to the insertion of microwires in the spinal cord and chronic ISMS, it was probably minor and insufficient to account for the similar muscle transformations induced by ISMS and NCS. The absence of appreciable damage is demonstrated by the preserved pattern of graded force generation produced by ISMS in chronically transected animals that had received thirty days of microwire implantation and stimulation (figure 12).

3.4.4 Onset of stimulation relative to time of ST

In the present study, ISMS and NCS were introduced 3 weeks following a complete T8 spinal cord transection, by which time ample muscle atrophy would have occurred along with slow-to-fast fibre-type transformation. Therefore, it is possible that neuronal properties would have been substantially altered by then resulting in pools of motoneurons with more homogenous passive and active properties (Heckmann et al., 2005). Such homogeneity would collapse the differences in membrane properties between various types of motoneurons and lead to near equal probability of activation of fast and slow motor units. ISMS and NCS would subsequently produce similar activation profiles of the motor units, leading to similar functional and phenotypic transformations.

While this is plausible, it cannot explain the preserved force generation characteristics produced in chronically transected animals (figure 12). After chronic ST and ISMS, gradual force recruitment could still be attained through ISMS indicating a differential recruitment of slow (small) and fast (large) motoneurons. Thus, changes in passive and active motoneuronal membrane properties that may have taken place after 3 weeks of ST may either have not been substantial enough to collapse the differential activation properties of small and large motoneurons, or were reversed after thirty days of ISMS.

3.4.5 Pattern of quadriceps activation through ISMS and NCS

According to Kernell et. al. the impetus for the transformation of motor units arises from the daily amount of activity imposed upon the

muscle (Kernell et al., 1987). Given that both ISMS and NCS underwent similar fast-to-slow transformations it is possible that both stimulation paradigms were activating a similar proportion of their motor units, both large and small. In the case of NCS the reversed recruitment order makes this almost certain since the whole population of motor units are recruited over a very small range of stimulus amplitudes. Furthermore, the instability of force evoked by the nerve cuff at submaximal stimulation levels makes stimulation at supramaximal levels, and the concomitant activation of all motor units, the only option for achieving stable force. The reversed recruitment order and need for supramaximal stimulation levels impose a tonic activity profile upon large, phasic motor units.

Since ISMS is capable of recruiting stable submaximal force it was anticipated that chronic stimulation with ISMS would maintain a relatively normal, mixed population of muscle fibres since the largest, motor units would not be activated. However, ISMS levels in this study were chosen to provide muscle contractions that resembled those obtained by NCS as closely as possible. Given that the transformation of ISMS muscle is so similar to that of NCS muscle it seems likely that the majority of motor units in the quadriceps muscle were recruited by ISMS leading to the same transformation seen with NCS. This can be supported by the fact that large forces can be evoked by trains of ISMS delivered through individual microwires (Mushahwar and Horch, 2000; Mushahwar et al., 2000; Snow et al., 2006).

Furthermore, it has been shown that activation of CNS tissues can be accomplished at very low stimulation amplitudes (Jankowska and Roberts, 1972). This corresponds to the finding that ISMS can activate tissues at lower stimulus thresholds than other FES methods (Mushahwar et al., 2004). Chronically, ISMS stimulus thresholds have been shown to increase in the first 10 days following implantation but remain stable thereafter (Mushahwar et al., 2000). In the current work we found that ISMS thresholds dropped significantly over the thirty day stimulation period while those for NCS did not. This result was unexpected in light of the previous work showing no changes in ISMS threshold; however, the previous work did not entail daily stimulation. Decreases in the threshold for ISMS over time will cause the recruitment of more motor units at the same stimulus amplitudes, thus expanding the population of recruited motor units in the quadriceps pool.

It is possible that the decrease in threshold for ISMS represents a plastic adaptation similar to those adaptations seen during training in chronically transected cats and rats (Edgerton et al., 2004). Transected spinal cords show an increase in inhibition which can be reversed with training or pharmacological intervention. Lowered stimulus threshold following chronic ISMS is likely explained by a similar mechanism whereby electrically induced spinal cord training results in more easily activated circuitry.

While full recruitment of motor units in the ISMS animals is likely a main contributor to the unanticipated fast-to-slow transformations in the quadriceps muscle, these effects are further compounded by the duration of daily activation. Four hours of continuous stimulation is in retrospect inappropriate for maintaining a mixed muscle phenotype. This duration of activation is akin to an endurance training paradigm in marathon runners, a population with proportionally higher representation of type-I and IIA fibre types in their leg muscles (Fitts and Widrick, 1996).

3.4.6 Summary and future directions

Thirty days of stimulation with either intraspinal microwires or a nerve cuff induced similar fast-to-slow transformations as measured by isometric twitch speed measures, sag profile and MHC content in rectus femoris muscles. This was surprising in light of a number of studies in intact and spinalized animals showing that ISMS recruits gradual, fatigue resistant force suggesting a more normal recruitment order. We verified directly the near-normal recruitment order of ISMS in an acute rat model and showed that recruitment order did not change in the ISMS animals used in the current work. Although it remains possible that there was a transient alteration of recruitment properties following transection, the most likely explanation for the current results is that the populations of motor units recruited by both NCS and ISMS were nearly identical. This led to the dramatic and similar fast-to-slow transformations in both stimulated legs. In the future, ISMS should be used to produce submaximal con-

tractions. Stable contraction levels at forces below 50% of maximal voluntary activation are easily achievable with ISMS in contrast to peripheral FES approaches (e.g. figure 12). Such contraction levels are more representative of the natural recruitment order and activation paradigms utilized for achieving the majority of daily activities (Henneman and Mendell, 1981). Furthermore, contractions against resistive loads as is the case in weight-bearing locomotion could also be applied to reduce the extent of muscle atrophy (Roy et al., 2002).

3.5 Tables and Figures

Table 3-1. Summary of Muscle Mass and Contractile Characteristics

	Intact		Intraspinal		Nerve Cuff
	Control	Stim	Control	Stim	Control
Mass (g)	3.36 ± 0.30	1.41 ± 0.46 (a)	1.74 ± 0.58 (a)	1.57 ± 0.23 (a,b)	2.07 ± 0.14 (a)
Force (N)	2.91 ± 1.65	2.14 ± 0.75	1.84 ± 0.97	2.99 ± 0.95	1.92 ± 0.63
TWFn (N/g)	0.85 ± 0.43	1.57 ± 0.54	1.05 ± 0.37	1.91 ± 0.60 (a,b)	0.94 ± 0.32
Fatigue Ratio	0.49 ± 0.03	0.51 ± 0.09	0.34 ± 0.16	0.46 ± 0.08 (b)	0.27 ± 0.09 (a)
Sag/No Sag	5 / 1	1 / 5	5 / 1	0 / 6	6 / 0

Quadriceps muscle mass, TWFn, fatigue ratio and sag test results are displayed above (mean ± SD). Muscle mass decreased in all treatment groups. TWFn was increased in the NCS group but not the ISMS group when compared to IC. Both NCS and ISMS stimulation groups showed fatigue ratios that were not different from IC. (a) significantly different from intact control, (b) significantly different from contralateral leg

Table 3-2. Summary of fibre cross-sectional area in the rectus femoris muscle of the control and electrically stimulated legs

	Intact	Nerve Cuff		Intraspinal	
	Control (μm^2)	Control (μm^2)	Stim (μm^2)	Control (μm^2)	Stim (μm^2)
Type-I	1327.7 ± 491.2	1073.9 ± 287.7	964.4 ± 204.5	1453.2 ± 767.5	1295.4 ± 55.7
Type-IIA	1518.1 ± 553.2	1261.5 ± 233.4	908.0 ± 214.2	1069.9 ± 405.9	1003.1 ± 318.2
Type-IID	4067.6 ± 1391.9	2911.1 ± 505.7	1529.1 ± 344.5 (a)	2528.7 ± 1481.5	1664.2 ± 470.4 (a)
Type-IIB	2946.8 ± 1092.8	1921.6 ± 342.0	1241.4 ± 395.4 (a)	1829.6 ± 922.0	1241.3 ± 424.5 (a)
Type-I/IIA	890.6 ± 668.0	945.7 ± 155.1	747.1 ± 142.3	981.8 ± 379.1	708.3 ± 290.2
Type-IIA/IIB	NA	1017.5 ± 488.6	1240.3 ± 246.9	1092.3 ± 602.6	1426.4 ± 444.1

Mean cross-sectional areas for each fiber type are displayed. Both NCS and ISMS stimulation legs showed a significant decrease in mean fiber cross-sectional area for type-IID and type-IIB fibers relative to intact control. (a) different from intact control

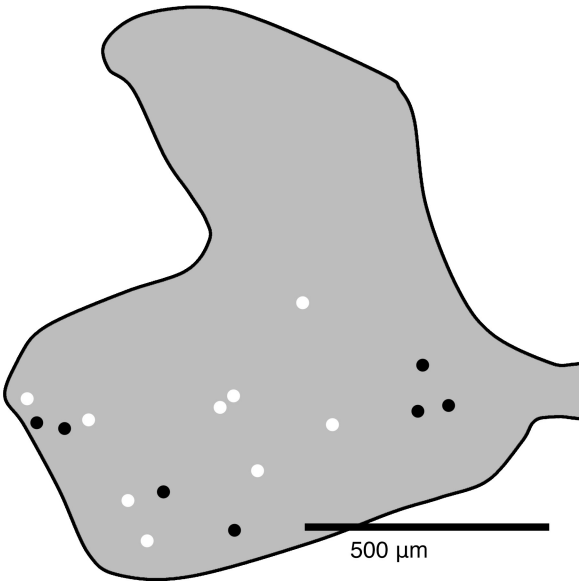

Figure 3-1. Microwire tip locations in the ventral horn

The locations of stimulated and sham implanted microwire tips were identified in immunostained spinal cord tissue sections and a composite diagram was created to show their locations. We located 16 of 24 microwire tips. We discovered 9 from unpulsed microwires (shown in white) and 7 from pulsed microwires (shown in black). All tips were found within the grey matter of the ventral horn.

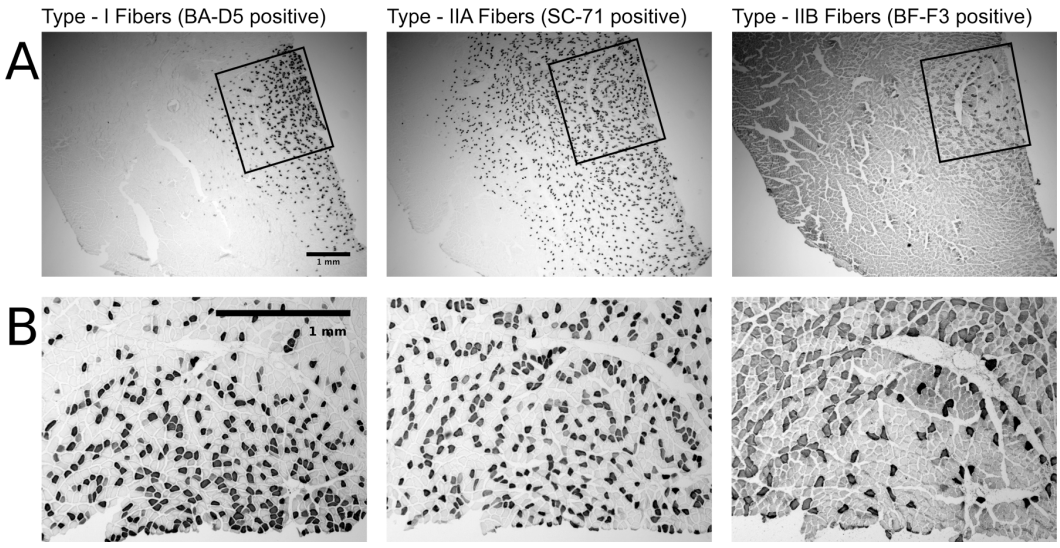

Figure 3-2. Selection of muscle areas for analysis.

The deepest and slowest areas of rectus femoris muscles were chosen for analysis because these areas contain a mixed content of myosin heavy chain (MHC) type-I, -IIA, -IID and –IIB fibers. Due to their heterogeneous mixture these areas are best suited to show both slow-to-fast and fast-to-slow transformations in MHC-based phenotype. A) Representative serial examples of the same intact control muscle at 1.6X magnification stained with a panel of antibodies for adult MHC. Rectangles demonstrate the area selected for analysis of fibers that contains the greatest concentrations of type-I and –IIA fibers and the lowest concentration of type-IIB fibers. B) The selected areas from (A) are shown here at 5X magnification. In intact control muscles this magnification allowed for the analysis of approximately 500 fibers from each muscle. The panel of antibodies allowed for the identification of stained pure type-I, -IIA, -IIB and, if no staining was detected, pure type-IID fibers. Hybrid fibers containing more than one MHC isoform (e.g. type-I/IIA fibers) were also identified

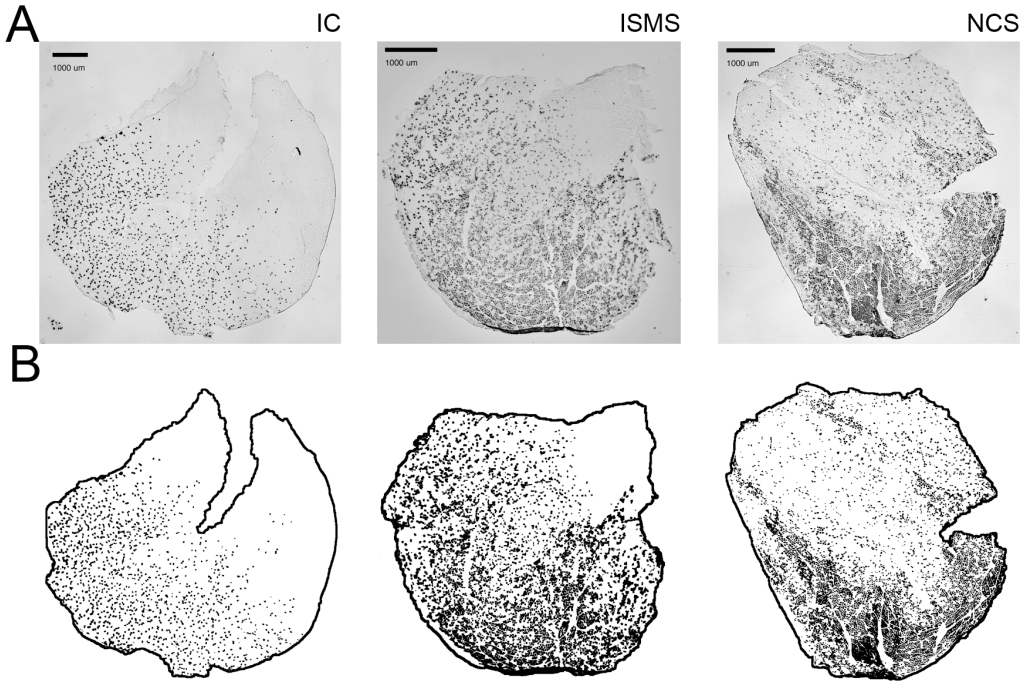

Figure 3-3. Whole muscle analysis of MHC IIA fibres in rectus femoris muscles.

Whole muscle analysis of MHC IIA fibres was performed on rectus femoris muscles. Whole muscle images (A) were binarized so that stained pixels were rendered completely black and all other pixels white (B). Image analysis software was used to quantify black pixels and express them as a fraction of all pixels within the muscle boundary.

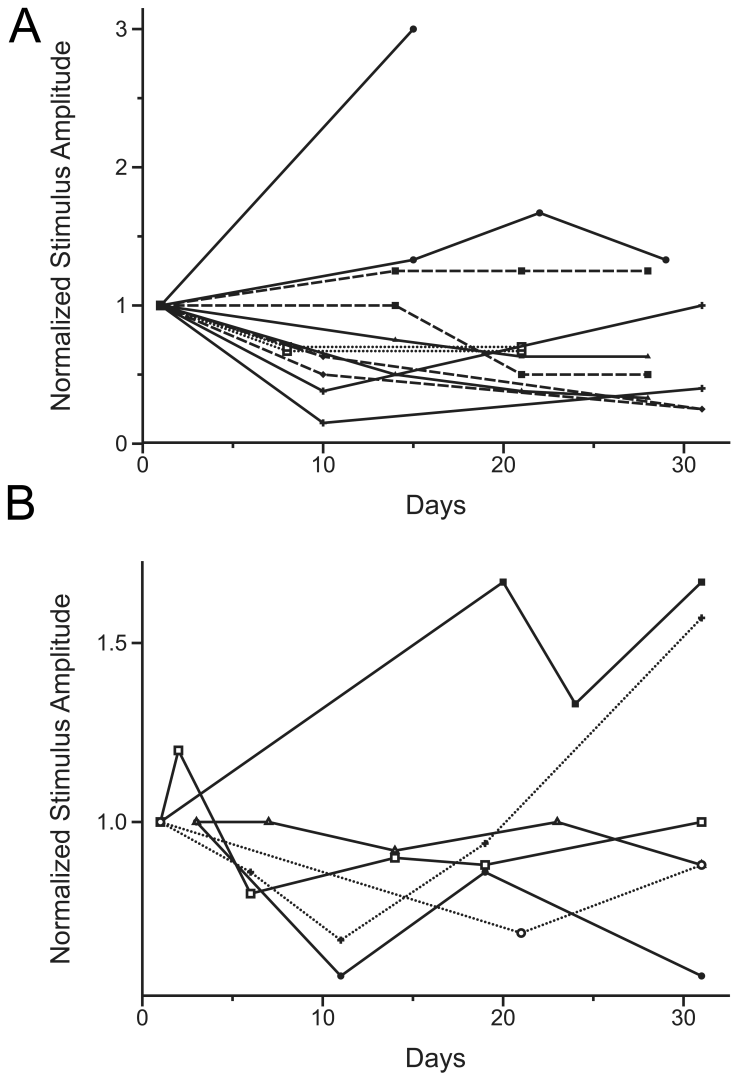

Figure 3-4. Stimulation thresholds for muscle activation.

Stimulation thresholds for muscle activation. Plots show threshold amplitudes normalized to the first day of stimulation for each microwire. Threshold is defined as the lowest stimulation amplitude which produces a visible muscle twitch. Threshold amplitudes for activation in intraspinal microwires (A) and nerve cuff electrodes (B) were noted throughout the thirty day stimulation period. For the ISMS thresholds in A, microwires from the same animal are displayed with paired symbols and line formats.

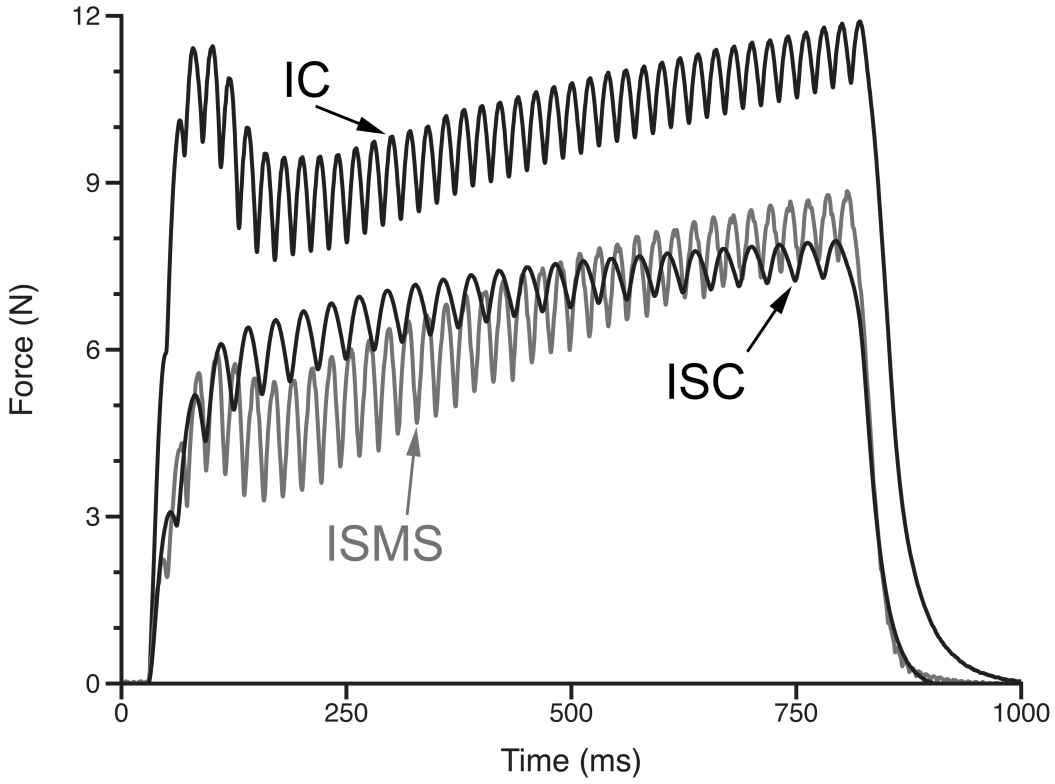

Figure 3-5. Examples of sag profiles in stimulated and unstimulated legs

Whole muscle unfused contractions due to stimulus trains with inter-pulse intervals of 1.25 x TTP were used to detect the presence or absence of sag. The IC and ISC legs show early potentiation of muscle force followed by sag indicating fast whole muscle twitch properties. The ISMS leg force trace shows potentiation of force with the absence of sag indicating slow whole muscle twitch properties. The ISC and ISMS examples are representative of all unstimulated and stimulated legs, respectively. Based upon the presence of sag (e.g. the IC and ISC unstimulated legs), or the absence of sag (e.g. the ISMS stimulated leg), force responses were categorized as 'sag' or 'no sag'. The results of this classification are in table 1.

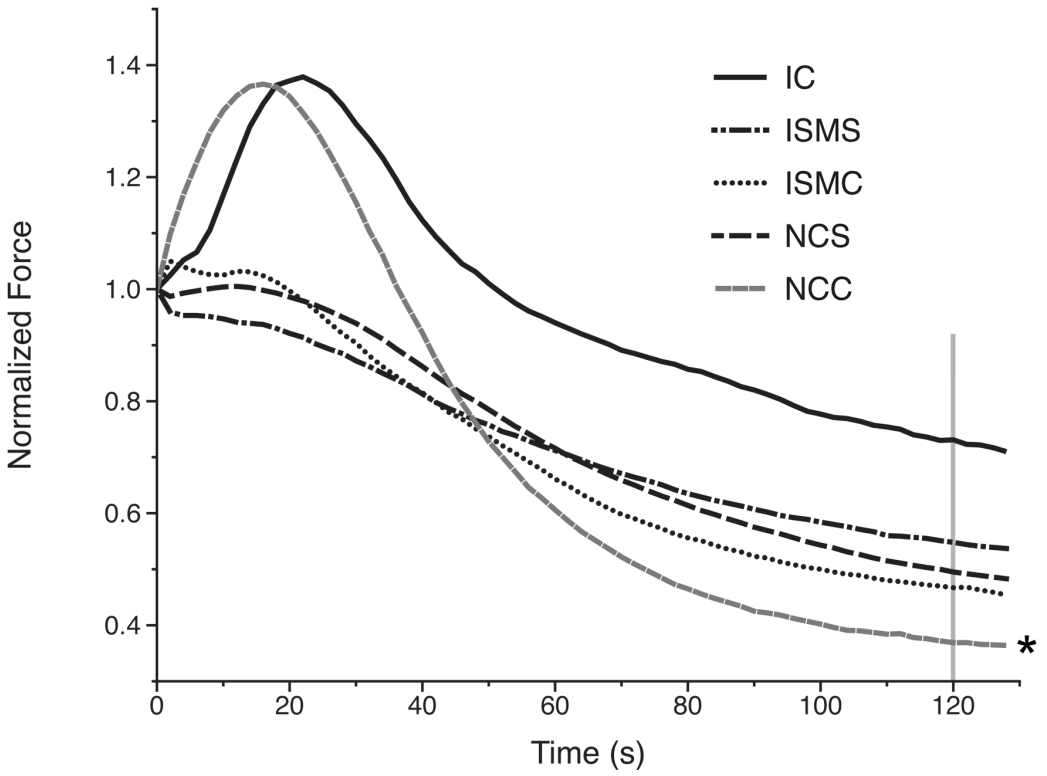

Figure 3-6. Fatigue profiles of forces evoked by repeated 40 Hz stimulus

Group mean forces are normalized to their respective mean peak force. Shown are force means from intact control (IC) legs, transected but unstimulated contralateral nerve cuff (NCC) and intraspinal (ISC) legs, and transected and stimulated nerve cuff (NCS) and intraspinal microstimulation (ISMS) legs. A fatigue ratio was calculated by dividing the force at 120 s by the peak force. Only the NCC legs showed a significant decline in fatigue index relative to NCS and IC legs (*). Fatigue ratio data for all legs is shown in table 1.

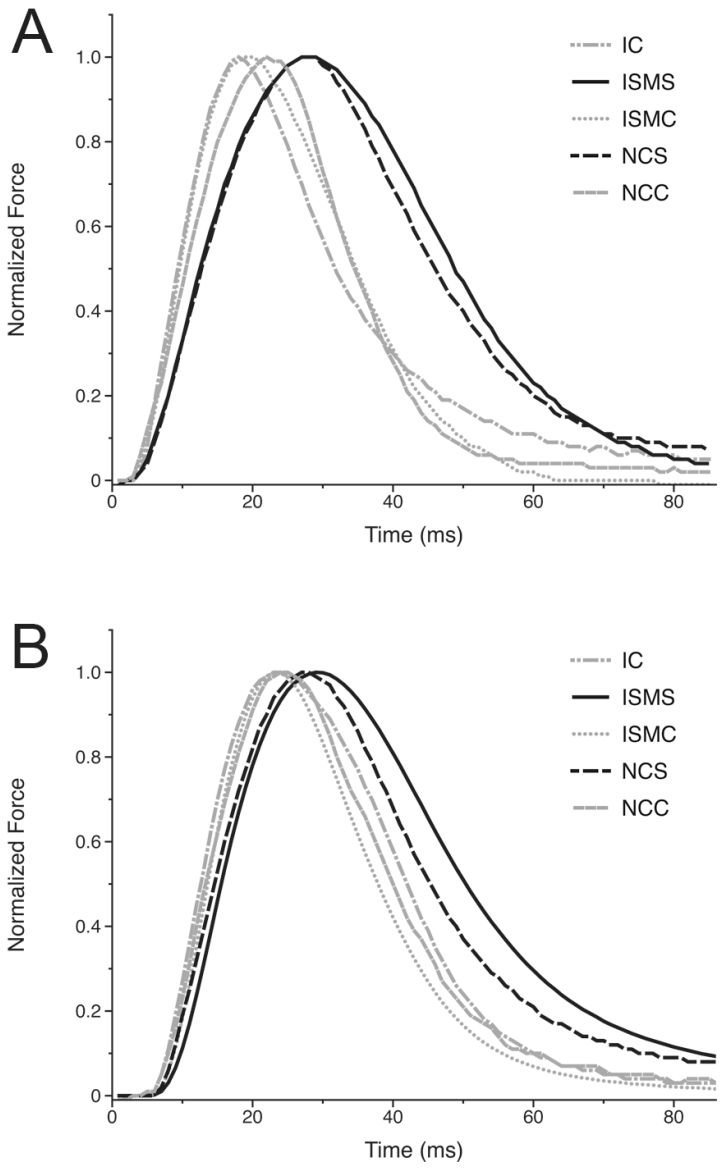

Figure 3-7. Normalized twitch force.

Graphs showing representative examples of (A) individual twitches normalized to their respective peak force and (B) group means normalized to their respective mean peak force. The traces are from intact control (IC) legs, transected but unstimulated nerve cuff (NCC) and intraspinal (ISC) control legs, and transected and stimulated nerve cuff (NCS) and intraspinal microstimulation (ISMS) legs.

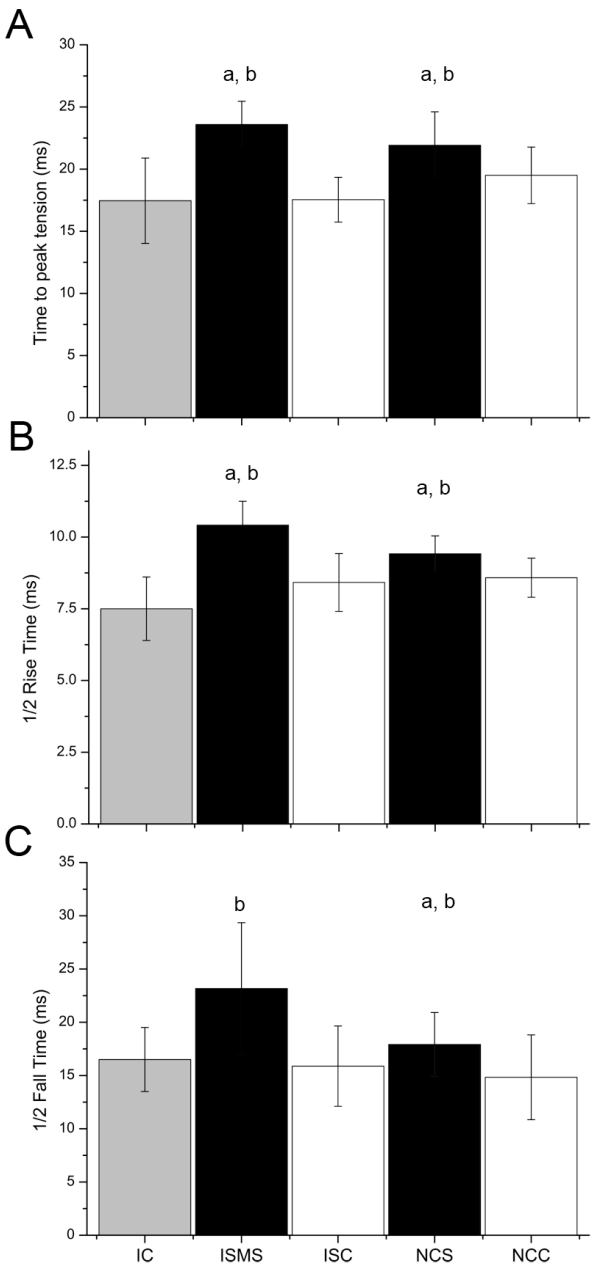

Figure 3-8. Summary of twitch width results.

(A) TTP increased in duration in both NCS and ISMS legs compared to NCC and ISMS control legs and the IC leg. (B) 1/2RT increased in both NCS and ISMS legs compared to NCC, ISC and IC legs. (C) 1/2FT increased in NCS and ISMS legs as compared to the NCC and ISMS legs. Only the ISMS legs showed a significant increase in 1/2FT compared to the IC leg. (a) different from intact control, (b) different from contralateral control

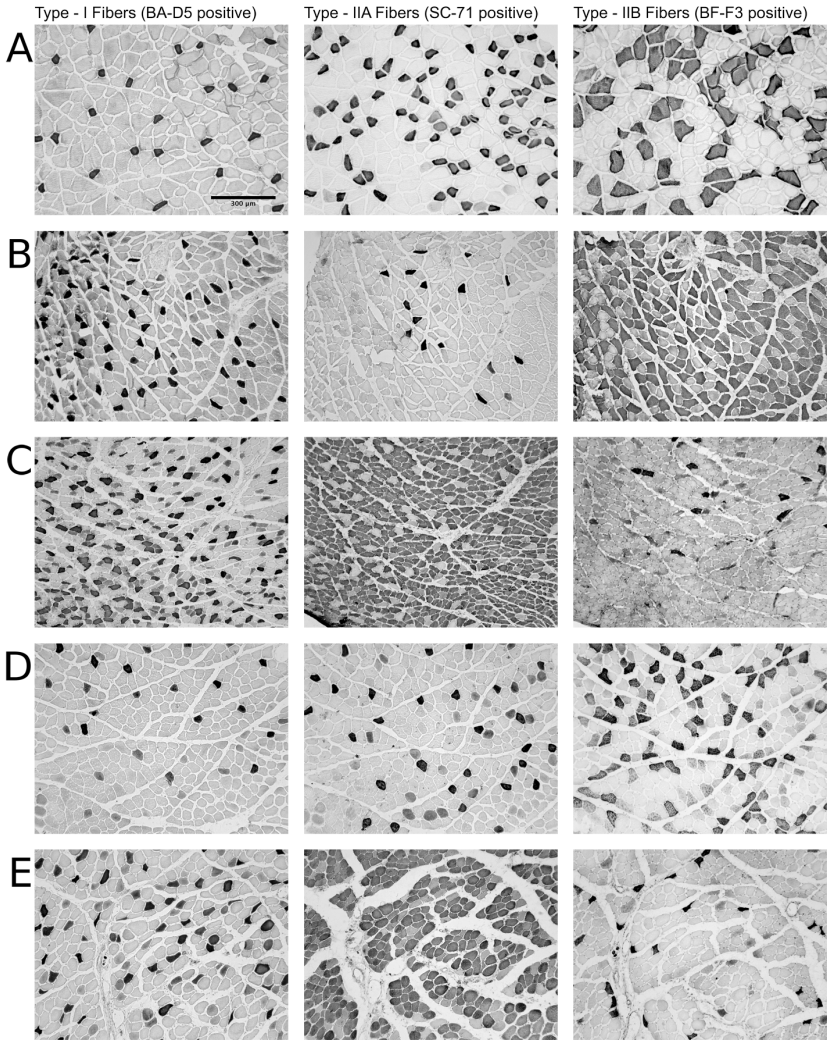

Figure 3-9. Myosin heavy chain (MHC) immunohistochemistry.

Representative examples of MHC staining from rectus femoris muscles at 5X magnification. (A) Intact control legs show a mixed phenotype with a preponderance of MHC type-IIB and unstained -IID fibers. Following spinal cord transection, unstimulated nerve cuff control (B) and intraspinal microwire control (D) legs show increases in MHC type-IIB fiber content and decreases in MHC type-IIA fiber content. Thirty days of stimulation through a nerve cuff (C) or intraspinal microwires (E) causes an increase in MHC type-IIA fiber content and a decrease in MHC type-IID content.

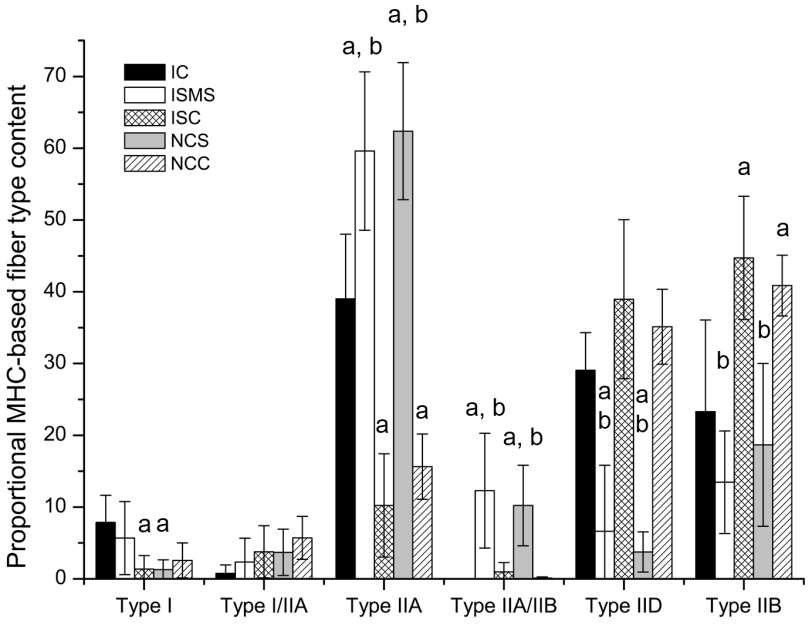

Figure 3-10. Proportional MHC-based fiber types from slow areas of rectus femoris.

Stimulation with either NCS or ISMS caused a fast-to-slow conversion as demonstrated by increases in type-IIA fiber content and corresponding decreases in type-IID fiber content as compared to the IC leg. Control NCC and ISC legs showed a slow-to-fast conversion as demonstrated by increases in type-IIB fiber content and decreases in type-IIA fiber content. (a) different from intact control, (b) different from contralateral control

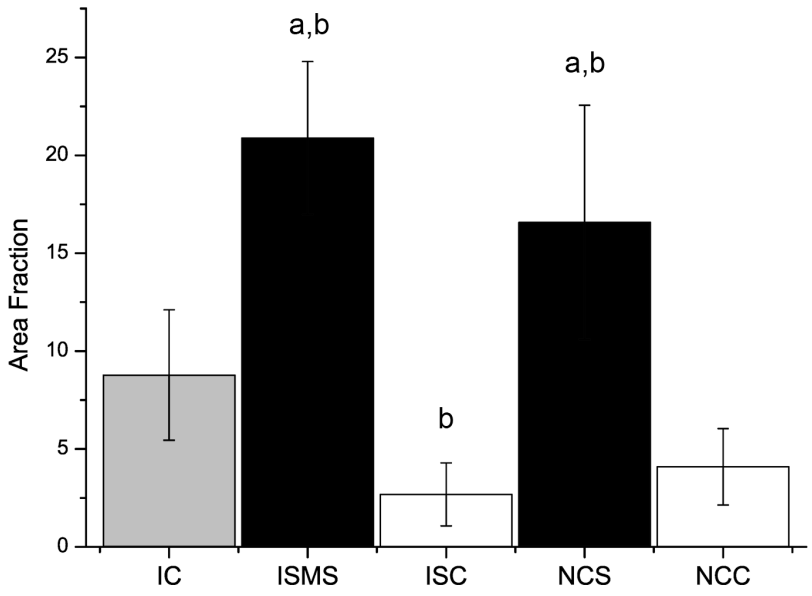

Figure 3-11. Whole muscle analysis of MHC IIA in rectus femoris

Whole muscle analysis of MHC IIA content showed an increase in IIA content in stimulated ISMS and NCS legs compared to control legs ISC and NCC and to the IC leg. (a) significantly different from intact control, (b) significantly different from contralateral control

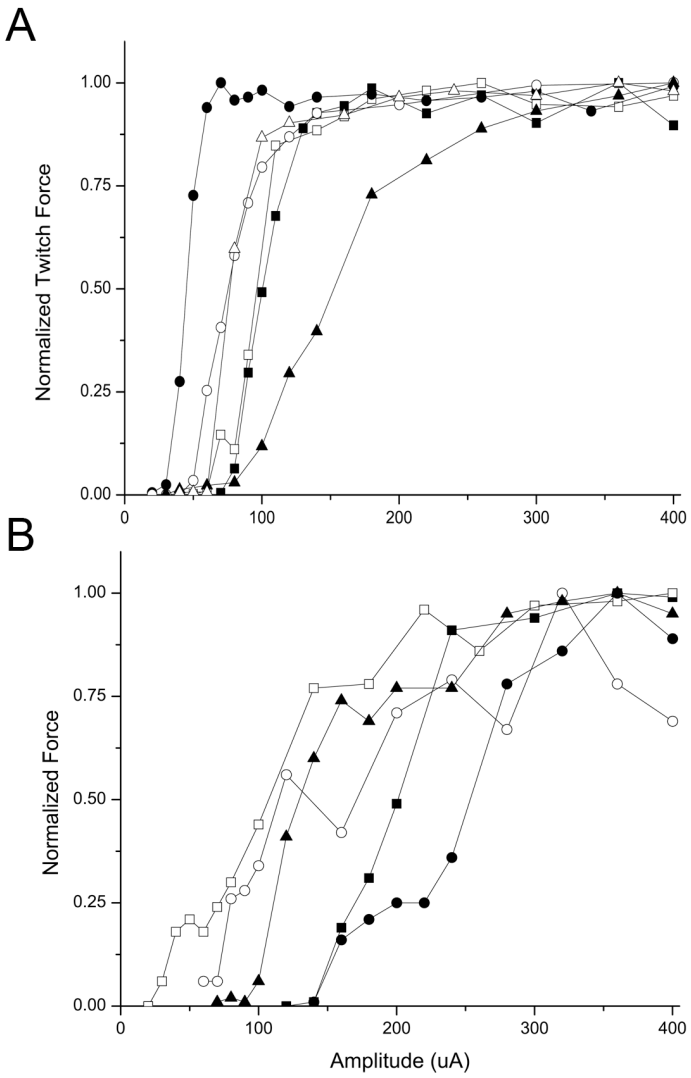

Figure 3-12. Recruitment Curves after ST and 30 days of stimulation

Normalized force recruited from A) 5 nerve cuffs or B) 5 ISMS microwires after 30 days of stimulation. Graphs show force recruited by 1 second long 50 pps trains of randomly assigned amplitudes. The mean slope of the force recruited from 10% to 90% of peak force was 3.4 fold sharper in the nerve cuff group.

3.6 Bibliography

Allen DG Lamb G & Westerblad H (2008) Skeletal muscle fatigue: cellular mechanisms. Physiol Rev, 88:287-332.

Andersen JL Mohr T Biering-Sorensen F Galbo H & Kjaer M (1996) Myosin heavy chain isoform transformation in single fibres from m. vastus lateralis in spinal cord injured individuals: effects of long-term functional electrical stimulation (FES). *Pflugers Arch***431**, 513-518.

Bamford JA Putman CT & Mushahwar VK (2005) Intraspinal microstimulation preferentially recruits fatigue-resistant muscle fibres and generates gradual force in rat. *J Physiol***569**, 873-884.

Burke RE Levine DN & Zajac FE, 3rd (1971) Mammalian motor units: physiological-histochemical correlation in three types in cat gastrocnemius. *Science***174**, 709-712.

Cope T & Pinter M (1995) The Size Principle: Still Working After All These Years. *News in Physiological Sciences News Physiol Sci***10**, 280-286.

Cuoco FA, Jr. & Durand DM (2000) Measurement of external pressures generated by nerve cuff electrodes. *IEEE Trans Rehabil Eng***8**, 35-41.

Dudley-Javoroski S & Shields R (2008) Muscle and bone plasticity after spinal cord injury: Review of adaptations to disuse and to electrical muscle stimulation. *J Rehabil Res Dev***45**, 283-296.

Durkovic R (2006) Functional consequences of motor unit recruitment order reversals following spinal cord transection in cat. *Somatosens Mot Res***23**, 25-35.

Edgerton V Tillakaratne N Bigbee A De Leon RD & Roy RR (2004) Plasticity of the spinal neural circuitry after injury. *Annu Rev Neurosci***27**, 145-167.

Fitts R & Widrick J (1996) Muscle mechanics: adaptations with exercise-training. *Exerc Sport Sci Rev***24**, 427-473.

Frigon A & Rossignol S (2006) Functional plasticity following spinal cord lesions. *Prog Brain Res***157**, 231-260.

Gallo M Gordon T Tyreman N Shu Y & Putman C (2004) Reliability of isolated isometric function measures in rat muscles composed of different fibre types. *Exp Physiol***89**, 583-592.

Gaunt RA Prochazka A Mushahwar VK Guevremont L & Ellaway PH (2006) Intraspinal Microstimulation Excites Multisegmental Sensory Afferents at Lower Stimulus Levels Than Local α?-Motoneuron Responses. *J Neurophysiol***96**, 2995-3005.

Gerrits H De Haan A Sargeant A Dallmeijer A & Hopman M (2000) Altered contractile properties of the quadriceps muscle in people with spinal cord injury following functional electrical stimulated cycle training. *Spinal Cord***38**, 214-223.

Gordon T Thomas CK Munson JB & Stein RB (2004) The resilience of the size principle in the organization of motor unit properties in normal and reinnervated adult skeletal muscles. *Can J Physiol Pharmacol***82**, 645-661.

Guevremont L Renzi C Norton J Kowalczewski J Saigal R & Mushahwar V (2006) Locomotor-related networks in the lumbosacral enlargement of the adult spinal cat: activation through intraspinal microstimulation. *IEEE Trans Neural Syst Rehabil Eng***14**, 266-272.

Hämäläinen N & Pette D (1997) Coordinated fast-to-slow transitions of myosin and SERCA isoforms in chronically stimulated muscles of euthyroid and hyperthyroid rabbits. *J Muscle Res Cell Motil***18**, 545-554.

Harris RL Putman C Rank M Sanelli L & Bennett D (2007) Spastic tail muscles recover from myofiber atrophy and myosin heavy chain transformations in chronic spinal rats. *J Neurophysiol***97**, 1040-1051.

Heckman C (1994) Alterations in synaptic input to motoneurons during partial spinal cord injury. *Med Sci Sports Exerc***26**, 1480-1490.

Heckmann CJ Gorassini MA & Bennett DJ (2005) Persistent inward currents in motoneuron dendrites: implications for motor output. *Muscle Nerve***31**, 135-156.

Henneman E & Mendell LM. 1981 Functional organization of motoneuron pool and its inputs. In Vol II, Motor Control, VD Brooks,Ed American Physiological Society.

Jankowska E & Roberts W (1972) An electrophysiological demonstration of the axonal projections of single spinal interneurones in the cat. *J Physiol***222**, 597-622.

Kernell D Eerbeek O Verhey BA & Donselaar Y (1987) Effects of physiological amounts of high- and low-rate chronic stimulation on fast-twitch muscle of the cat hindlimb. I. Speed- and force-related properties. *Journal of Neurophysiology***58**, 598-613.

Lau B Guevremont L & Mushahwar V (2007) Strategies for generating prolonged functional standing using intramuscular stimulation or intraspinal microstimulation. *IEEE Trans Neural Syst Rehabil Eng***15**, 273-285.

Munson J Foehring R Lofton S Zengel J & Sypert G (1986) Plasticity of medial gastrocnemius motor units following cordotomy in the cat. *J Neurophysiol***55**, 619-634.

Mushahwar VK Collins DF & Prochazka A (2000) Spinal cord microstimulation generates functional limb movements in chronically implanted cats. *Exp.Neurol***163**, 422-429.

Mushahwar VK & Horch KW (2000) Muscle recruitment through electrical stimulation of the lumbo-sacral spinal cord. *IEEE Trans.Rehabil.Eng***8**, 22-29.

Mushahwar V Aoyagi Y Stein R & Prochazka A (2004) Movements generated by intraspinal microstimulation in the intermediate gray matter of the anesthetized, decerebrate, and spinal cat. *Can J Physiol Pharmacol***82**, 702-714.

Mushahwar V & Horch K (1998) Selective activation and graded recruitment of functional muscle groups through spinal cord stimulation. *Ann N Y Acad Sci***860**, 531-535.

Mushahwar V Jacobs P Normann R Triolo R & Kleitman N (2007) New functional electrical stimulation approaches to standing and walking. *J Neural Eng***4**, S181-97.

Nicolopoulos-Stournaras S & Iles J (1983) Motor neuron columns in the lumbar spinal cord of the rat. *J Comp Neurol***217**, 75-85.

Pette D & Staron RS (2001) Transitions of muscle fiber phenotypic profiles. *Histochem.Cell Biol***115**, 359-372.

Pette D & Vrbova G (1999) What does chronic electrical stimulation teach us about muscle plasticity? *Muscle Nerve***22**, 666-677.

Roy RR Talmadge R Hodgson J Zhong H Baldwin K & Edgerton V (1998) Training effects on soleus of cats spinal cord transected (T12-13) as adults. *Muscle Nerve***21**, 63-71.

Roy RR Zhong H Hodgson J Grossman E Siengthai B Talmadge R & Edgerton V (2002) Influences of electromechanical events in defining skeletal muscle properties. *Muscle Nerve***26**, 238-251.

Saigal R Renzi C & Mushahwar VK (2004) Intraspinal microstimulation generates functional movements after spinal-cord injury. *IEEE Trans.Neural Syst.Rehabil.Eng***12**, 430-440.

Sedgewick J (2008) Scientific imaging with Photoshop: methods, measurement, and output. New Riders, Berkeley, CA.

Snow S Horch K & Mushahwar V (2006) Intraspinal microstimulation using cylindrical multielectrodes. *IEEE Trans Biomed Eng***53**, 311-319.

Talmadge RJ (2000) Myosin heavy chain isoform expression following reduced neuromuscular activity: potential regulatory mechanisms. *Muscle Nerve***23**, 661-679.

Talmadge RJ Roy RR Caiozzo VJ & Edgerton VR (2002) Mechanical properties of rat soleus after long-term spinal cord transection. *J.Appl.Physiol***93**, 1487-1497.

Talmadge R Roy RR & Edgerton V (1999) Persistence of hybrid fibers in rat soleus after spinal cord transection. *Anat Rec***255**, 188-201.

Yakovenko S Kowalczewski J & Prochazka A (2007) Intraspinal stimulation caudal to spinal cord transections in rats. Testing the propriospinal hypothesis. *J Neurophysiol***97**, 2570-2574.

Chapter 4

Chronic intraspinal microstimulation causes limited damage and inflammation in rat[‡]

4.1 Introduction

Spinal cord injury represents a devastating neurological impairment with potentially life-threatening implications. Following a spinal cord injury, a host of challenges to quality of life arise and typically involve impaired bladder and bowel function, respiration, skin and muscle health, freedom of movement, and general independence. Previous interventions have applied functional electrical stimulation (FES) to address these problems with some success (Prochazka et al., 2001).

Intraspinal microstimulation (ISMS) is an FES approach that targets central nervous system structures and has been investigated for its ability to produce weight-bearing standing (Lau et al., 2007) and stepping (Saigal et al., 2004) in cats. Others have proposed different central FES paradigms to aid in voiding the bladder (Grill et al., 1999; Pikov et al., 2007), restore hearing loss (McCreery, 2008) or reduce the effects of Parkinson's disease (Lozano et al., 2002). When considering such interventions it is important to evaluate the potential damage that they may cause as well as any plastic adaptations that may occur due to the implantation of and stimulation through chronically implanted microwires.

---

‡ A version of this chapter has been submitted for publication to the journal Biomaterials.

The insertion of intraspinal microwires and subsequent electrical stimulation could potentially cause damage within the spinal cord. Merely the act of implanting foreign bodies into central neural tissue is associated with initial traumatic injury and an ongoing inflammatory response (Biran et al., 2005). When considering nerve stimulation previous authors have shown that much of the damage comes from any mechanical strain upon the nerve (Agnew and McCreery, 1990). Central stimulation paradigms have the advantage of anchoring neural prostheses to hard, bony tissue and implanting microelectrodes within relatively immobile central neural tissues. Nevertheless, the damage done to central structures by mechanically mismatched or unstable implants could be severe.

In addition to mechanical damage the ongoing electrical stimulation may cause trauma due to the injection of current. This can occur due to potential cytotoxic effects at the electrode-tissue interface (Mortimer, 1981) or due to the flow of current across the neural structures (McCreery et al., 1990). In addition, the duty cycle of electrically excited neurons can be damaging if the interaction between stimulus frequency and daily stimulus duration reaches harmful levels (McCreery et al., 2004). Thus, even if the discrete pulse parameters are not injurious the aggregate chronic stimulation protocol may become so if the neural structures are excited at too high a rate or for too long.

Previous work has examined the damage induced by continuous stimulation in the feline cochlear and subthalamic nuclei (McCreery et al., 1994; McCreery et al., 2006). Safe upper limits for stimulation were identified at 3-4 nC/phase, however, the electrodes used in these experiments were relatively large in diameter and these experiments involved stimulus frequencies as high as 500 pulses per second (pps). In the sacral spinal cord the same authors discovered that functional increases in bladder pressure, when stimulating through single microelectrodes, were not achieved until stimulation levels reached 40 nC/phase at 20 pps (McCreery et al., 2004). This level of stimulation proved to be damaging during two 12 hour bouts of continuous stimulation on successive days although lesser duty cycles of 5% and 10% produced no, or minimal histological damage, respectively.

Following injury, the spinal cord retains its ability to learn and adapt to external stimuli (de Leon et al., 1998a,b). The spinal cord can respond to patterned or unpatterned stimuli and modify the motor output produced. This can occur in a very short period of time and it has been suggested that this represents a learning process similar to long-term potentiation or depression observed in the hippocampus (Edgerton et al., 2004). In addition to short-term changes there are task-specific, long-term biochemical adaptations within the spinal cord in response to activity (Cai et al., 2006). To date we are unaware of any investigations into the plasticity induced by repetitive electrical stimulation in the spinal cord, although

it may be expected that any increased activity of motor networks would produce similar biochemical and pharmacological adaptations.

A hallmark of ISMS is the gradual recruitment of force due to the orderly, preferential recruitment of small, fatigue-resistant motor units (Bamford et al., 2005). The recruitment order of ISMS is produced due to the excitation of fibers in passage and the subsequent transsynaptic activation of motoneurons through a larger network of afferent projections, interneurons and propriospinal neurons (Gaunt et al., 2006; Mushahwar et al., 2007). This, in combination with some direct activation of motoneurons produces a near-normal recruitment order that partially explains the fatigue-resistance produced by ISMS in synergistic movements such as standing and stepping (Saigal et al., 2004; Lau et al., 2007). Gradual force recruitment has been observed in intact and spinal cord transected animals indicating that the near-normal recruitment of motor units is not affected following the loss of supraspinal input. It is important to determine whether these force recruitment characteristics will remain unchanged following chronic ISMS. An alteration of these properties might indicate damage to the neural structures surrounding the implanted microwires.

The purpose of the current work was to evaluate the response of the rat spinal cord to microwire implantation and 30 days of ISMS. Immunohistochemical stains were used to reveal any damage induced by the insertion of microwires and subsequent stimulation protocol. In addition, an

attempt was made to examine the degree of activity-induced plasticity caused by chronic ISMS. This was examined directly at the spinal cord level and functionally by evaluating the functional recruitment of force following microwire implantation and chronic ISMS for 30 days. The experimental protocol involved daily stimulation through 2 microwires on one side of the spinal cord. On the contralateral side 2 microwires were implanted as sham controls and were not used for stimulation. Stimulation proceeded daily for 4 hours with a 50% duty cycle of 1 s on and 1 s off. This protocol was chosen to approximate the anticipated duration of daily use of the ISMS system upon clinical translation. The degree to which this protocol could induce damage and/or plasticity in the spinal cord was assessed. This study is the first to examine these issues following chronic, daily ISMS.

4.2 Methods

4.2.1 Animals

Experiments were performed on a total of 13 female Sprague-Dawley rats weighing 225-275 g. All procedures were approved by the University of Alberta Animal Welfare Committee and were in keeping with the guidelines for scientific research animals approved by the Canadian Council on Animal Care.

4.2.2 Spinal cord transection

Aseptic transection of the spinal cord at the eighth thoracic vertebra (T8) was carried out as follows. Under 2.0 % isofluorane anesthesia a

laminectomy was performed to expose the T8 spinal segment. A complete transection of the spinal cord was performed and the cord was closely inspected to ensure that no tracts remained intact. Surgical mesh was inserted into the cavity to minimize bleeding and a thin layer of plastic film was glued in place over the laminectomy site to prevent the invasion of connective tissues. The wound was sutured closed and analgesics (buprenorphine 0.015 mg/kg sc) and antibiotics (enroflaxacin 1.0 mg/kg sc) were administered. Analgesics were subsequently administered as needed along with a one week course of daily antibiotics. Rat bladders were expressed manually 3 times per day for 2 weeks and once daily thereafter. Animals were singly housed and cages were inspected daily and changed at least twice per week. A total of 10 animals were transected in this manner. In order to account for the effects of spinal cord transection alone, 4 of these 10 animals received only the transection and were classified as spinal cord transected control (ST).

4.2.3 ISMS Implant

After a 2 week recovery period a second laminectomy was performed on the 6 remaining transected animals to expose spinal cord segments T13 and L1. ISMS microwire arrays were implanted as described previously in rats (Bamford et al., 2005; Yakovenko et al., 2007) (see figure 4-1). Arrays of 4 microwires, 1.5 mm in depth, were manufactured according to established protocols (Guevremont et al., 2006) from 30 μm diameter platinum-iridium wire insulated with 4 μm polyimide except for

the tip (California Fine Wire, Grover Beach, CA, USA). After sterilization the arrays were inserted with two microwires on each side of the midline of the spinal cord and 2 mm spacing between rostral and caudal microwires. Microwire tips were targeted at the quadriceps motoneuron pool which has previously been mapped (Nicolopoulos-Stournaras and Iles, 1983).

When microwires are placed in the grey matter ISMS produces gradual recruitment of force from selected muscles. Therefore, these properties can be used during implantation to aid in targeting microwire tips to the ventral horn. Stimulus test trains were delivered to ensure quadriceps activation and recruitment of gradual force indicating accurate placement of microwire tips within the ventral grey matter. Microwires were fixed to the dura mater with individual drops of cyanoacrylate at their point of insertion and routed upon the dorsal surface of the dura mater to the base of the T12 vertebrae where they were collectively sutured to the dura mater using 8-0 silk (figure 4-1). A thin layer of plastic film was glued over the implantation site to prevent the adherence of overlaying muscle to the implanted array. At the T12 spinous process microwires were routed through a silastic tube to a headpiece (MS363, PlasticsOne, Roanoke, VA, USA) which was fixed to the rat skull using stainless steel screws and dental acrylic. Muscle and skin layers were sutured and analgesics were administered (buprenorphine 0.015 mg/kg sc). All animals were given a one week recovery period during which they received daily bladder expression.

4.2.4 Stimulation protocol

One side of the spinal cord was selected for daily stimulation and was designated ISMS while the contralateral side was chosen as the unstimulated sham control and was designated intraspinal microwire control (ISC). The ISMS side was stimulated for 4 consecutive hours of every day for 30 days through the two ipsilateral microwires while the contralateral ISC side received no stimulation. Individual ISMS pulses were 200 μs in duration, biphasic, charge balanced, cathodic-first. Stimulus trains at 25 pps were delivered through each microwire in an interleaved manner to produce 50 pps contractions at the quadriceps muscle. Interleaved stimulation presents interposed stimulus pulses from multiple electrodes at evenly spaced intervals. Stimulation proceeded for 1 second followed by 1 second of rest and was carried out at a level sufficient to produce functional contractions of the quadriceps muscle. Stimulus thresholds for quadriceps activation were checked approximately every 10 days and, when necessary, stimulus amplitudes were adjusted to maintain functional contractions. In order to accomplish this, stimulus amplitudes were maintained between 140 - 260 μA, or 28 - 52 nC per phase. As a function of the stimulus threshold for quadriceps activation this represented a mean of 2.55 ± 0.87 times threshold. Stimulating at these levels produced functional contractions from the ipsilateral quadriceps muscle in each animal throughout the 30 day stimulation period.

4.2.5 Functional assessments in terminal experiments

Functional muscle recruitment was compared in 3 intact animals and 3 of the 6 animals that underwent chronic ISMS. Under isofluorane anesthesia animals were positioned in a stereotaxic array and the quadriceps tendon was sutured to a force transducer (Interface MB-5, Interface Inc., Scottsdale, AZ, USA). In the intact rats, pairs of ISMS microwires were implanted ipsilaterally, targeting the quadriceps motoneuron pool as with the chronic implants. Force recruitment curves were generated by stimulating through each microwire at 25 pps. In the same experiment a second set of force recruitment curves were generated by stimulating through both microwires interleaved together at 25 pps to produce an aggregate 50 pps. Stimulation amplitude was varied randomly from subthreshold to a maximal amplitude of 400 μA and the evoked forces were recorded. Using the same protocol, force recruitment curves were generated at 25 pps from 5 ISMS microwires in 3 animals that had been stimulated with ISMS for 30 days through the chronically implanted microwires. In both intact and chronically implanted animals, forces from each microwire were normalized to the peak force evoked during the contraction and plotted against stimulus amplitude above threshold.

4.2.6 Perfusion and Tissue Handling

One day after the final day of chronic ISMS (i.e. the 31st day) animals were sacrificed and spinal cords were removed. The animals were perfused through the heart with approximately 200 ml of saline delivered at a rate of 40 ml/min and then with 200 ml of 4% formalin solution at the

same rate. Microwires were removed and the spinal cords were excised from the animals and soaked in formalin solution overnight. Subsequently, cords were transferred to 20% sucrose/phosphate buffered saline (PBS) at pH 7.4 for cryoprotection. Cryoprotectant solution was changed daily for 7 days until all cords sank to the bottom of the solution. Cords were embedded in cryostat tissue mounting medium and frozen by submersion in melting isopentane cooled in liquid nitrogen. Cords were subsequently stored at -80° C until serial cross sections of 20 µm thickness were cut using a cryostat and mounted onto slides (Superfrost plus gold, Fisher Scientific, PA, USA).

4.2.7 Immunohistochemistry

In order to evaluate the potential damage done by microwire implantation and ISMS for 30 days, a panel of immunohistochemical stains was performed. We applied primary antibodies to serial sections mounted on slides to reveal neuronal cell bodies (NeuN, clone A60), cytoskeletal disruption (Map-2, clone HM-2), reactive astrocytes marked by upregulated glial fibrillary acidic protein (GFAP, clone GA5), macrophages and microglia (ED-1) and synaptic terminals (Synaptophysin, polyclonal). Each of these immunohistochemical stains was repeated along the spinal cord segment where microwires were known to be implanted. Repetitions of each stain were performed at 200 µm intervals. As such, the separation between serial tissue sections immunostained with a given antibody was 200 µm in either the rostral or caudal direction. Before staining, a stan-

dard antigen retrieval technique was applied. Briefly, slides with mounted tissue cross-sections were incubated at 95° C for 20 min in 10 mM citrate buffer at pH 6.0. Slides in buffer were then removed from the heat and left to cool at room temperature for 20 min until an approximate temperature of 50° C was reached. Slides were then rinsed in distilled water and a standard immunohistochemical staining procedure was followed.

Washing in PBS-tween and then PBS was carried out between each step. Slides were incubated for 1 hour at room temperature in blocking solution containing PBS-tween, 1% bovine serum albumin, 10% horse serum and avidin-D blocking agent (Vector Laboratories, Burlingame, CA, USA). The blocking step for the Synaptophysin clone was identical except for the substitution of goat serum for an equal amount of horse serum. Primary antibodies were applied overnight at 4° C (NeuN 1:2000; Map-2 1:2000; ED-1 1:800; GFAP 1:400; Synaptophysin 1:800) in blocking solution which also included biotin blocking agent (Vector Laboratories). On the following day sections were incubated in 0.3% H_2O_2 in PBS for 15 minutes. Secondary antibodies were applied for 1 hour at room temperature with rat adsorbed, biotinylated horse anti-mouse IgG (Vector Laboratories, for NeuN and Map-2, ED-1, GFAP) diluted 1:400 in the appropriate blocking solution or with biotinylated goat anti-rabbit IgG (Vector Laboratories, for Synaptophysin) diluted 1:400 in appropriate blocking solution. Sections were incubated for 1 hour at room temperature with Vectastain ABC Reagent (Vector Laboratories) in PBS and immunoreactivity was visualized by

applying diaminobenzidine, H_2O_2 and NiCl in 50 mM tris-HCl (Vector Laboratories). To halt the developing reaction, sections were rinsed with distilled water and dehydrated in solutions of increasing ethanol concentration before being rinsed in xylene and mounted with Entallan mounting medium.

4.2.8 Imaging and Post-Processing

Pictures of stained serial sections were taken with an upright microscope (Leica DMLS, Leica Microsystems, Wetzlar, Germany) and attached digital camera (Spot Insight, Diagnostic Instruments, Sterling Heights, MI, USA) and then post-processed using commercial imaging software (Photoshop CS4, Adobe Systems Incorporated, San Jose, CA, USA). Standard post-processing methods were applied to images including the adjustment of brightness and contrast according to approved methods (Sedgewick, 2008).

Neuronal density was measured by counting the number of $NeuN^+$ cells in the vicinity of implanted microwire tips in the ventral horns of both ISMS and ISC sides of the chronically implanted animals and in matched areas in the ST control group. The number of positive cells was divided by the area analyzed to give a measurement of neuronal density in ISMS, ISC and ST control groups, expressed as cells/mm^2. When analyzing ISMS and ISC spinal tissue neither scar tissue, nor the path of the implanted microwire were included in the counting area. This was done to avoid counting areas where no $NeuN^+$ cells could possibly be found.

The immunostaining for ED-1 proved to be the most sensitive measure for detecting microwire tracks. As such, we measured the rostrocadual extent of the immune response by considering the distance from the microwire microwire track to the most rostral and caudal points where a track of ED-1 immunoreactivity conforming to the track of an implanted microwire could still be detected. The analysis of ED-1, GFAP, synaptophysin and Map-2 staining was carried by qualitative observations of spinal cord cross-sections by an experienced researcher who was blinded as to which microwire tracks were stimulated and which were sham control.

4.2.9 Statistics

All analyses were performed with a computerized software package (SPSS 17.0, SPSS Inc., Chicago, IL, USA). Differences were determined using one-way ANOVA and Tukey HSD post hoc analyses. Where appropriate, paired t-tests were performed between results from the ISMS side and the contralateral unstimulated ISC side. All data are presented as mean ± standard deviation. Differences were considered significant at $P < 0.05$.

4.3 Results

4.3.1 Pulsed and unpulsed microwire tips were located in the ventral grey matter

The locations of implanted pulsed and unpulsed intraspinal microwire tips were verified directly in spinal cord cross-sectional slices. The locations of ISMS microwire tips are shown in figure 4-2. Of 24 microwires implanted in 6 animals, a total of 16 were located on stained tissues. Pre-

sumably, some sections showing the microwire tips were lost during tissue processing including sectioning on the cryostat and immunohistochemical staining. Since the diameter of implanted microwires is only 30 μm it is possible that the loss of a few 20 μm thick tissue sections in certain areas would make the localization of all microwire tips impossible. As shown in figure 4-2, all of the microwire tips which could be located were in the ventral grey horn.

4.3.2 Stimulus thresholds of intraspinal microwires decreased over time

The stimulus threshold amplitudes for quadriceps muscle activation were tested on the first day of ISMS and approximately every ten days thereafter (figure 4-3). Mean threshold for muscle activation with ISMS microwires dropped significantly from 118.2 μA ± 45.1 μA to 67.8 μA ± 25.1 μA by the end of the 30 days of stimulation. This represented a mean decrease in threshold of 33.6% ± 38.2%. Regression curves were fitted for the relationship of stimulus threshold vs time. The mean slope of these curves was -1.61 ± 1.67 indicating the decline in stimulus threshold during the 30 day period. A single microwire failed permanently on the fourteenth day of stimulation while the remaining 11 out of 12 lasted throughout the 30 day stimulation period. Stimulus thresholds decreased in 8 of the remaining microwires, increased in 2 microwires and showed no overall change in 1 microwire.

4.3.4 Functional recruitment of muscle is unaltered after chronic ISMS

The slopes of the regression between amplitude and normalized force in intact animals were 0.0034 ($R^2 = 0.68$) and 0.0038 ($R^2 = 0.79$) for individual microwires pulsed at 25 pps and through two microwires interleaved at 50 pps, respectively (figure 4-4 A,B). Following chronic ISMS the slope of the same regression between amplitude and normalized force with microwires pulsed at 25 pps was 0.0034 ($R^2 = 0.78$, figure 4-4C). An analysis of covariance indicated that the slopes of these regressions were not significantly different from one another. Given this, we conclude that the recruitment of force through ISMS is not altered following spinal cord transection and 30 days of daily ISMS. As expected, this also shows that the recruitment of force through 2 microwires pulsed at 25 pps in an interleaved manner which produces an aggregate 50 pps is not altered from the recruitment from each microwire pulsed individually at 25 pps. ISMS continues to activate the neural circuitry of the spinal cord of chronically stimulated animals in the same manner as in the acute animals. This suggests that chronic ISMS does not cause sufficient damage to compromise the underlying neural networks that produce graded force recruitment.

4.3.5 Inflammation and reactive gliosis surrounding implanted microwires was unaffected by chronic stimulation

Microwires were affixed to the T12 spinous process and run along the dorsal surface of the dura mater. In two cases, microwires invaginated into the dorsal funiculi of the spinal cord (figure 4-5). This caused some deformation of the grey matter and recruitment of monocytes to surround

the embedded microwires (figure 4-5C). Encapsulation of the microwires with connective tissue and an increase in GFAP immunoreactivity were noted (figure 4-5D). In these instances damage to the dorsal grey matter did not appear to be severe as there was strong NeuN immunoreactivity in the dorsal horn suggesting that dorsal neurons were not affected by the deformation of the dorsal horn and surrounding white matter (figure 4-5B). In addition, Map-2 immunoreactivity, a marker of the neuronal cytoskeleton (Kikuchi et al., 1999; Gonzalez et al., 2008), was strong and uniform suggesting that the damage was limited (figure 4-5A). Nevertheless we did observe displacement and deformation of dorsal white matter, the functional consequences of this damage are unknown.

Microwires within the spinal cord were encapsulated with connective tissue and surrounded by reactive astrocytes staining for GFAP along the length of the microwire (figure 4-6). In addition, a strong ED-1 response in the microwire track demonstrated the recruitment of macrophages and microglia to the damaged area (figure 4-6). The extent of encapsulation, reactive astrocytosis and immune response did not appear to vary along the length of the microwire track or at the tip. The ED-1 immunoreactivity proved to be the best way to identify microwire tracks as ED-1 labeling was elevated up to 200 μm from the microwire track. We observed an elevation in ED-1 labeling in all microwire tracks at the next most rostral or caudal spinal cord cross sections which were 200 μm away. However, the ED-1 response had faded by the next cross section, a total of

400 μm distance from the microwire track. In some spinal cord sections we noted pieces of insulation along the microwire tracks of both pulsed and unpulsed microwires and, in some instances, at the dorsal cord surface at the site of microwire penetration (figure 4-5B and 4-6H). We believe portions of the insulation were stripped from the microwires during explantation as they appeared to be free of encapsulating tissues and often appeared to rest on top of the spinal cord section as they were the first pieces to become focused when adjusting the distance between the stage and the optical objective. This suggests that these pieces came loose during explantation and not at some point during the 30 day stimulation period.

4.3.6 Neuronal density was unaltered around pulsed and unpulsed microwires

Immunoreactivity against the NeuN antibody showed strong staining of neurons throughout the grey matter in spinal tissue from ISMS, ISC and ST unimplanted animals (figure 4-7). Insertion of microwires caused both the death of some neurons and the displacement of others along the shaft of the implanted microwire and subjacent to the tip. Subsequent stimulation, however, did not cause an observable worsening of the damage caused by insertion. Staining for NeuN was strong and uniform throughout the grey matter and $NeuN^+$ cells were located immediately adjacent to the connective tissue surrounding microwire shafts and tips. Counts of $NeuN^+$ cells in the ventral grey matter showed no significant differences in mean neuronal density between ISMS, ISC and ST groups (fig-

ure 4-8A). A regression analysis indicated that there was no significant correlation between increasing charge and a decrease in neuronal density (figure 4-8B). The range of neuronal densities in ventral grey matter was 180 - 264 NeuN cells/mm^2, 187 - 316 NeuN cells/mm^2 and 193 - 313 NeuN cells/mm^2 in ST, pulsed ISMS and unpulsed ISC spinal cords, respectively. The nearly identical ranges between ISMS and ISC suggest stimulation up to 48 nC/phase and 25 pps for 4 hours per day does little to damage nearby neurons.

4.3.7 Structural damage and synaptic reorganization

Tissue stained with the Map-2 antibody displayed strong staining of motoneurons and neural processes in the ventral horn (figure 4-9). Motoneurons displayed staining around the edges of the soma with projections from the soma also stained. Projections into the white matter were clearly demarcated. The staining pattern demonstrated with the Map-2 antibody was consistent with previous reports of Map-2 immunoreactivity in the spinal cord (Kikuchi et al., 1999; Gonzalez et al., 2008). We could find no observable differences in staining pattern or intensity between ISMS, ISC and ST controls. Moreover, a survey of tissues within 200 μm of implanted microwires showed no observable alteration in the intensity or distribution of staining that would indicate damage to the cytoskeleton of neurons.

Tissues stained with the synaptophysin antibody displayed punctate staining around the edges of large motoneurons in the ventral horn with

some less intense staining of the soma (figure 4-10). The staining pattern of the synaptophysin antibody was similar to that observed previously around spinal cord motoneurons (Nacimiento et al., 1995). There were no observable differences in staining pattern or intensity between ISMS, ISC and ST controls. Likewise, there were no apparent changes in tissue immunoreactivity to the synaptophysin antibody from ISMS, ISC and ST control groups within 200 μm of implanted microwires.

4.4 Discussion

4.4.1 Overview

Intraspinal microstimulation is a paradigm of electrical stimulation designed to reanimate paralyzed muscle by exciting directly the neural circuits in the spinal cord which control the muscles below the level of a spinal lesion. This involves the chronic implantation of fine microwires into spinal tissue and subsequent stimulation at levels sufficient to excite neural tissue adequately to produce desired levels of functional muscle activation. Multiple microwires are needed for the coordinated activation of muscle synergies necessary for complex movements such as standing and walking. In the current work we found that the mechanical implantation of microwires was followed by their encapsulation by reactive astrocytes and monocytes. Despite this, there was no significant decrease in neuronal density and no apparent disruption of the cytoskeletal elements in the ventral horn surrounding the implant. This is encouraging given the exaggerated mechanical mismatch between the size of the rat spinal cord and the

30 μm diameter microwires that were implanted in this study. Typically, these microwires are implanted in cats with much larger spinal cords and have demonstrated very little damage (Prochazka et al., 2001). Furthermore, the damage caused by implantation was not exacerbated by subsequent chronic stimulation for 30 days at a level sufficient to activate strongly the quadriceps muscle in rat. Although there were significant decreases in the stimulus threshold of the quadriceps muscle group we found no apparent increase in synaptic terminal density on motoneurons and no change in the recruitment of force by ISMS following 30 days of chronic ISMS. We conclude that functional activation of skeletal muscle through ISMS can be achieved safely, however, more compliant implants insulated by more robust polymeric materials would further minimize the mechanical damage associated with chronic implantation.

4.4.2 Functional recruitment

Motor units recruited during voluntary or reflex actions follow a specified order proceeding from smallest to largest. This is known as the size-principle and is explained by the rheobase current for motoneurons as well as the organization of synaptic input to motoneurons (Cope and Pinter, 1995). Following spinal cord transection in cats the principle of ordered recruitment according to motor unit size can be lost and a disordered recruitment profile can be observed transiently (Heckman, 1994; Durkovic, 2006). Although the reasons for disrupted recruitment order are uncertain it may be explained by an increase in the magnitude of hetero-

nymous EPSPs to extensor motoneuron pools following transection (Frigon and Rossignol, 2006). One report of this phenomenon also suggested that the increase in EPSPs is largest in FF and FR motoneurons shortly after transection (Munson et al., 1986). The size of EPSP magnitudes does return to normal after several months which roughly coincides with the return of an ordered recruitment pattern. ISMS takes advantage of the extant circuitry in the spinal cord by activating a larger network of afferent projections, interneurons and propriospinal neurons in order to produce a graded recruitment of force (Bamford et al., 2005; Gaunt et al., 2006; Mushahwar et al., 2007).

Given the possibility of disordered recruitment following spinal transection and the possibility of plastic alterations to spinal cord circuits with chronic ISMS it was important to determine if ISMS would continue to produce similar force recruitment properties as it does in intact animals. In the current work we showed that the slope of the relationship between normalized force and stimulus amplitude obtained from intact animals is not altered following chronic transection and 30 days of ISMS indicating the continuing ability of ISMS to recruit force in a gradual manner.

4.4.3 Ongoing inflammatory response

A clear finding in this study is that chronic ISMS for 30 days did not cause damage to the spinal cord. There is damage caused by the mere insertion of microwires and resultant foreign-body response, however, this

was limited. Upon removal of the chronically implanted microwires a track could be clearly seen in stained tissues, although this was extremely difficult to detect in cross-sectional slices before immunostaining. Immunostaining for ED-1 proved to be the best indicator of the microwire track location as ED-1 immunoreactivity was contained only in and around the microwire tracks. An elevated immunoreactivity for ED-1 was observed at 200 μm dorsal and caudal to the microwire tracks but not at 400 μm. In cross-sectional slices beyond this point no indication of implantation could be found indicating that the immune response caused by microwire insertion was limited to a distinct area surrounding the microwire implants which extended further than 200 μm but less than 400 μm in rostral and caudal directions.

The classical understanding of spinal cord damage suggests that activated monocytes are recruited within the first few days following injury and that this response subsides in the following weeks (Norenberg et al., 2004). Our results showed that there was a persistent inflammatory response to the intraspinal microwires 38 days after implantation. The implantation tracks of chronically implanted microwires were found to contain clusters of ED-1$^+$ cells indicating an ongoing inflammatory response. This may be explained by the fact that the implants in question cannot be broken down and absorbed by the immune system, thus incurring an ongoing response. Other authors found similar results with silicon electrodes implanted in rat cerebral cortex for up to 4 weeks (Biran et al., 2005).

These authors showed that an acute stab wound with the microelectrode produced no lasting macrophage/microglia recruitment at 4 weeks while the implanted electrode produced a persistent inflammatory response similar to our own. The existence of an inflammatory response, ongoing after 38 days, raises the issue of long-term stability and safety of implanted microwires. Activated microglia and macrophages are responsible for the release of compounds such as cytokines and tumor necrosis factor-α (Kwon et al., 2004). These factors encourage the continuing immune response and can have cytotoxic effects.

Previous authors have also shown a decrease in neuronal content surrounding their implanted microelectrodes and suggested that the cause might be the cytotoxic elements released by the ongoing inflammatory response they observed (Biran et al., 2005; Biran et al., 2007). Similar to their findings, we observed a persistently elevated ED-1 immunoreactivity and yet we showed no significant decrease in neuronal density around either pulsed or unpulsed microwires. The difference may lie in the nature of the implanted electrodes. Their implanted microelectrodes have a very different footprint measuring 200 μm wide by 15 μm thick at the base and tapering to 33 μm wide and 2 μm thick at the tip. In addition, due to their silicon construction those implants are much stiffer than our 30 μm diameter platinum-iridium microwires. It is reasonable to expect that stiffer implants might produce greater damage as more flexible electrodes are

better able to yield with any movement in the surrounding tissue. Indeed, the same authors concluded that the decreased neuronal content surrounding a neural implant tethered to the skull, as opposed to a floating design, may have been due to the combination of micromotion of the implant within the tissue and the stiffness of silicon implants (Biran et al., 2007).

Previous work with deep brain stimulation (DBS) implants in humans showed no ongoing inflammatory response or tissue damage in autopsied brains from patients who had active implants for up to 70 months before their deaths (Haberler et al., 2000). This suggests that the persistent immune response observed around the implanted microwires in our study will ultimately recede. The same work also demonstrated well preserved neurons and synaptophysin-immunoreactive bodies close to the implantation tracks, a finding similar to our own.

4.4.4 Reactive gliosis

In addition to the ongoing recruitment of monocytes we observed the encapsulation of the microwires as evidenced by a thin layer of connective tissue surrounding the implant site, bordered by a gliotic layer immunoreactive for GFAP. We observed reactive gliosis surrounding the implanted microwires, both in the ventral horn and at the dorsal surface where microwires were routed to a silastic tube. There were no observable difference between the encapsulation of pulsed or unpulsed microwires. The thickening of the glial sheath in the weeks following implantation has

been associated with the degradation of signal and ultimate failure of recording electrodes (Grill et al., 2009). In the case of stimulating electrodes such as ours the glial sheath is likely to be less of an impediment to operation. Reactive gliosis around neural implants is a common finding (Grill et al., 2009) and has been shown to persist for years as evidenced by autopsies of deep brain stimulators implanted into human patients (Haberler et al., 2000). The progression of encapsulation surrounding the implant, specifically the increase in GFAP immunoreactivity, has been implicated in the increased tissue adherence and resistance to removal of chronically implanted electrodes (McConnell et al., 2007). This may explain our observation that some of our chronically implanted microwires retained some surrounding scar tissue when removed, leaving both a tissue residue on the microwire and, in one case, an enlarged cavity in the spinal cord with no sign of connective tissue or a glial scar. Other authors have noted similar findings with silicon microelectrodes at 2 and 4 weeks after implantation (Turner et al., 1999). At later time periods the glial sheath becomes more compact and the adherence between tissue and electrode surface is lessened resulting in less damage when electrodes are removed.

In concert with this finding we observed pieces of polyimide insulation at multiple locations around the microwire tracks in the tissue cross-sections. Presumably, these pieces were stripped off from the implanted microwires. These pieces were gold in color and were found within and around the microwire tracks (see figure 4-5B and 4-6H). It is unclear when

the insulation was removed but we suspect that it occurred during the withdrawal of microwires from spinal tissue and not during the 30 day stimulation period. We believe this because the insulation pieces were found surrounding both pulsed and unpulsed microwires. In addition, the deposition of these pieces was uniform along the length of the microwire track instead of being focused at the microwire tip where stimulation occurred. Pieces of insulation appeared to be free from encapsulation by connective tissues and, when intermingled with tissues, were observed to be resting on top of the tissues.

4.4.5 Structural damage

Synaptic reorganization during recovery from trauma can be visualized by alterations in neuronal cytoskeleton and synaptic input via immunoreactivity for Map-2 and synaptophysin, respectively (Nacimiento et al., 1995; Kikuchi et al., 1999; Gonzalez et al., 2008). In normal conditions Map-2 immunoreactivity reveals neurons and dendrites (Yu et al., 2000) while synaptophysin immunoreactivity on motoneurons is punctate and discontinuous revealing synaptic inputs onto the neuron (Gilerovich et al., 2008). Following trauma, diminished Map-2 staining indicates structural damage to the neuron while a decrease or absence of staining for synaptophysin around the soma indicates a loss of descending, propriospinal and afferent input. Synaptophysin immunoreactivity is ultimately restored following spinal cord trauma suggesting a reorganization of neural input to the motoneurons that can occur in as little as 21 days in upper lumbar

segments. In the current work we observed no difference between ISMS, ISC and ST controls in synaptophysin immunoreactivity surrounding motoneurons in the ventral horn. These observations align closely with previous descriptions of punctate, discontinuous synaptophysin staining patterns around undamaged neurons suggesting that any loss of synaptophysin immunoreactivity following spinal transection was restored in all groups by the time of the terminal experiments. Importantly, the chronic implantation of microwires and subsequent ISMS did not cause a loss of synaptic input to the motoneuronal soma. Our results are similar to those with chronic DBS implants in human patients showing regular staining for synaptophysin in close proximity to pulsed electrode tracks (Haberler et al., 2000). Likewise, we observed strong Map-2 staining of motoneurons and perineural areas indicating no obvious damage to the cytoskeleton of neurons and neurites in close proximity to both pulsed and unpulsed microwires.

4.4.6 Plasticity

We have previously shown that chronic implants in the cat spinal cord undergo an increase in stimulus threshold within the first 10-15 days followed by long periods of stable thresholds (Mushahwar et al., 2000). Presumably this was due to the effect of encapsulation around the microwire tip. Given these previous results we were surprised by our current result that stimulus thresholds decreased in the first two weeks following the initiation of stimulation and then appeared to stabilize. This may be

explained by the fact that the previous work showing increases in stimulus threshold did not entail daily stimulation as the current work did. It is possible that the significant decline in stimulus threshold for quadriceps muscle is the result of a mechanism similar to that seen during training in chronically transected cats and rats (Edgerton et al., 2004). The authors of this work showed an increase in the expression of markers of inhibitory neurotransmitters in the transected cord which was reversed with activity in the form of physical training. A decrease in the stimulus threshold could be achieved through a similar mechanism following chronic activation of circuits by electrical stimulation.

4.4.7 Microwire design

The current work represents the first attempt to use a rat model to evaluate our ISMS implants chronically. The rat spinal cord is considerably smaller than that of the cat, our previous animal model. This makes accurately targeting the microwire tips to the ventral horn more challenging and creates a mechanical mismatch between the 30 μm diameter microwires and the smaller cord diameter of the rat. Some of the damage caused by insertion of the microwires can be attenuated by addressing the materials, design and implantation techniques relevant to ISMS microwires. The invagination of microwires into the dorsal horn (figure 4-5) is likely due to a downwards force upon the microwire which may have occurred during or after the implantation. During the implant it is possible that the microwire was inserted with too much force, causing the mi-

crowire to be pushed into the tissue along with the inserted tip and shaft. However, it seems more likely that this occurred afterwards due to downwards pressure placed upon the implant by the muscle and skin layers sutured closed over the implant. Given that this damage has not been observed in cat implants it may be related to the relatively smaller space between the spinal cord and the muscle layers in the rat and thus this particular form of damage seems unlikely to occur in cat or human procedures. The polyimide insulation used in the current design has been shown to be relatively non-toxic and compliant (Polikov et al., 2005), however, we found that this insulation was stripped from the microwires during explantation. Although we do not believe this occurred prior to explantation it may indicate that the robustness of the insulation material needs to be improved.

A great deal of controversy and mixed results surround the question of speed of implant insertion into the tissue, perhaps owing largely to the wide array of electrode designs currently in use (as reviewed by Polikov et al., 2005). When inserting stiffer arrays, some authors have suggested implantation at high speed using microdrivers (Rousche and Normann, 1992). However, given the advantages of flexible microwires in yielding with the motion of the surrounding tissue it seems that hand implantation at relatively slow speeds remains the best option for our flexible microwire implants. Some of the microelectrodes used by others have rounded tips which can cause a compaction of neurons around the microwire tip

(McCreery et al., 2000). We observed a similar phenomenon in one instance (figure 4-7C), however, this was not common with our implants, likely due to the fact that our microwires have sharpened tips which are better able to advance through tissue than a rounded tip.

4.4.8 Conclusions

In summary, we found that implantation of intraspinal microwires caused encapsulation with connective tissue and reactive astrocytes and an inflammatory response which persisted until the terminal experiment. There was, however, no diminishing of neuronal density in the ventral horn near the microwire tracks, nor any observable sign of cytoskeletal damage. Microwires which were used for daily stimulation at up to 48 nC/phase and 25 pps showed no more damage than those which remained unpulsed. In comparison to spinal controls we conclude that chronic ISMS produces limited damage due to the initial insertion of microwires which is not apparently worsened by daily stimulation at levels sufficient to cause functional activation of the quadriceps muscle group. Moreover, the force recruitment properties of ISMS were unaltered following spinal transection and 30 days of ISMS. Although chronic activation of spinal cord circuitry can reasonably be expected to encourage activity-induced plasticity we observed no alteration in the pattern of staining with the synaptophysin antibody. Taken collectively, these results are very encouraging, especially given the dramatic mechanical mismatch between the relatively small rat spinal cord and the 30 μm diameter microwires, however, it

would be prudent to continue the effort to limit damage during implantation. This can be accomplished by redesigning the microwires with more compliant and robust materials and by examining the techniques of implantation.

4.5 Figures

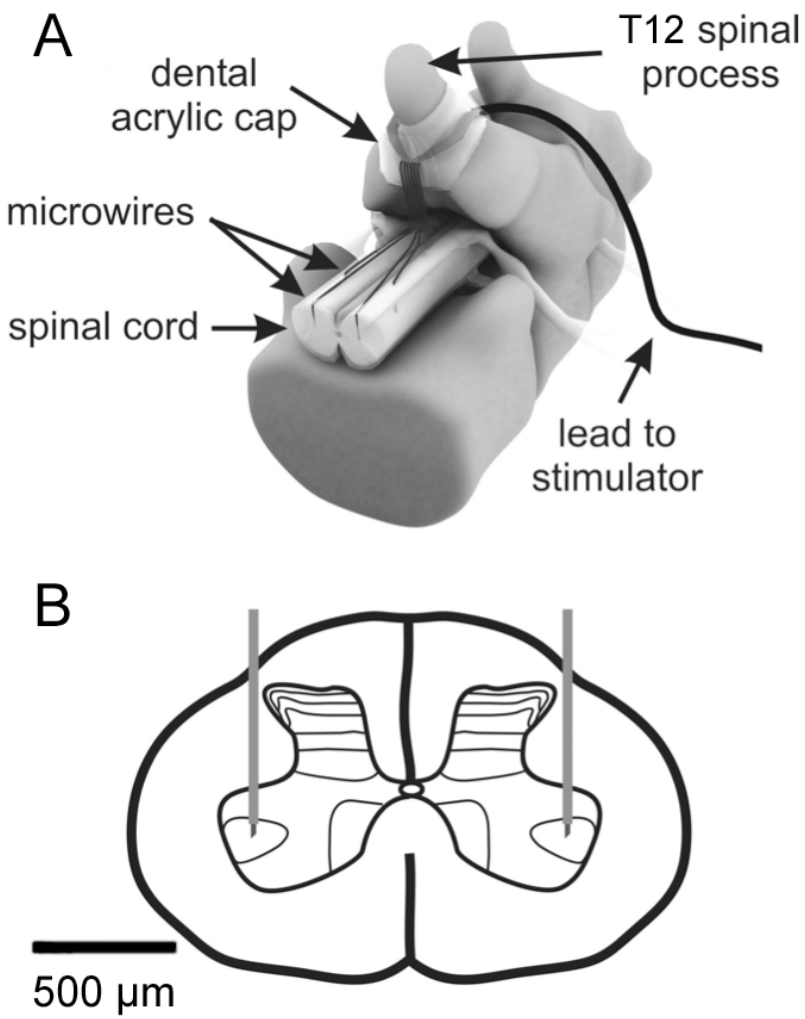

Figure 4-1: Schematic of the intraspinal implant

A laminectomy was performed at the T13 level in the rat to expose the lumbar enlargement for implantation of microwire arrays. A) An example of an 8 microwire array is shown including the dental acrylic cap which secures the lead to the T12 spinous process. B) Microwires with exposed tips are implanted contralaterally into the spinal cord with the tips targeting lamina IX in the ventral horn.

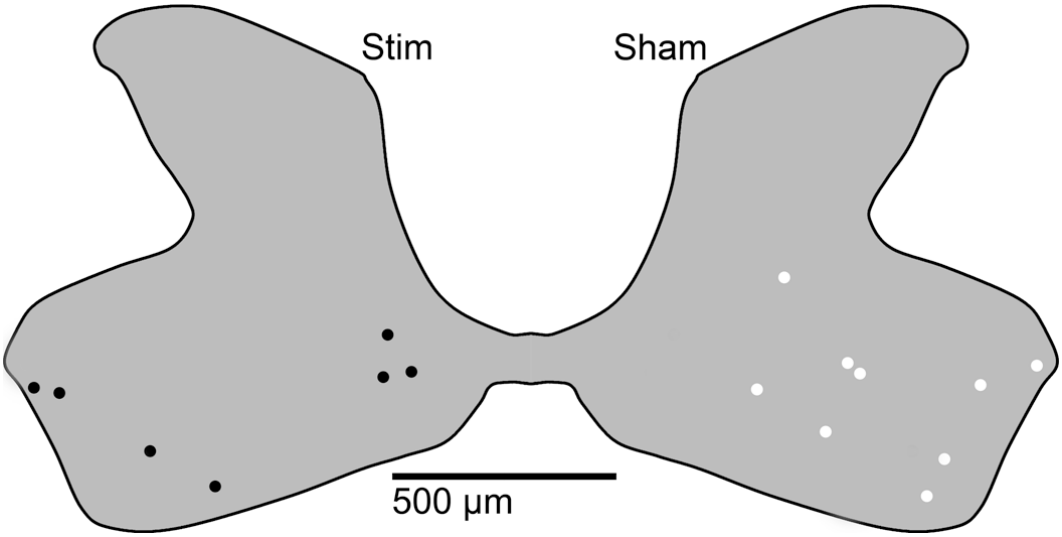

Figure 4-2 Summary of located microwire tips

The locations of stimulated and sham implanted microwire tips were identified in immunostained spinal cord tissue sections and a composite diagram was created to show their locations. We located 16 of 24 microwire tips, 9 from unpulsed microwires (shown in white) and 7 from pulsed microwires (shown in black). All tips were found within the grey matter of the ventral horn.

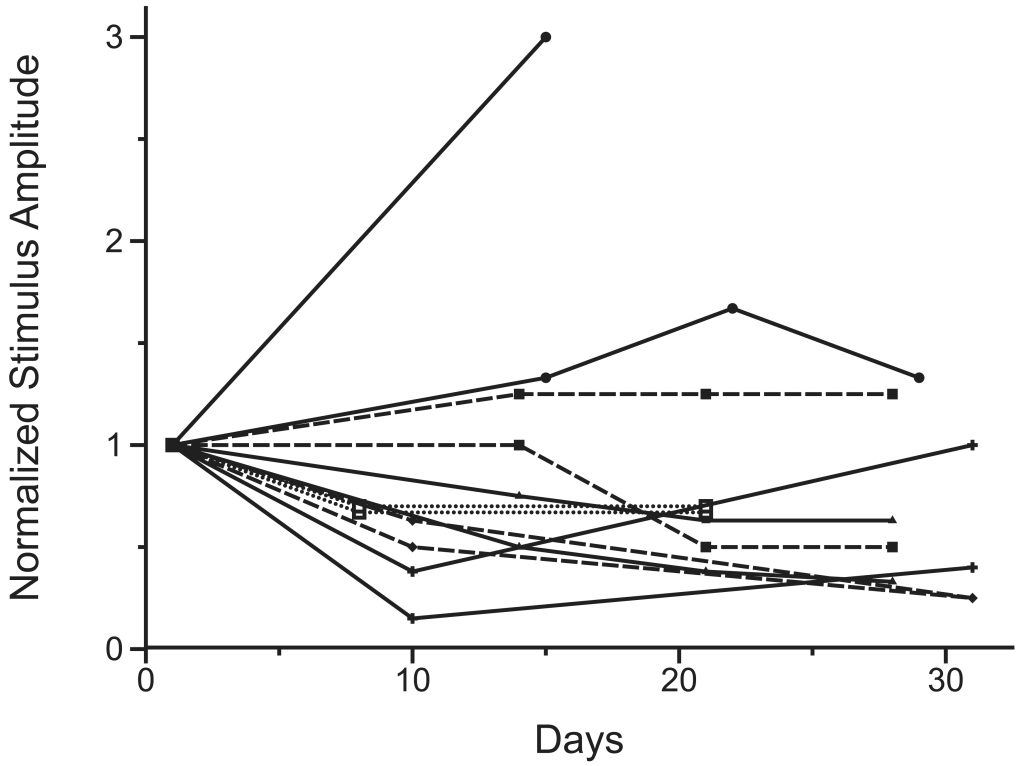

Figure 4-3 Activation thresholds from pulsed microwires during the 30 day stimulation period

ISMS thresholds for quadriceps muscle activation for the 12 stimulating microwires are shown normalized to their respective stimulus thresholds determined on the first day of stimulation. There was a significant decline in mean threshold amplitude from 118.2 μA ± 45.1 μA on the first day of stimulation to 67.8 μA ± 25.1 μA at the end of the stimulation period. The stimulus threshold for 1 microwire increased sharply before the microwire failed permanently on day 14. Of the remaining 11 microwires 8 had decreases in stimulus threshold, 2 had increases and 1 microwires had no overall change. Pairs of ipsilateral microwires in each animal are indicated by matching symbols and lines.

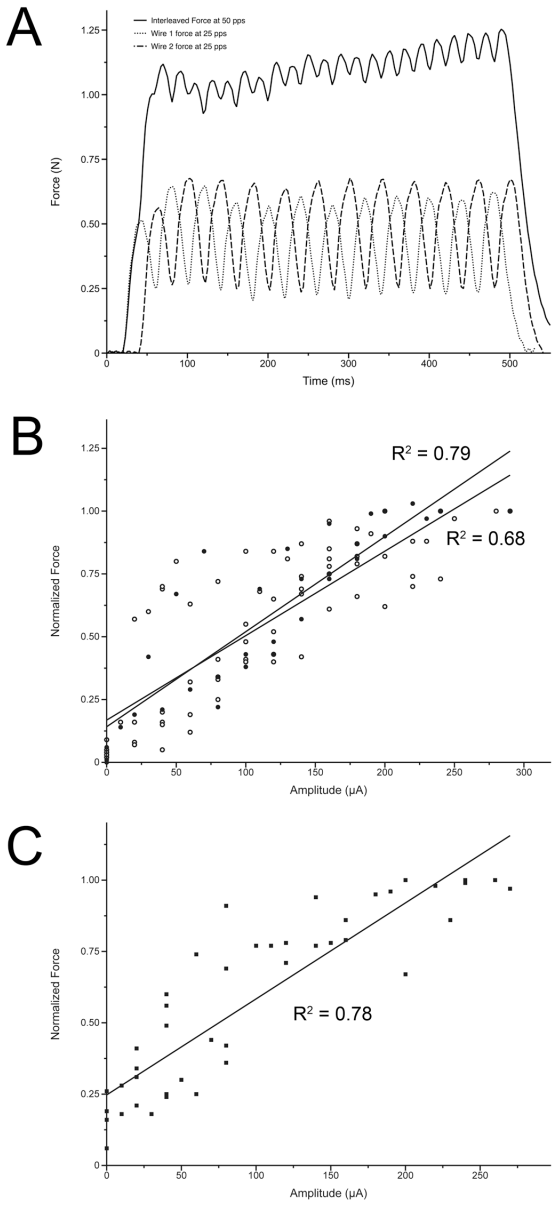

Figure 4-4 Force recruitment curves from intact and chronically spinalized and stimulated animals

(A) Examples are shown of forces recruited from individual ISMS microwires at 25 pps and from the resultant 50 pps product of interleaved stimulation through these microwires. (B) The relationship between normalized force and supra-threshold amplitude in intact animals from 6 individual microwires at 25 pps (open circles) is shown in comparison to the same relationship generated by the resultant 50 pps (filled circles) product of interleaved stimulation in the same intact animals. C) Following 30 days of chronic spinal transection and ISMS the relationship between normalized force and supra-threshold amplitude is shown.

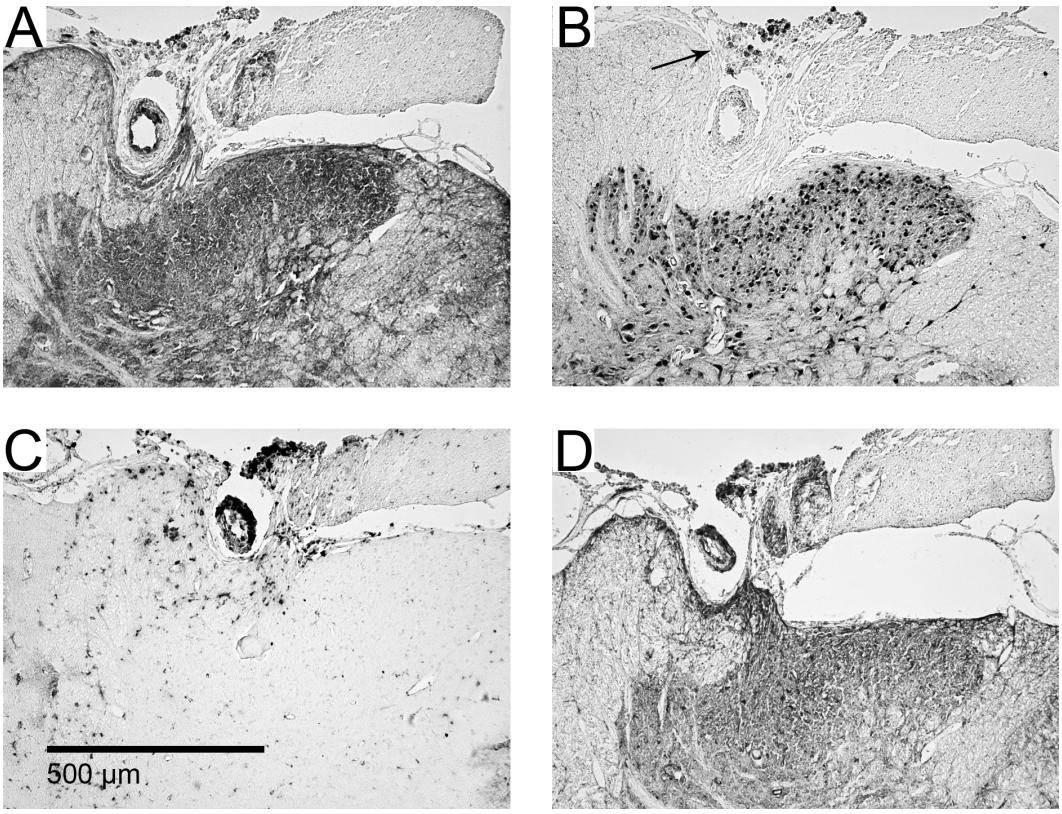

Figure 4-5 Dorsal horn invagination by implanted microwires

Serial images from one example of dorsal horn damage due to invagination of microwires running across the dorsal surface of the spinal cord. Immunohistochemical stains for A) Map-2, B), NeuN, C) ED-1 and D) GFAP. Encapsulation of the microwire occurred with some deformation of the dorsal grey matter. Some pieces of insulation pulled off from the microwires and can be seen in panel B as dark spots indicated by the arrow.

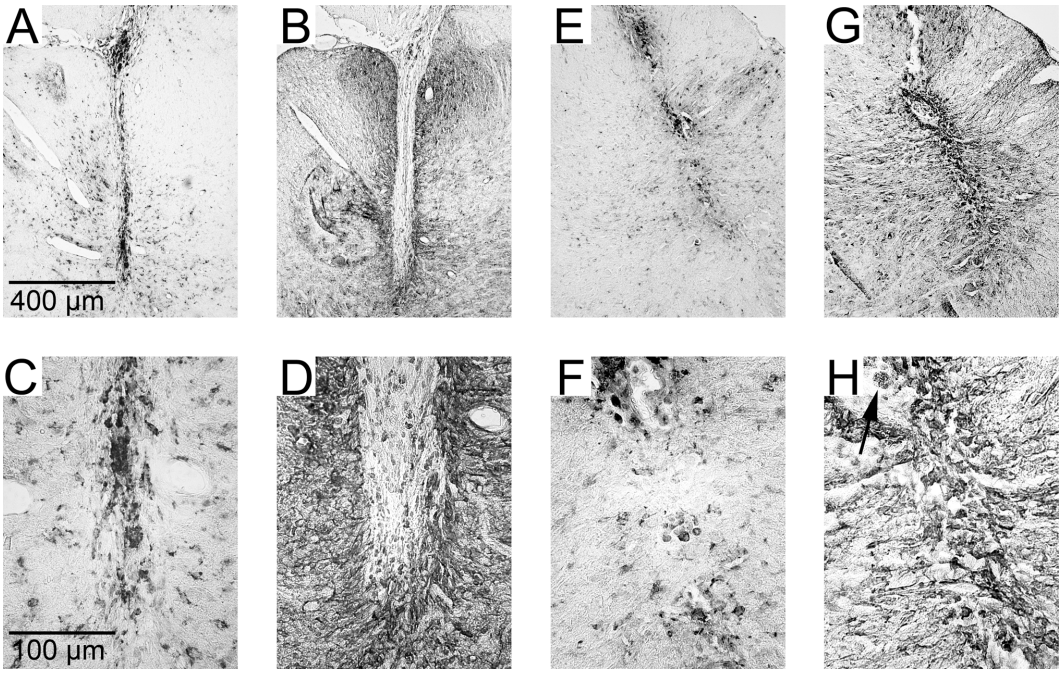

Figure 4-6 Pulsed and unpulsed microwire tracks

Examples of pulsed microwire electrode tracks (A,B,E,G) and tips (C,D,F,H). Pulsed electrodes (E,G,F,H) and unpulsed electrodes (A,B,C,D) displayed an ongoing inflammatory response as evidence by immunoreactivity for ED-1 (A,E,C,F). Encapsulation by a thin connective tissue layer and by GFAP immunoreactive astrocytes (B,G,D,H) was found along the entire track and at the electrode tip. The arrow in panel H indicates a piece of insulative material that was removed during explantation and was found in the microwire track.

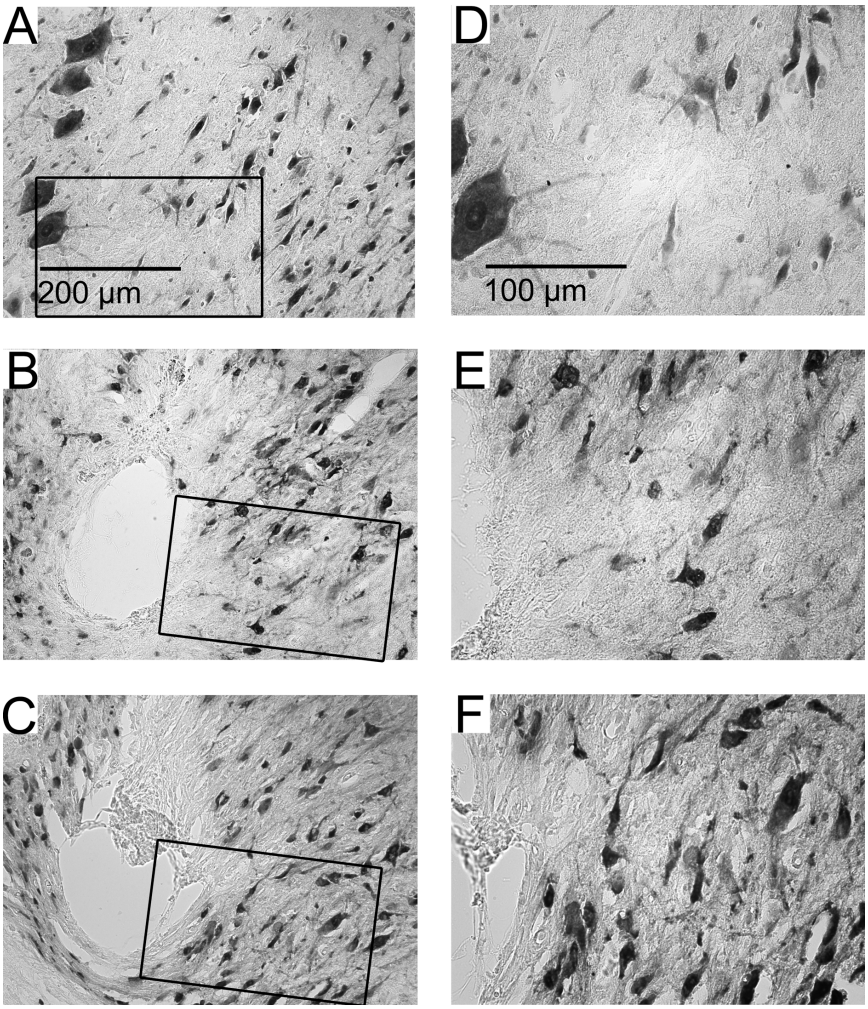

Figure 4-7 Neuronal density around microwires and in control tissue

Examples are shown of NeuN staining in spinal control tissue A,D), around an unpulsed electrode track B,E) and around a pulsed electrode track C,F). Boxed Outlines in A,B,C indicate the enlarged areas in D,E,F. Darkly stained $NeuN^{+}$ neurons can be seen surrounding the tracks of both pulsed and unpulsed electrodes near the tip. The microwire tracks are gaps in the tissue indicated by the black arrows. Explantation of the microwire tips caused some tearing of the tissue surrounding the microwire tracks in panels B and C. In panel C the tissue adjacent to the microwire track can be seen to be compressed by the microwire indicating some distortion around the tip of this microwire.

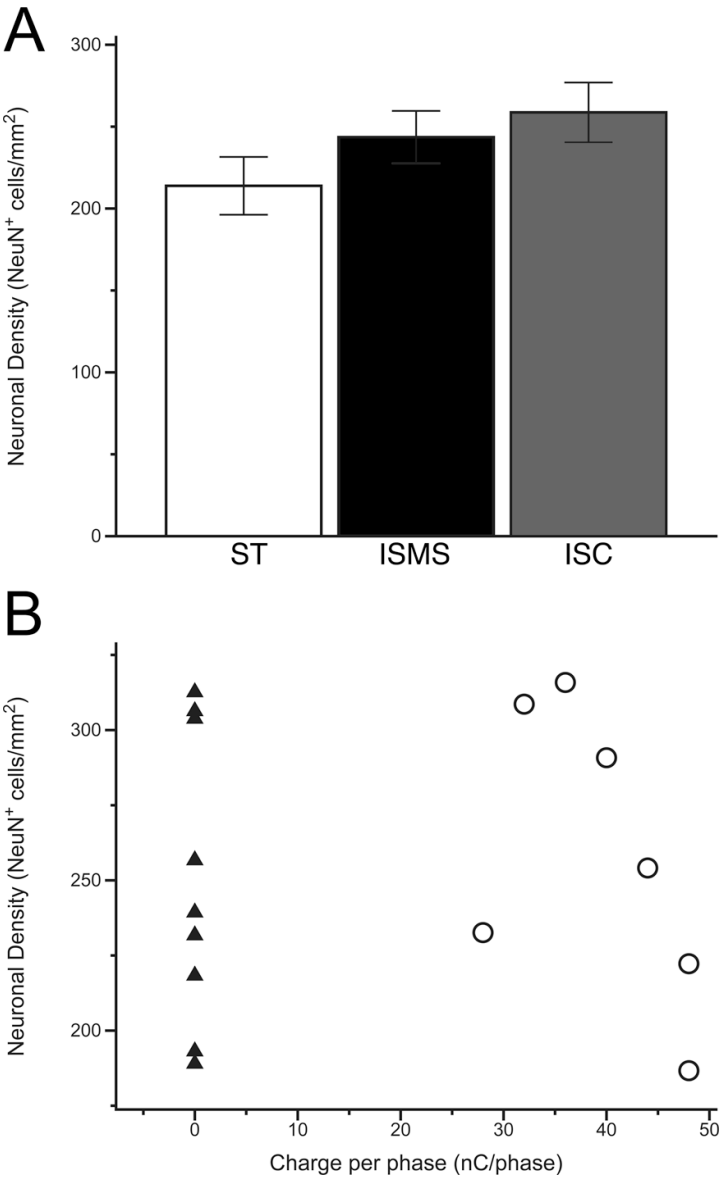

Figure 4-8 Quantification of neuronal density

Determination of neuronal density was made by counting NeuN immuno-reactive cells in the ventral horn of ST, ISMS and ISMC spinal tissue. A) Neuronal density was not decreased in ISMS or ISMC groups as compared to the spinal transected control. B) When plotted against charge per phase the range of neuronal density was virtually identical between the ISMS side (open circles) and the unstimulated ISC side (filled triangles).

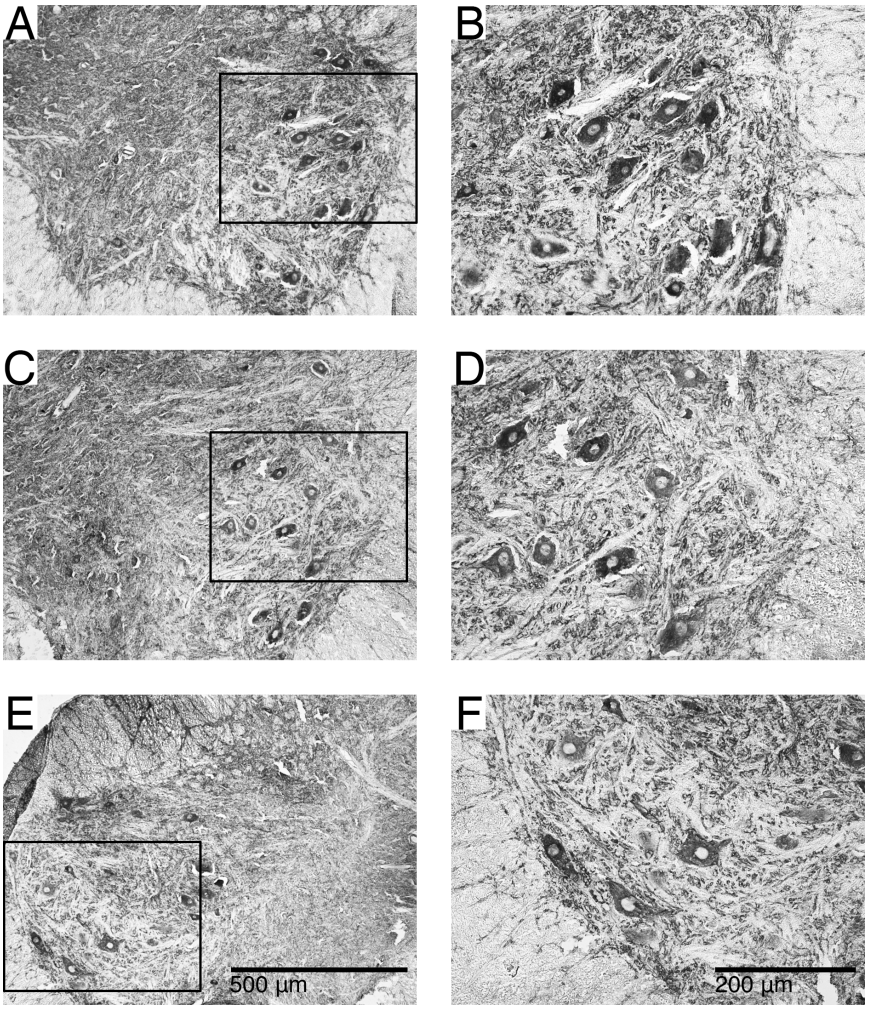

Figure 4-9 Cytoskeletal structure visualized with Map-2

Examples showing Map-2 immunoreactivity in the ventral horns of ST (A,B), ISMS (C,D) and ISC (E,F) groups. Black outlines in A,E,C indicate the enlarged areas in B,D,F. Strong staining of motoneurons in the ventral horn and neurites was noted including projections into the surrounding white matter. No apparent differences between any of the groups was noted.

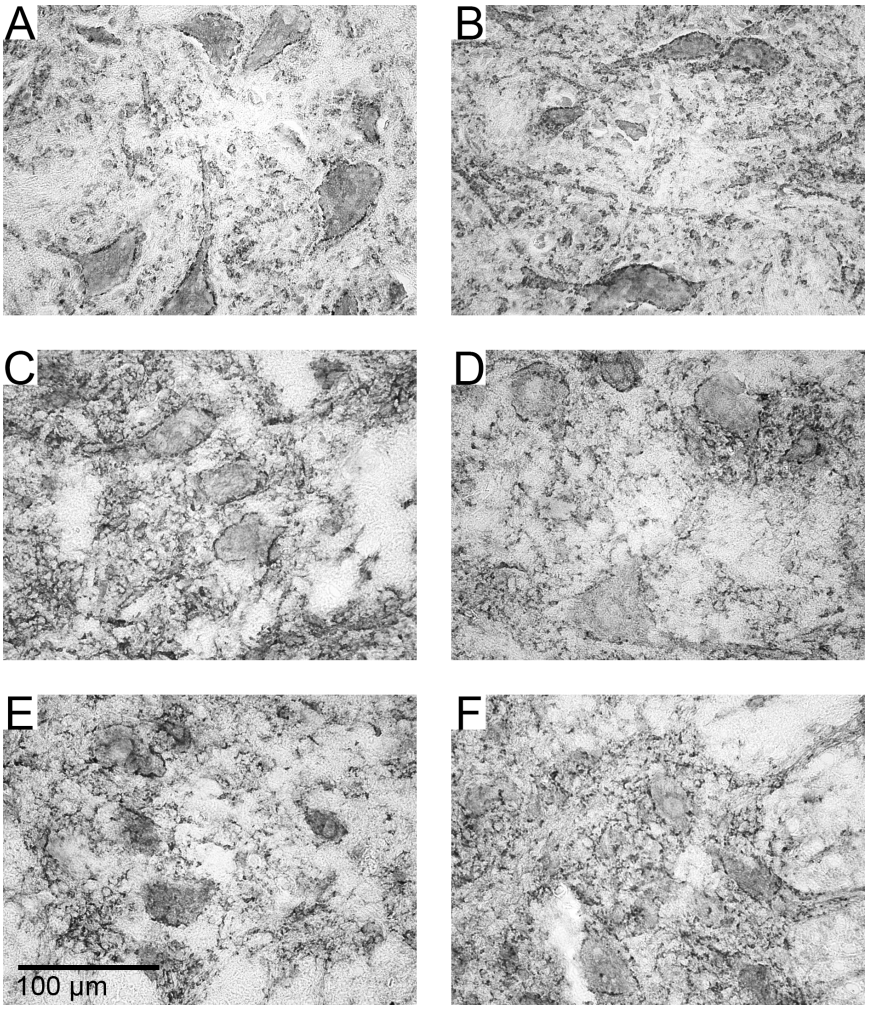

Figure 4-10 Synaptic inputs to motoneurons visualized with synaptophysin immunoreactivity

Two examples from each group showing synaptophysin immunoreactivity in the ventral horns of ST (A,B), ISMS (C,D) and ISC (E,F) groups. Punctate and discontinuous staining around motoneurons in the ventral horn and noted suggesting axosomatic inputs at these locations. No apparent differences between any of the groups was noted.

4.6 Bibliography

Agnew, WF, McCreery, DB (1990) Considerations for safety with chronically implanted nerve electrodes. Epilepsia, 31 Suppl 2:S27–32.

Bamford, JA, Putman, CT, Mushahwar, VK (2005) Intraspinal microstimulation preferentially recruits fatigue-resistant muscle fibres and generates gradual force in rat. J Physiol, 569:873–884.

Biran, R, Martin, DC, Tresco, PA (2007) The brain tissue response to implanted silicon microelectrode arrays is increased when the device is tethered to the skull. J Biomed Mater Res A, 82:169–178.

Biran, R, Martin, DC, Tresco, PA (2005) Neuronal cell loss accompanies the brain tissue response to chronically implanted silicon microelectrode arrays. Exp.Neurol, 195:115–126.

Cai, LL, Courtine, G, Fong, AJ, Burdick, JW, Roy, RR, Edgerton, VR (2006) Plasticity of functional connectivity in the adult spinal cord. Philos Trans R Soc Lond B Biol Sci, 361:1635–1646.

Cope, TC, Pinter, MJ (1995) The Size Principle: Still Working After All These Years. News in Physiological Sciences News Physiol Sci, 10:280–286.

De Leon RD Hodgson J Roy RR & Edgerton V (1998a) Locomotor capacity attributable to step training versus spontaneous recovery after spinalization in adult cats. J Neurophysiol, 79:1329-1340.

De Leon RD Hodgson J Roy RR & Edgerton V (1998b) Full weight-bearing hindlimb standing following stand training in the adult spinal cat. J Neurophysiol, 80:83-91.

Durkovic, RG (2006) Functional consequences of motor unit recruitment order reversals following spinal cord transection in cat. Somatosens Mot Res, 23:25–35.

Edgerton, VR, Tillakaratne, NJ, Bigbee, AJ, De Leon, RD, Roy, RR (2004) Plasticity of the spinal neural circuitry after injury. 27:145–167.

Frigon, A, Rossignol, S (2006) Functional plasticity following spinal cord lesions. Prog Brain Res, 157:231–260.

Gaunt, RA, Prochazka, A, Mushahwar, VK, Guevremont, L, Ellaway, PH (2006) Intraspinal Microstimulation Excites Multisegmental Sensory Afferents at Lower Stimulus Levels Than Local {alpha}-Motoneuron Responses. J Neurophysiol, 96:2995–3005.

Gilerovich, EG, Moshonkina, TR, Fedorova, EA, Shishko, TT, Pavlova, NV, Gerasimenko, YP, Otellin, VA (2008) Morphofunctional characteristics of the lumbar enlargement of the spinal cord in rats. Neurosci Behav Physiol, 38:855–860.

Gonzalez, SL, Lopez-Costa, JJ, Labombarda, F, Deniselle, MC, Guennoun, R, Schumacher, M, De Nicola, AF (2008) Progesterone Effects on Neuronal Ultra-

structure and Expression of Microtubule-associated Protein 2 (MAP2) in Rats with Acute Spinal Cord Injury. Cell Mol Neurobiol,

Grill, WM, Bhadra, N, Wang, B (1999) Bladder and urethral pressures evoked by microstimulation of the sacral spinal cord in cats. Brain Res, 836:19–30.

Grill, WM, Norman, SE, Bellamkonda, RV (2009) Implanted Neural Interfaces: Biochallenges and Engineered Solutions. Annu Rev Biomed Eng,

Guevremont, L, Renzi, CG, Norton, JA, Kowalczewski, J, Saigal, R, Mushahwar, VK (2006) Locomotor-related networks in the lumbosacral enlargement of the adult spinal cat: activation through intraspinal microstimulation. IEEE Trans Neural Syst Rehabil Eng, 14:266–272.

Haberler, C, Alesch, F, Mazal, PR, Pilz, P, Jellinger, K, Pinter, MM, Hainfellner, JA, Budka, H (2000) No tissue damage by chronic deep brain stimulation in Parkinson's disease. Ann Neurol, 48:372–376.

Heckman, CJ (1994) Alterations in synaptic input to motoneurons during partial spinal cord injury. Med Sci Sports Exerc, 26:1480–1490.

Kikuchi, H, Doh-ura, K, Kawashima, T, Kira, J, Iwaki, T (1999) Immunohistochemical analysis of spinal cord lesions in amyotrophic lateral sclerosis using microtubule-associated protein 2 (MAP2) antibodies. Acta Neuropathol, 97:13–21.

Kwon, BK, Tetzlaff, W, Grauer, JN, Beiner, J, Vaccaro, AR (2004) Pathophysiology and pharmacologic treatment of acute spinal cord injury. Spine J, 4:451–464.

Lau, B, Guevremont, L, Mushahwar, VK (2007) Strategies for generating prolonged functional standing using intramuscular stimulation or intraspinal microstimulation. IEEE Trans Neural Syst Rehabil Eng, 15:273–285.

Lozano, AM, Dostrovsky, J, Chen, R, Ashby, P (2002) Deep brain stimulation for Parkinson's disease: disrupting the disruption. Lancet Neurol, 1:225–231.

McConnell, GC, Schneider, TM, Owens, DJ, Bellamkonda, RV (2007) Extraction force and cortical tissue reaction of silicon microelectrode arrays implanted in the rat brain. IEEE Trans Biomed Eng, 54:1097–1107.

McCreery, D, Lossinsky, A, Pikov, V, Liu, X (2006) Microelectrode array for chronic deep-brain microstimulation and recording. IEEE Trans Biomed Eng, 53:726–737.

McCreery, D, Pikov, V, Lossinsky, A, Bullara, L, Agnew, W (2004) Arrays for chronic functional microstimulation of the lumbosacral spinal cord. IEEE Trans.Neural Syst.Rehabil.Eng, 12:195–207.

McCreery, DB, Agnew, WF, Yuen, TG, Bullara, L (1990) Charge density and charge per phase as cofactors in neural injury induced by electrical stimulation. 37:996–1001.

McCreery, DB (2008) Cochlear nucleus auditory prostheses. Hear Res, 242:64–73.

McCreery, DB, Yuen, TG, Agnew, WF, Bullara, LA (1994) Stimulus parameters affecting tissue injury during microstimulation in the cochlear nucleus of the cat. Hear Res, 77:105–115.

McCreery, DB, Yuen, TG, Bullara, LA (2000) Chronic microstimulation in the feline ventral cochlear nucleus: physiologic and histologic effects. Hear Res, 149:223–238.

Mortimer, JP (1981) Motor Prostheses. In: Vol II, Motor Control (Brooks, VD, ed), pp 155–187. Bethesda: American Physiological Society.

Munson, JB, Foehring, RC, Lofton, SA, Zengel, JE, Sypert, GW (1986) Plasticity of medial gastrocnemius motor units following cordotomy in the cat. J Neurophysiol, 55:619–634.

Mushahwar, VK, Collins, DF, Prochazka, A (2000) Spinal cord microstimulation generates functional limb movements in chronically implanted cats. Exp.Neurol, 163:422–429.

Mushahwar, VK, Jacobs, PL, Normann, RA, Triolo, RJ, Kleitman, N (2007) New functional electrical stimulation approaches to standing and walking. J Neural Eng, 4:S181–97.

Nacimiento, W, Sappok, T, Brook, GA, Toth, L, Schoen, SW, Noth, J, Kreutzberg, GW (1995) Structural changes of anterior horn neurons and their synaptic input caudal to a low thoracic spinal cord hemisection in the adult rat: a light and electron microscopic study. Acta Neuropathol, 90:552–564.

Nicolopoulos-Stournaras, S, Iles, JF (1983) Motor neuron columns in the lumbar spinal cord of the rat. J Comp Neurol, 217:75–85.

Norenberg, MD, Smith, J, Marcillo, A (2004) The pathology of human spinal cord injury: defining the problems. J Neurotrauma, 21:429–440.

Pikov, V, Bullara, L, McCreery, DB (2007) Intraspinal stimulation for bladder voiding in cats before and after chronic spinal cord injury. J Neural Eng, 4:356–368.

Polikov, VS, Tresco, PA, Reichert, WM (2005) Response of brain tissue to chronically implanted neural electrodes. J Neurosci Methods, 148:1–18.

Prochazka, A, Mushahwar, VK, McCreery, DB (2001) Neural prostheses. J.Physiol, 533:99–109.

Rousche, PJ, Normann, RA (1992) A method for pneumatically inserting an array of penetrating electrodes into cortical tissue. Ann Biomed Eng, 20:413–422.

Saigal, R, Renzi, C, Mushahwar, VK (2004) Intraspinal microstimulation generates functional movements after spinal-cord injury. IEEE Trans.Neural Syst.Rehabil.Eng, 12:430–440.

Sedgewick, J (2008) Scientific imaging with Photoshop : methods, measurement, and output. New Riders: Berkeley, CA.

Turner, JN, Shain, W, Szarowski, DH, Andersen, M, Martins, S, Isaacson, M, Craighead, H (1999) Cerebral astrocyte response to micromachined silicon implants. Exp Neurol, 156:33–49.

Yakovenko, S, Kowalczewski, J, Prochazka, A (2007) Intraspinal stimulation caudal to spinal cord transections in rats. Testing the propriospinal hypothesis. J Neurophysiol, 97:2570–2574.

Yu, WR, Westergren, H, Farooque, M, Holtz, A, Olsson, Y (2000) Systemic hypothermia following spinal cord compression injury in the rat: an immunohistochemical study on MAP 2 with special reference to dendrite changes. Acta Neuropathol, 100:546–552.

Chapter 5
General discussion

5.1 Discussion

Currently, ISMS remains an experimental technique that requires further testing before clinical trials can be attempted. In order to progress towards a clinically viable treatment it was necessary to address lingering questions about the recruitment properties of ISMS. In addition, the plastic adaptations to the muscle and spinal cord needed to be evaluated, including the extent of any injury resulting from daily ISMS use. ISMS is not the only FES system that holds promise for restoring motor function following spinal cord injury (section 1.4); however, it has proven to be capable of generating complex synergies such as weight-bearing standing and stepping through relatively simple stimulation patterns (Saigal et al., 2004; Lau et al., 2007). Advances in stimulation methods and control systems have continued to improve the results obtained with ISMS and encourage further research (Snow et al., 2006; Guevremont et al., 2007). This work has attempted to complement these studies by clarifying the force recruitment characteristics of ISMS in acute and chronic models and examining the plasticity and damage induced by ISMS in muscle and spinal cord. This represents a substantial advance in our knowledge regarding an emerging FES paradigm and how it excites the underlying neuromuscular apparatus.

Although ISMS had been shown to produce gradual recruitment of force (Mushahwar and Horch, 1998) the mechanisms of this effect had not been examined. In the study outlined in chapter 2 we confirmed previous work showing that ISMS recruits force significantly more gradually than does a nerve cuff in rat quadriceps muscle. Moreover, we examined the recruitment of muscle fibers directly by determining which fibers had been active during stimulation. We demonstrated that ISMS at 3.0X threshold recruited significantly more slow and fatigue-resistant muscle fibers than did a nerve cuff. When considering this data against the populations of MHC-based muscle fiber classifications we determined that ISMS was preferentially recruiting slow muscle fibers while the nerve cuff was preferentially recruiting fast muscle fibers. These results were the first to provide a detailed explanation of the force-recruitment characteristics of ISMS and they explain the previous findings that ISMS can produce gradual force recruitment and fatigue-resistant contractions.

Given these results it seemed reasonable to expect that chronic ISMS might produce a muscle that was more physiologically normal in terms of its distribution of MHC-based fiber types and resultant functional properties. The reversed motor unit recruitment order common in peripheral FES procedures, when applied chronically, can result in a homogeneous muscle comprised of only slow muscle fibers (Andersen et al., 1996; Roy et al., 1998). This has the secondary effects of decreasing muscle cross-sectional area and reducing the muscle's possible range of force out-

puts (Gordon et al., 1997). In the study presented in chapter 3 we found that the muscle transformation produced by ISMS was similar to that produced by the nerve cuff in regards to both contractile elements and functional properties. This suggests that total daily stimulation time may be more important than recruitment order in determining the final muscle phenotype and associated functional properties (Kernell et al., 1987). This work was the first attempt at chronic ISMS for a period that simulated the total daily time that an implant would need to function in a human.

The effects of daily, chronic ISMS on spinal cord plasticity and damage were unknown. In the study in chapter 4 we considered the damage and the plasticity in the spinal cord as a result of chronic ISMS. We found that the insertion of microwires causes limited damage in line with what has been shown for other chronic implants in CNS tissue (Haberler et al., 2000). However, the chronic excitation of neural tissue with ISMS amplitudes sufficient to cause functional quadriceps contractions did not further this damage. Moreover, the force recruitment properties of ISMS were identical to those in acute experiments suggesting that any damage induced by the insertion of microwires and subsequent stimulation did not compromise the neural networks in the spinal cord which might have altered the functional characteristics of ISMS. This was the first work to use a chronic rat model of ISMS which entailed a relatively large mismatch between the size of the spinal cord and the diameter and stiffness of the implanted 30 μm microwires. Given this fact, our observation of a limited

damage response due to implantation and no furtherance of this response with chronic ISMS is encouraging.

5.2 Future directions

Despite the encouraging results with ISMS presented here and elsewhere, some engineering challenges need to be addressed in order to encourage more research into this technique and to advance towards clinical trials. These challenges can be generally placed into three categories. Namely, manufacture of the microwire array, implantation procedures and control strategies.

Currently the manufacture of ISMS arrays is a challenging process requiring a day of hand labor. Furthermore, the manufactured arrays are fragile and cannot be modified at the time of implant to adjust to the unique circumstances of each procedure. In order for ISMS to become more widely utilized, a more standardized approach to array manufacture must be developed. Preferably this would include the ability to customize the length and depth of the microwire arrays in order to accommodate individualized measurements taken using magnetic resonance imaging before manufacture. Previous results have also suggested that the mechanical separation of individual microwires from one another grants the ability to flex with micromotion of the spinal cord which is a critical factor in preventing damage and ensuring long-term stability (Polikov et al., 2005). The results in chapter 4 suggest that any new implant should take care not

to compromise the flexibility of the microwire. It may also be necessary to consider different insulation materials given that the stripping of the microwires during explantation demonstrated some weakness in the bonding of insulation to the microwires. These results, however, are not dispositive as it could be argued that these implants have proven to be stable over the long-term (Prochazka et al., 2001) and that the stripping of insulation only occurred during explantation of microwires, a process applied here only for diagnostic examination of the spinal cord.

The development of better designs for microwire arrays should also streamline the implantation procedure. Currently, the arrays require individual implantation of each microwire by hand, occasionally leading to misplacement of the microwire tips (Guevremont and Mushahwar, 2008). A simplified procedure would preferably allow the surgeon to implant an array of microwires in one step but retain the mechanical separation of microwires that is critical to limiting damage. Current work is proceeding into the development of platforms into which multiple microwires could be embedded, conceptually similar to the Utah array implant (Rousche and Normann, 1992), which would then be inserted in one step. The platform would be constructed of an adsorbent material such as a hydrogel polymer that could be stiff during implantation but would subsequently become compliant when saturated with liquid. Other alternatives include the use of dissolvable polymers that might be absorbed by the body following the implant. In both cases the goal would be to simplify and standard-

ize the implantation procedure while ensuring that microwires remain detached from one another.

ISMS can produce graded, fatigue-resistant force and complex multijoint synergies utilizing simple, tonic stimulation patterns from a few implanted microwires (Mushahwar et al. 2007). However, the ultimate goal of the work is to optimize this result by employing advanced stimulation and control strategies. As mentioned in section 1.4, an FES system employing multiple electrode contacts can take advantage of interleaved stimulation strategies to reduce fatigue and produce a fused contraction (McDonnall et al., 2004). ISMS already utilizes multiple microwires to improve selectivity and take advantage of an interleaved stimulation protocol. To further this advantage, work has proceeded into increasing the number of electrode contacts along a shaft without increasing the number of implanted shafts. In order to accomplish this, electrodes have been designed with multiple contacts along the length of the shaft, providing multiple stimulation sites in the dorsal-ventral plane (Snow et al., 2006). Further work should consider applying these advancements while maintaining the smallest possible shaft diameter in order to limit insertion damage and maximize the flexibility of the electrodes.

In order to maximize the fatigue-resistance of ISMS, interleaved stimulation using a closed-loop controller has been applied (Lau et al., 2007). In order to optimize this feature, feedback systems need to be de-

veloped which can provide accurate data about limb kinematics and forces. Although this may be accomplished with external sensors such as accelerometers and force sensors further work should consider the possibility of incorporating neural data recorded in real-time from afferent fibers. The ultimate realization of this model would be to provide a brain-machine interface that would read the intentions of the user, apply the appropriate stimulation strategy and then modify this strategy based upon feedback from sensory afferents in the limb. It may even be possible to close this loop by providing this input to the brain in order to restore perception of the motor task to the user. These last improvements in the brain-machine interface would likely require significant breakthroughs in the design of recording electrodes as well as our understanding of how neural activity in the brain creates sensation in the consciousness of the individual.

5.3 Conclusion

ISMS has produced graded, fatigue-resistant force in the execution of selected multijoint synergies using relatively simple electrodes, stimulation protocols and control strategies. As we expand our knowledge of ISMS properties we are able to tailor the design and implantation of microwire arrays to optimize these results. Advances in the engineering of the ISMS implant will capitalize on the inherent advantages of ISMS and aid in the development of a clinically viable procedure to restore motor function fol-

lowing SCI. If successful, this technique could dramatically improve the quality of life and independence of those living with paralysis.

5.4 Bibliography

Andersen JL Mohr T Biering-Sorensen F Galbo H & Kjaer M (1996) Myosin heavy chain isoform transformation in single fibres from m. vastus lateralis in spinal cord injured individuals: effects of long-term functional electrical stimulation (FES). Pflugers Arch, 431:513-518.

Gordon T Tyreman N Rafuse VF & Munson JB (1997) Fast-to-slow conversion following chronic low-frequency activation of medial gastrocnemius muscle in cats. I. Muscle and motor unit properties. Journal of Neurophysiology, 77:2585-2604.

Guevremont, L, Mushahwar, VK (2008) Tapping into the spinal cord for restoring function after spinal cord injury. In: Neuroengineering (DiLorenzo, DJ, Bronzino, JD, eds), pp 19–1 to 19-25. Boca Raton: CRC Press.

Guevremont, L, Norton, JA, Mushahwar, VK (2007) Physiologically based controller for generating overground locomotion using functional electrical stimulation. J Neurophysiol, 97:2499–2510.

Haberler C Alesch F Mazal P Pilz P Jellinger K Pinter M Hainfellner J & Budka H (2000) No tissue damage by chronic deep brain stimulation in Parkinson's disease. Ann Neurol, 48:372-376.

Kernell D Eerbeek O Verhey BA & Donselaar Y (1987) Effects of physiological amounts of high- and low-rate chronic stimulation on fast-twitch muscle of the cat hindlimb. I. Speed- and force-related properties. Journal of Neurophysiology, 58:598-613.

Lau, B, Guevremont, L, Mushahwar, VK (2007) Strategies for generating prolonged functional standing using intramuscular stimulation or intraspinal microstimulation. IEEE Trans Neural Syst Rehabil Eng, 15:273–285.

McDonnall, D, Clark, GA, Normann, RA (2004) Interleaved, multisite electrical stimulation of cat sciatic nerve produces fatigue-resistant, ripple-free motor responses. IEEE Trans.Neural Syst.Rehabil.Eng, 12:208–215.

Mushahwar V & Horch KW (1998) Selective activation and graded recruitment of functional muscle groups through spinal cord stimulation. Ann N Y Acad Sci, 860:531-535.

Mushahwar V Jacobs P Normann R Triolo R & Kleitman N (2007) New functional electrical stimulation approaches to standing and walking. J Neural Eng, 4:S181-97.

Polikov, VS, Tresco, PA, Reichert, WM (2005) Response of brain tissue to chronically implanted neural electrodes. J Neurosci Methods, 148:1–18.

Prochazka, A, Mushahwar, VK, McCreery, DB (2001) Neural prostheses. J.Physiol, 533:99–109.

Rousche, PJ, Normann, RA (1992) A method for pneumatically inserting an array of penetrating electrodes into cortical tissue. Ann Biomed Eng, 20:413–422.

Roy RR Talmadge R Hodgson J Zhong H Baldwin K & Edgerton V (1998) Training effects on soleus of cats spinal cord transected (T12-13) as adults. Muscle Nerve, 21:63-71.

Saigal, R, Renzi, C, Mushahwar, VK (2004) Intraspinal microstimulation generates functional movements after spinal-cord injury. IEEE Trans.Neural Syst.Rehabil.Eng, 12:430–440.

Snow, S, Horch, KW, Mushahwar, VK (2006) Intraspinal microstimulation using cylindrical multielectrodes. IEEE Trans Biomed Eng, 53:311–319.